

January 01, 2008

## A family of space-time block codes for wireless communications

Ning Yang  
*Northeastern University*

---

### Recommended Citation

Yang, Ning, "A family of space-time block codes for wireless communications" (2008). *Electrical Engineering Dissertations*. Paper 1.  
<http://hdl.handle.net/2047/d10017732>

This work is available open access, hosted by Northeastern University.

**A FAMILY OF SPACE-TIME BLOCK CODES FOR  
WIRELESS COMMUNICATIONS**

A Thesis Presented

by

**Ning Yang**

to

The Department of Electrical and Computer Engineering

in partial fulfillment of the requirements

for the degree of

**Doctor of Philosophy**

in

Electrical Engineering

Northeastern University

Boston, Massachusetts

August 2008

© Copyright by Ning Yang 2008  
All Rights Reserved

**NORTHEASTERN UNIVERSITY**  
**Graduate School of Engineering**

Thesis Title: A Family of Space-Time Block Codes for Wireless Communications

Author: Ning Yang

Department: Electrical and Computer Engineering

Approved for Thesis Requirement for the Doctor of Philosophy Degree

---

Thesis Advisor Prof. Masoud Salehi

---

Date

---

Thesis Committee Member Prof. John G. Proakis

---

Date

---

Thesis Committee Member Prof. Hanoch Lev-Ari

---

Date

---

Thesis Committee Member Prof. David Brady

---

Date

---

Department Chair Prof. Ali Abur

---

Date

Graduate School Notified of Acceptance:

---

Associate Dean of Engineering Dr. Yaman Yener

---

Date



## Abstract

It is well known that the performance of the wireless communication systems can be enhanced by using multiple transmit and receive antennas, which is generally referred to as the MIMO technique, and has been incorporated into the IEEE 802.11n standard, i.e. one of the Wi-Fi systems. The MIMO technique has also been adopted by the 3GPP Long Term Evolution (LTE) and the 3GPP2 Ultra Mobile Broadband (UMB) standards. The space-time coding is a promising way to realize the gain in the wireless communications system using MIMO. The space time block code, and the orthogonal space time block code in particular have been proposed in research and implemented in practical wireless communication systems due to their low computational complexity in maximum likelihood decoding implementation. However, the code rates of the orthogonal space time block codes are usually lower than  $3/4$  when the number of transmit antennas is greater than two, which limit their throughput. To increase the code rate and the throughput of the orthogonal space time block code for more than two transmit antennas, a family of new space-time block codes (STBC) for 3 and 4 transmit antennas in a MIMO wireless communication system have been proposed in this Ph.D. research. These new codes are orthogonal and achieve full diversity, full rate using “Triple QPSK” modulation, which is proposed in this research. We investigated the performance of these STBCs when the channel state information (CSI) is perfectly known at the receiver. The CSI is not known to the transmitter in all of the studies in this dissertation. An analytical bound of the probability of bit error is developed and the Monte Carlo simulation is used when investigating these new STBC codes.

In practical wireless communication system, the CSI is generally not available at the receiver and it is usually estimated by the receiver through the pilot signals or training signals known to the receiver. No matter what channel estimation method

is used, the estimate of CSI will not match the CSI exactly and is noisy. The performance of these new STBCs using the “Triple QPSK” modulation when the estimate of the CSI is employed to detect the symbol is investigated in this dissertation. An upper bound of the bit error probability is developed when the noisy CSI is used to detect the symbols. The performance of the new STBCs using the “Triple QPSK” modulation is also evaluated using Monte Carlo simulation.

When the CSI is not available to either the receiver or the transmitter, the differential encoding and decoding algorithm is applied to these new STBCs, which use the “Triple QPSK” modulation. The results showed that these orthogonal STBCs achieve full diversity full rate using ”Triple-QPSK” modulation with differential detection. This provides a means of achieving space diversity and multiplexing gain without the CSI. A new differential encoding and decoding algorithm is proposed and analyzed for STBCs with 3 transmit antennas, whose transmission matrix is not square matrix, as part of this Ph.D. research. The STBCs using this algorithm achieve full diversity the MIMO system can possibly provide.

# Acknowledgements

First, I would like to thank my advisor Professor Masoud Salehi, for his guidance and support throughout my entire Ph.D. program of study. It is a pleasure to work with him. I would also like to express my gratitude to Professors John G. Proakis, David Brady and Hanoch Lev-Ari for serving on my graduate committee, and giving me valuable feedback on every aspects of my graduate study.

I would like to thank my friends at Northeastern, and at the Communication and Digital Signal Processing Center in particular, for their friendship. They made my experience at Northeastern University enjoyable.

Much of my Ph.D. study was done when I was working full time in the industry. The support from my colleagues, friends, and management at Qualcomm, Inc., Teradyne, Inc., Analog Devices Inc., Verizon Communications, Inc. and the former GTE Laboratories, Inc. are highly appreciated.

Last, but not least, the support and understanding from my family, my wife Judy, my sons Andrew and Victor are appreciated. The original vision and expectation of my parents made it possible for me to study for a Ph.D. degree in the United States.

# Contents

|                                                                       |            |
|-----------------------------------------------------------------------|------------|
| <b>Acknowledgements</b>                                               | <b>iii</b> |
| <b>1 Introduction to Multiple Antenna Communications Systems</b>      | <b>1</b>   |
| 1.1 Characteristics of Fading Channel . . . . .                       | 2          |
| 1.2 Diversity Techniques . . . . .                                    | 4          |
| 1.3 The MIMO System . . . . .                                         | 5          |
| 1.4 The MIMO Channel . . . . .                                        | 7          |
| 1.5 Capacity of the MIMO Channel . . . . .                            | 9          |
| 1.6 Diversity and Multiplexing Gain . . . . .                         | 14         |
| <b>2 Space Time Codes</b>                                             | <b>17</b>  |
| 2.1 The Design Criterion for Space-Time Codes . . . . .               | 17         |
| 2.2 Space-Time Trellis Code . . . . .                                 | 21         |
| 2.3 Space-Time Block Code . . . . .                                   | 24         |
| 2.3.1 STBCs from Real Orthogonal Designs . . . . .                    | 27         |
| 2.3.2 STBC from Complex Orthogonal Designs . . . . .                  | 28         |
| 2.4 High Rate STBC from Complex Designs . . . . .                     | 31         |
| <b>3 A New Family of Space-Time Block Codes</b>                       | <b>37</b>  |
| 3.1 New STBC for Three Transmit Antennas . . . . .                    | 39         |
| 3.2 Performance of the New STBC for Three Transmit Antennas . . . . . | 45         |
| 3.3 New STBC for Four Transmit Antennas . . . . .                     | 50         |

|          |                                                                                 |            |
|----------|---------------------------------------------------------------------------------|------------|
| 3.4      | Performance of the New STBC for Four Transmit Antennas . . . . .                | 53         |
| <b>4</b> | <b>Performance of Space-Time Block Codes with Imperfect Channel Information</b> | <b>57</b>  |
| 4.1      | Performance of STBC with Noisy CSI . . . . .                                    | 57         |
| 4.2      | Performance of Alamouti STBC with Noisy CSI using QPSK . . . . .                | 62         |
| 4.2.1    | System Model . . . . .                                                          | 65         |
| 4.2.2    | Performance Analysis of STBC . . . . .                                          | 66         |
| 4.2.3    | Performance Results . . . . .                                                   | 73         |
| <b>5</b> | <b>A New Family of Differentially Encoded Space Time Block Codes</b>            | <b>76</b>  |
| 5.1      | Differential STBC for Three Transmit Antennas . . . . .                         | 79         |
| 5.2      | Differential Detection for New STBC with “triple-QPSK” . . . . .                | 87         |
| <b>6</b> | <b>Concluding Remarks</b>                                                       | <b>92</b>  |
| <b>A</b> | <b>Confidence Intervals</b>                                                     | <b>97</b>  |
|          | <b>Bibliography</b>                                                             | <b>101</b> |

# List of Figures

|     |                                                                                     |    |
|-----|-------------------------------------------------------------------------------------|----|
| 1.1 | Block Diagram of MIMO System . . . . .                                              | 6  |
| 1.2 | Diagram to Derive Antenna Correlation . . . . .                                     | 9  |
| 1.3 | Ergodic Capacity of MIMO System . . . . .                                           | 12 |
| 1.4 | 10% Outage Capacity of MIMO System . . . . .                                        | 14 |
| 1.5 | Error Probability vs SNR for Different Diversity Orders $d$ . . . . .               | 16 |
| 2.1 | A Four-State Space-Time Trellis Code, $N_T=2$ . . . . .                             | 22 |
| 2.2 | The Alamouti Scheme . . . . .                                                       | 25 |
| 3.1 | Signal Constellation of the “triple QPSK” . . . . .                                 | 41 |
| 3.2 | BER of the New STBC with $R_2$ and $R_3$ . . . . .                                  | 44 |
| 3.3 | Trellis Diagram of the “triple QPSK” Modulation . . . . .                           | 46 |
| 3.4 | BER of Orthogonal STBC and New STBC, $N_T=3$ . . . . .                              | 47 |
| 3.5 | BER of New STBC and Orthogonal STBC with Same Rate, $N_T=3$ . . . . .               | 48 |
| 3.6 | Performance of the New Full Rate STBC, $N_T=3$ . . . . .                            | 49 |
| 3.7 | BER of Quasi-Orthogonal STBC and New STBC, $N_T = 4$ . . . . .                      | 54 |
| 3.8 | Performance of the New Full Rate STBC, $N_T = 4$ . . . . .                          | 55 |
| 4.1 | Performance of the New STBC with Noisy CSI $\sigma_e^2 = 0.2\%$ , $N_T=3$ . . . . . | 60 |
| 4.2 | Performance of the New STBC with Noisy CSI $\sigma_e^2 = 1\%$ , $N_T=3$ . . . . .   | 60 |
| 4.3 | Performance of the New STBC with Noisy CSI $\sigma_e^2 = 5\%$ , $N_T=3$ . . . . .   | 61 |
| 4.4 | Performance of the New STBC with Noisy CSI $\sigma_e^2 = 0.2\%$ , $N_T=4$ . . . . . | 63 |
| 4.5 | Performance of the New STBC with Noisy CSI $\sigma_e^2 = 1\%$ , $N_T=4$ . . . . .   | 63 |

|     |                                                                                                      |    |
|-----|------------------------------------------------------------------------------------------------------|----|
| 4.6 | $P_b$ affected by Channel Profile, Pilot SNR and Data SNR . . . . .                                  | 74 |
| 4.7 | $P_b$ affected by Pilot SNR and Data SNR . . . . .                                                   | 74 |
| 4.8 | $P_b$ affected by Channel Profile and Data SNR . . . . .                                             | 75 |
| 5.1 | Performance of the STBC Using Differential Detection, QPSK With<br>Three Transmit Antennas . . . . . | 86 |
| 5.2 | Performance of the STBC with Differential Detection, 16-QAM, $N_T=3$                                 | 86 |
| 5.3 | Performance of the Differential STBC with 16-QAM, $N_T = 2,3,4$ . . .                                | 87 |
| 5.4 | Performance of the New STBC using “triple QPSK” with Differential<br>Detection, $N_T=3$ . . . . .    | 89 |
| 5.5 | Performance of the New STBC using “triple QPSK” with Differential<br>Detection, $N_T=4$ . . . . .    | 90 |



# Chapter 1

## Introduction to Multiple Antenna Communications Systems

With rapid expansion of the Internet and development of related services, the Internet has become an indispensable part of daily life creating a need for high speed communication systems. Although wired communication systems have been serving this need, the desire to communicate from anywhere at anytime drives the demand for high speed wireless systems. The proliferation of consumer electronics with the capability to process large amounts of data, such as cell phones with digital camera, wireless home audio/visual networks, wireless local area networks for homes and businesses, etc. also helps to increase the demand for reliable high speed wireless communication systems. As a result, the data rate of wireless communication systems has increased substantially in recent years. To further increase the data rate and improve reliability, we have to overcome the main bottleneck in the wireless communication systems, which usually is the wireless channel.

The wireless channel introduces many challenges for the designer. Two of the primary challenges are the impairments resulting from multipath fading and the Doppler frequency shift, both imposing detrimental effects on the received signal and degrading the performance of the wireless communication system. Diversity techniques are

frequently employed to combat the multipath fading and the Doppler frequency shift effects, thus improving the performance of wireless communication systems [1]. The essence of all diversity techniques is to transmit several replicas of the same signal over several channels, resulting in a significant reduction in the probability that all signals fade simultaneously.

## 1.1 Characteristics of Fading Channel

Many factors in a radio signal propagation influence the characteristics of a wireless channel [2], including multipath propagation, velocity of the mobile, and transmission bandwidth of the signal. The presence of surrounding objects reflecting and scattering in the channel creates a constantly changing environment that dissipates the signal energy in amplitude, phase, and time. These effects result in multiple versions of the transmitted signal to arrive at the receiving antenna, displaced with respect to one another in time and spatial orientation. The relative motion between the base station and the mobile unit results in a random frequency modulation due to a different Doppler shifts on each of the multipath components. The Doppler shift,  $f_d$  is given by

$$f_d = \frac{v}{c/f_c} \cdot \cos(\theta) \quad (1.1)$$

where  $v$  is the velocity of the mobile,  $c = 3 \times 10^8 m/sec$  is the velocity of the light,  $f_c$  is the carrier frequency, and  $\theta$  is the angle between the the direction of the mobile movement and the direction of arrival of the radio wave.

Doppler spread is a measure of the spectral broadening caused by the time rate of change of the mobile radio channel and is defined as the range of frequency over which the received Doppler spectrum is essentially non-zero. When a pure sinusoidal tone of frequency  $f_c$  is transmitted, the received signal spectrum, called the Doppler spectrum, will have components in the range  $f_c - f_d$  to  $f_c + f_d$ , where  $f_d$  is the Doppler shift given by Equation (1.1). If the bandwidth of the baseband signal is

much greater than the Doppler spread, the effects of Doppler spread are negligible at the receiver. Coherence time  $T_c$  is the time domain dual of the Doppler spread and is inversely proportional to the Doppler spread, i.e.  $T_c \approx 1/f_d$ , where  $f_d = v f_c/c$  is the maximum Doppler shift. Coherence time is a statistical measure of the time duration over which the channel impulse response is essentially invariant, and quantifies the similarity of the channel response at different times. If the coherence time is defined as the time over which the time correlation function is above 0.5, then the coherence time is approximately [2]

$$T_c \approx \frac{9}{16\pi f_d} \quad (1.2)$$

The Doppler spread in frequency domain and the coherence time in time domain characterize the time varying nature of the frequency dispersiveness of the channel.

The time dispersiveness properties of wide band multipath channel are most commonly quantified by their mean excess delay,  $\bar{\tau}$  and rms delay spread,  $\sigma_\tau$ . The mean excess delay is the first moment of the power delay profile and is defined as [2]

$$\bar{\tau} = \frac{\sum_k P(\tau_k)\tau_k}{\sum_k P(\tau_k)} \quad (1.3)$$

where  $\tau_k$  is the delay of the  $k$ th multipath and  $P(\tau_k)$  is the power of the  $k$ th multipath. The rms delay spread is the square root of the second central moment of the power delay profile and is defined as [2]

$$\sigma_\tau = \sqrt{\bar{\tau}^2 - (\bar{\tau})^2} \quad (1.4)$$

where

$$\bar{\tau}^2 = \frac{\sum_k P(\tau_k)\tau_k^2}{\sum_k P(\tau_k)} \quad (1.5)$$

The coherence bandwidth is a defined relation from the rms delay spread. Coherence bandwidth is a statistical measure of the range of frequencies over which the channel can be considered correlated. If the coherence bandwidth is defined as the bandwidth

over which the frequency correlation function is above 0.9, the coherence bandwidth,  $B_c$  is approximately [2]

$$B_c \approx \frac{1}{50\sigma_\tau} \quad (1.6)$$

## 1.2 Diversity Techniques

Conventional diversity techniques include time diversity, frequency diversity, polarization diversity, and space diversity. In time diversity, the same information signal is transmitted in several time slots, in such a way that the successive time slots are separated by more than the coherence time of the channel [1]. In time diversity signals with the same information content pass through channel realizations that are independent of each other and thus the received signals in each time slot experience independent fadings. The replicas of the transmit signal are provided to the receiver in the form of redundancy in temporal domain. Generally, the forward error control coding in conjunction with time interleaving is considered as one form of time diversity.

Frequency diversity techniques involve transmitting the same information over several carrier frequencies. The separation of adjacent carriers is selected to be no less than the coherent bandwidth of the channel [1], which guarantees that the radio waves transmitted on different carrier frequencies experience independent fading. The replicas of the transmitted signal are delivered to the receiver as redundancy in the frequency domain. In TDMA systems, frequency diversity is obtained using a non-linear equalizer when multipath delays are a significant fraction of symbol interval. In a direct sequence CDMA system, the RAKE receiver is used to obtain frequency diversity.

It has been shown [3] that signals received on two orthogonal polarizations in wireless communication systems exhibit uncorrelated fading statistics. Thus the signals received on vertical and horizontal polarization can be combined together, and the combined signal achieves diversity gain in a fading channel. However, in this case only

two diversity branches are available since there are only two orthogonal polarizations.

Space diversity techniques employ multiple transmit and receive antennas. The antennas are separated far enough that the signals have significantly different propagation paths and hence experience independent fading. Space diversity techniques are preferred over time or frequency diversity because they do not incur extra time or bandwidth, which are valuable resources in wireless communication systems. Sometimes polarization diversity can be regarded as a special case of space diversity techniques. An adaptive antenna array is an example of conventional space diversity, where the intelligence of the multi-antenna algorithm lies in the selection of the weights on each signal path for signal combining at the receiver and beamforming at the transmitter. In the development of space-time coding for multiple transmit and receive antenna systems, which are generally known as multiple input, multiple output (MIMO) systems, the emphasis is to find encoding and decoding algorithms for the transceiver. Space-time codes are implemented by employing forward error control coding techniques across the time and space domains. The resulting signal is transmitted over  $N_T$  transmit antennas.

### 1.3 The MIMO System

Let's consider a MIMO wireless communication system that has  $N_T$  transmit and  $N_R$  receive antennas. The block diagram of this system is shown in Figure 1.1. The information source is a bit stream that is fed to the transmitter block, which consists of data processing including data compression and forward error control encoding, and space time encoder/modulator. The space time code (STC) function produces several separate symbol streams that range from independent, partially redundant to fully redundant [4], and each stream is sent to one of the transmit antennas. After frequency up conversion, filtering and amplification, the signals are transmitted over the wireless channel.

At the receiver, the signals are received by all  $N_R$  antennas. The received signal

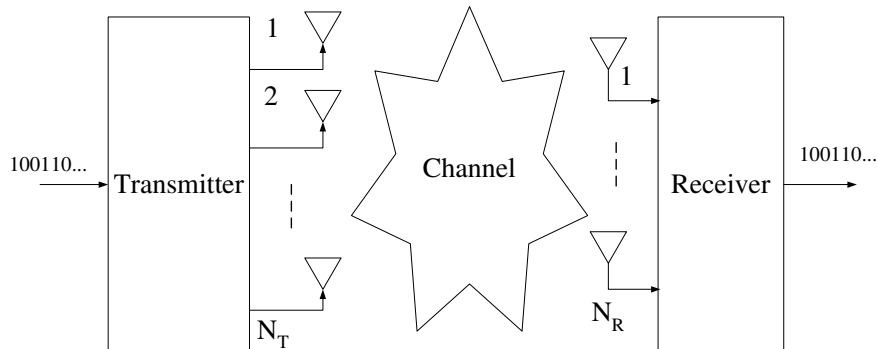


Figure 1.1: Block Diagram of MIMO System

at each receive antenna is a linear superposition of the signals received from all  $N_T$  transmit antennas plus noise. After amplification, filtering and frequency down conversion, the space-time decoder combines the received signals from the  $N_R$  receive antennas into a single symbol stream and detects the transmitted bit streams by data processing including forward error decoding and data de-compression.

The mathematical model for the lowpass equivalent of the MIMO system shown in Figure 1.1, at time slot  $t$ , can be given by [5]

$$r_t^m = \sqrt{\frac{\rho}{N_T}} \sum_{n=1}^{N_T} \alpha_{m,n} c_t^n + \eta_t^m, \quad 1 \leq m \leq N_R, 1 \leq t \leq l \quad (1.7)$$

where  $r_t^m$  denotes the received signal at antenna  $m$ ,  $\alpha_{m,n}$  is the channel coefficient from transmit antenna  $n$  to receive antenna  $m$ ,  $c_t^n, n = 1, 2, \dots, N_T$  is the space-time encoded signal transmitted from the  $n$ th transmit antenna at time slot  $t$ ,  $\eta_t^m$  is noise

sample at receive antenna  $m$  at time  $t$  being modeled as independent samples of circular complex Gaussian random variable with zero mean and variance  $N_0/2$  per complex dimension,  $\rho$  is the signal to noise ratio (SNR) at the receiver, and  $l$  is the number of symbols in a transmission frame. In equation (1.7), we assume that  $N_0 = 1$  and we use this assumption in most places of this dissertation.

The channel coefficient  $\alpha_{m,n}$  is a complex Gaussian random variable with zero mean and unit variance. The envelope of  $\alpha_{m,n}$  is Rayleigh distributed and the resulting channel model is referred to as a Rayleigh fading channel, which is the fading model used in this dissertation. When the mean of channel coefficient  $\alpha_{m,n}$  is not zero, the envelope of  $\alpha_{m,n}$  is Ricean distributed and the resulting channel is generally referred to as a Ricean channel model.

The channel is assumed to be quasi-static, i.e., the channel coefficients change once per frame, and memoryless, i.e. the channel coefficients on one frame are independent from those on other frames.

The constellation energy used by the communication scheme is normalized to unity at the transmitter. When the channel coefficients have unit variance, the variable  $\rho$  in Equation (1.7) is indeed the SNR at the receiver. The average energy of the transmitted symbols from each antenna is normalized such that the total transmit power is equal to that of a single transmit antenna system.

## 1.4 The MIMO Channel

In the MIMO system we considered in Figure 1.1, which has  $N_T$  transmit and  $N_R$  receive antennas, there are  $N_T N_R$  single input single output (SISO) channels formed by each transmit and receive antenna pair. Their channel coefficients can be represented by  $\alpha_{m,n}, m = 1, 2, \dots, N_R; n = 1, 2, \dots, N_T$ , which is the SISO channel from the  $n$ th transmit antenna to the  $m$ th receive antenna. The composite MIMO channel coefficients can be expressed by the  $N_R \times N_T$  matrix

$$\mathbf{H} = \begin{pmatrix} \alpha_{1,1} & \alpha_{1,2} & \cdots & \alpha_{1,N_T} \\ \alpha_{2,1} & \alpha_{2,2} & \cdots & \alpha_{2,N_T} \\ \vdots & \vdots & \ddots & \vdots \\ \alpha_{N_R,1} & \alpha_{N_R,2} & \cdots & \alpha_{N_R,N_T} \end{pmatrix} \quad (1.8)$$

In this study, this fading channel,  $\mathbf{H}$  is Rayleigh channel and quasi-static and memoryless, i.e.  $\mathbf{H}$  stays constant during one transmission frame and changes independently from one frame to the next.

The elements  $\alpha_{m,n}$  in the channel matrix  $\mathbf{H}$  in Equation (1.8) are independent and identically distributed (i.i.d.) random variables. In practical MIMO systems, there are correlations among the elements in the channel matrix  $\mathbf{H}$ , which are influenced by the spacing between antennas, angle of arrival, angle of departure, power azimuth spectrum and power delay profile in the transmitter and receivers. A diagram used to derive antenna correlation in a MIMO system given by [4] is illustrated in Figure 1.2. In this diagram, the  $i$ th ray from transmit antenna  $n$  to receive antenna  $m$  going through one single bounce is shown. If the base station antenna is higher than its surroundings, it is often the case that only waves transmitted within azimuth angle  $\theta \in [\Theta - \Delta, \Theta + \Delta]$  can reach the mobile [4]. Then,  $\Theta$  is defined as the angle of arrival and  $\Delta$  is defined as angle spread. Let us denote the distribution of scattering in azimuth angle, as seen by the base station, by  $p(\theta)$ . This function  $p(\theta)$  is referred to as a power azimuth spectrum. The power delay profile is the power distribution in the delay time.

Thus, when all these factors are taken into account, the channel matrix can be expressed by [4]

$$\mathbf{H}_{general} = (\mathbf{R}_{rx})^{1/2} \mathbf{H} (\mathbf{R}_{tx})^{1/2} \quad (1.9)$$

where  $\mathbf{H}_{general}$  is the channel matrix with all factors modeled,  $\mathbf{R}_{rx}$  denotes the antenna correlation matrix at the receiver and  $\mathbf{R}_{tx}$  denotes the antenna correlation matrix at the transmitter. In this work, only channel matrix  $\mathbf{H}$  with i.i.d. elements are

considered, in which case  $\mathbf{R}_{\mathbf{r}\mathbf{x}}$  and  $\mathbf{R}_{\mathbf{t}\mathbf{x}}$  are identity matrices.

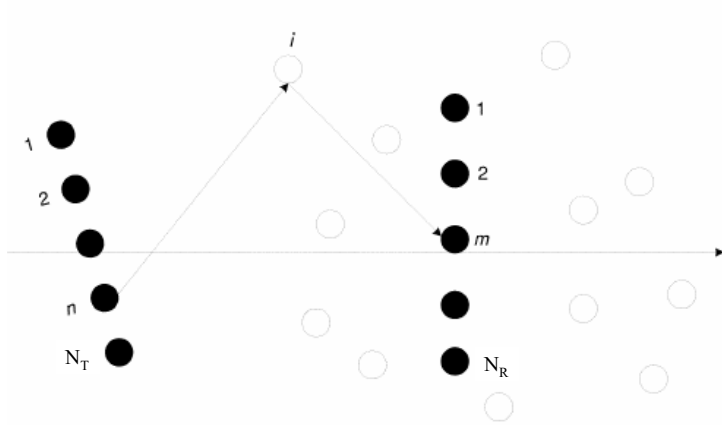


Figure 1.2: Diagram to Derive Antenna Correlation

In matrix form, the received signal at antenna  $m$  at time slot  $t$  given in Equation (1.7) can be written as

$$\mathbf{r}_t = \sqrt{\frac{\rho}{N_T}} \mathbf{c}_t \mathbf{H}_t^T + \mathbf{n}_t \quad (1.10)$$

where  $\mathbf{r}_t$  is  $1 \times N_R$ ,  $\mathbf{H}_t^T$  is a transpose of the  $N_R \times N_T$  complex channel matrix  $\mathbf{H}_t$ ,  $\mathbf{c}_t$  is the  $1 \times N_T$  transmit signal vector, and  $\mathbf{n}_t$  is a circular  $1 \times N_R$  complex random Gaussian noise vector.

## 1.5 Capacity of the MIMO Channel

In general, there are two notions of capacity for fading channels; ergodic capacity and outage capacity [6], [7], corresponding to the mean and tail behavior of the mutual information between the input and output of the channel. It has been shown [6], [8]

that the capacity of wireless communication systems can be significantly increased by using multiple transmit and receive antenna. We assume that the realization of the random channel coefficient matrix  $\mathbf{H}$ , i.e. the channel state information (CSI) is known at the receiver but not at the transmitter. Generally the receiver can obtain the CSI through pilot signal or known training signals sent by the transmitter. This scenario is close to the way wireless communication systems work in practice. It is harder for the transmitter than for the receiver to have the CSI since the transmitter obtains the CSI via a feedback channel from the receiver. The feedback channel usually consumes extra bandwidth, time, and power, which are valuable resources. If the transmit codewords span an infinite number of independently fading blocks, the Shannon capacity, also known as ergodic capacity, can be achieved by choosing the transmit signal  $\mathbf{c}$  to be circularly symmetric complex Gaussian vector. Assuming that the transmitted signal vector is composed of  $N_T$  statistically independent equal power components each with a Gaussian distribution, the received signal is linearly related to the transmitted signal as represented by Equation (1.7) and (1.10). We assume that  $E\{\mathbf{nn}^H\} = \mathbf{I}_{N_R}$ , where  $E()$  stands for the expectation, that is, the noises corrupting the different receivers are independent. The transmitter is constrained in its total power, which is normalized to 1,

$$E\{\mathbf{c}^H \mathbf{c}\} \leq 1 \tag{1.11}$$

Equivalently, since  $\mathbf{c}^H \mathbf{c} = tr(\mathbf{c}\mathbf{c}^H)$ , where  $tr()$  is the trace of a matrix, and expectation and trace commute,

$$tr(E\{\mathbf{c}\mathbf{c}^H\}) \leq 1 \tag{1.12}$$

Since the receiver knows the realization of  $\mathbf{H}$ , the channel output is the pair  $(\mathbf{r}, \mathbf{H}) = (\sqrt{\frac{\rho}{N_T}} \mathbf{c}\mathbf{H}^T, \mathbf{H})$ . The mutual information between the input and output is

[6]

$$\begin{aligned}
I(\mathbf{c}; \mathbf{r}) &= I(\mathbf{c}; (\mathbf{r}, \mathbf{H})) \\
&= I(\mathbf{c}; \mathbf{H}) + I(\mathbf{c}; \mathbf{r}|\mathbf{H})
\end{aligned} \tag{1.13}$$

which can be further simplified to

$$\begin{aligned}
I(\mathbf{c}; \mathbf{r}) &= I(\mathbf{c}; \mathbf{r}|\mathbf{H}) \\
&= E_{\mathbf{H}}\{I(\mathbf{c}; \mathbf{r}|\mathbf{H} = H)\}
\end{aligned} \tag{1.14}$$

where matrix  $H$  is a realization of random matrix  $\mathbf{H}$ . Another way to calculate the mutual information between  $\mathbf{c}$  and  $\mathbf{r}$  is

$$\begin{aligned}
I(\mathbf{c}; \mathbf{r}) &= \mathcal{H}(\mathbf{r}) - \mathcal{H}(\mathbf{r}|\mathbf{c}) \\
&= \mathcal{H}(\mathbf{r}) - \mathcal{H}(\mathbf{n})
\end{aligned} \tag{1.15}$$

where  $\mathcal{H}(\cdot)$  is the entropy. So maximizing  $I(\mathbf{c}; \mathbf{r})$  is equivalent to maximizing  $\mathcal{H}(\mathbf{r})$ . If  $\mathbf{c}$  is zero mean with covariance matrix  $E\{\mathbf{c}\mathbf{c}^H\} = Q$ , then  $\mathbf{r}$  is zero mean with covariance matrix  $E\{\mathbf{r}\mathbf{r}^H\} = HQH^H + I_{N_R}$  [6],  $\mathcal{H}(\mathbf{r})$  is the largest when  $\mathbf{r}$  is circularly symmetric complex Gaussian, which is the case when  $\mathbf{c}$  is circularly symmetric complex Gaussian. So we will focus on the circularly symmetric complex Gaussian  $\mathbf{c}$ , in which the mutual information between  $\mathbf{c}$  and  $\mathbf{r}$  is maximized and given by [6]

$$\begin{aligned}
\max\{I(\mathbf{c}; \mathbf{r})\} &= \Psi(Q, H) \\
&= \log [\det (I_{N_R} + HQH^H)]
\end{aligned} \tag{1.16}$$

Thus, we need to maximize

$$\begin{aligned}
\Psi(Q) &= E_H\{\Psi(Q, \mathbf{H})\} \\
&= E_H\{\log [\det (I_{N_R} + \mathbf{H}Q\mathbf{H}^H)]\}
\end{aligned} \tag{1.17}$$

over all possible choices of covariance matrix  $Q$  subject to  $tr(Q) \leq 1$  [6]. The optimal  $Q$  must be in the form of  $\kappa I$ , where  $\kappa$  is constant and  $I$  is identity matrix. It is clear that the maximum is obtained when  $\kappa$  is the largest possible, which is  $\rho/N_T$ . Therefore, the ergodic capacity of the fading channel is calculated and expressed as [6], [7]

$$C = E \left\{ \log \left[ \det \left( \mathbf{I}_{N_R} + \frac{\rho}{N_T} \mathbf{H}\mathbf{H}^H \right) \right] \right\} \quad (1.18)$$

where  $\mathbf{I}_{N_R}$  is a  $N_R \times N_R$  identity matrix,  $\rho$  is the SNR,  $()^H$  is the Hermitian transpose on matrix,  $C$  is the channel capacity, and the unit of  $C$  is bits per second per Hz.

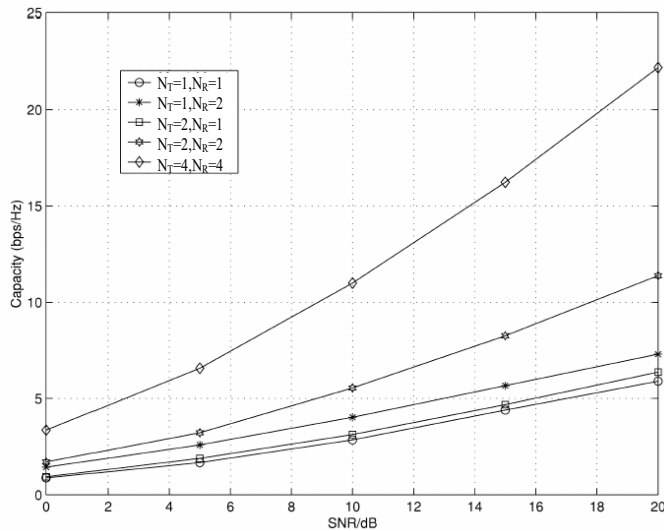


Figure 1.3: Ergodic Capacity of MIMO System

The ergodic capacity  $C$  of Rayleigh MIMO channel with several antenna configurations versus SNR are plotted in Figure 1.3 [9]. The number of antennas at the

transmitter and receiver ranges from 1 to 4. As expected, the ergodic capacity of a MIMO channel increases as the SNR increases. At a given SNR, the ergodic capacity of the MIMO channel increases when the number of antennas at either the transmitter or the receiver increases. It is noted that the ergodic capacity of a single input multiple output ( $1 \times N_R$ ) channel is greater than the ergodic capacity of a corresponding multiple input and single output ( $N_T \times 1$ ) channel for the same number of antennas. This is due to the fact that in the absence of CSI at the transmitter, the multiple input and single output channels do not offer as much transmit diversity gain as the receive diversity offered by the single input and multiple output channels.

At high SNR, the ergodic capacity of the fading channel is given as [6]

$$C = \min(N_R, N_T) \cdot \log(\text{SNR}) + o(1) \quad (1.19)$$

where the unit of  $C$  is bits/sec/Hz and  $o(1)$  represents a term independent of SNR. This clearly shows that the ergodic capacity of the MIMO channel is linearly increasing with the minimum of the number of transmit and receive antennas. This potential gain in capacity has motivated a lot of research to design codes to achieve this gain.

In cases when low latency is required, and the transmit codeword is of limited length, the Shannon capacity is zero, because there is always a nonzero probability that the given channel realization will not support the rate no matter how small the rate we want to communicate. Therefore another measure of channel capacity is needed when the codewords are of short length. We define the  $q\%$  outage capacity  $C_{out,q}$  as the information rate that is guaranteed for  $(100 - q)\%$  of the channel realizations [7] and it can be described as

$$\Pr(I(input; output) \leq C_{out,q}) = q\% \quad (1.20)$$

where  $I(input; output)$  stands for the mutual information between the input and output of the channel per channel use.

The outage capacity of several MIMO configuration as function of the SNR is shown in Figure 1.4, where the outage is 10% [9]. The outage capacity increases as the SNR increases. At a certain SNR, the outage capacity increases when the number of antennas at either the transmitter or the receiver increases. As a matter of fact, the behavior of 10% outage as a function of SNR,  $N_T$ , and  $N_R$  is almost identical to the behavior of the ergodic capacity.

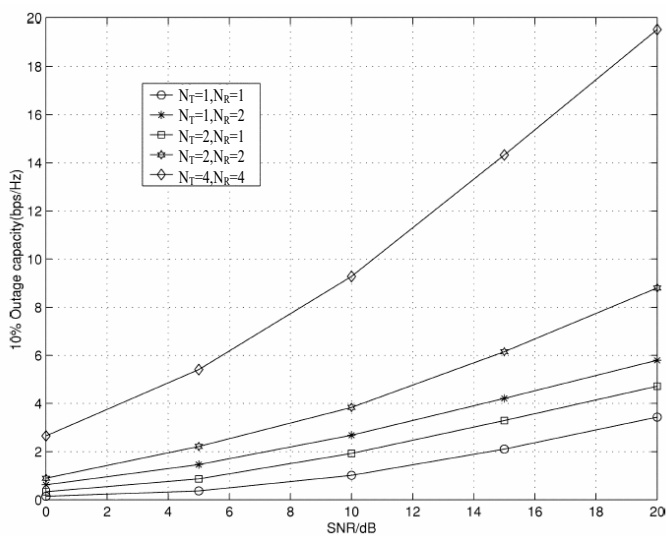


Figure 1.4: 10% Outage Capacity of MIMO System

## 1.6 Diversity and Multiplexing Gain

The diversity order or diversity gain is defined as the negative of the slope of the logarithm of the bit error rate (BER) versus the logarithm of the SNR curve [10] and

expressed by

$$d = - \lim_{SNR \rightarrow \infty} \frac{\log(P_e(SNR))}{\log(SNR)} \quad (1.21)$$

where  $P_e$  is the probability of error. This leads to the general relationship between probability of error and the diversity order in wireless communication system. A more explicit formula of probability of error as function of SNR and diversity order  $d$  is given in [11]

$$P_e \leq \binom{2d-1}{d} \frac{1}{(4 \cdot SNR)^d} \quad (1.22)$$

where  $P_e$  is probability of error. In particular, the error probability decreases as the  $d$ th power of SNR, corresponding to a slope of  $-d$  in the error probability vs SNR curve in dB/dB scale. The probability of error vs SNR with several diversity orders  $d$  as specified in Equation (1.22) are illustrated in Figure 1.5.

The BER achieved by a space-time code with higher diversity order decreases faster than the BER of a space-time code with lower diversity order when the SNR increases. The maximum diversity order a MIMO system with  $N_T$  transmit and  $N_R$  receive antennas can offer is  $N_T N_R$  [5], which is the total number of fading gains that one can average over. On the other hand, the fading in the channel can be beneficial in the MIMO system through increasing the degrees of freedom available to communicate [10]. If the path gains between individual transmit and receive antenna pairs fade independently, the channel matrix  $\mathbf{H}$  is well conditioned with high probability, thus multiple parallel spatial channels are created [10]. By transmitting independent information in parallel through these spatial channels, the data rate can be increased, which is called spatial multiplexing [12]. Let  $R$  in b/s/Hz be the rate of the code. A space-time coding scheme is said to achieve spatial multiplexing gain  $r$  if

$$r = \lim_{SNR \rightarrow \infty} \frac{\log(R(SNR))}{\log(SNR)} \quad (1.23)$$

The maximum value of  $r$  is  $\min(N_T, N_R)$ , which is the number of degrees of freedom.

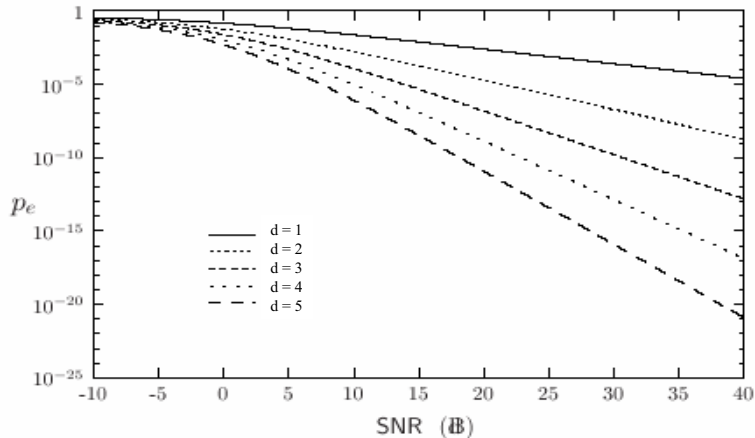


Figure 1.5: Error Probability vs SNR for Different Diversity Orders  $d$

A MIMO system can provide both diversity and spatial multiplexing gains. Maximizing one type of gain may not necessarily maximize the other. Given a MIMO channel, both gains can be simultaneously obtained, but there is a fundamental tradeoff between the diversity and multiplexing gain. Higher spatial multiplexing gain comes at the price of lower diversity gain. Consider a duration of  $l$  symbols. As long as the block length  $l \geq N_R + N_T - 1$ , the optimal diversity gain  $d^*(r)$  achievable by any coding scheme of block length  $l$  and multiplexing gain  $r$  is precisely  $(N_R - r)(N_T - r)$  [10]. This suggests that there are  $r$  transmit and  $r$  receive antennas that are used for multiplexing, and the remaining  $N_T - r$  transmit and  $N_R - r$  receive antennas that provide diversity in the MIMO system with  $N_T$  transmit and  $N_R$  receive antennas. It is noticed that the optimal tradeoff does not depend on  $l$  as long as  $l \geq N_R + N_T - 1$ .

# Chapter 2

## Space Time Codes

As stated in chapter 1, the capacity of a fading channel can be increased dramatically with the employment of multiple transmit and receive antennas. The capacity of the MIMO channel increases linearly with  $\min(N_T, N_R)$  at high SNR values. This capacity increase is achieved without increasing the total transmit power or the bandwidth. This shows that the spatial dimension is effectively another resource that we can exploit in wireless communication systems design. To reach this goal, we need to design channel codes that encode across both time and space, i.e. the multiple transmit antennas. This motivates the development of space-time codes.

### 2.1 The Design Criterion for Space-Time Codes

Generally speaking, the received signal can be modeled by Equation (1.7) in a MIMO system. When the CSI,  $\alpha_{m,n}, 1 \leq m \leq N_R; 1 \leq n \leq N_T$ , is available at the receiver, the maximum likelihood detector computes the decision metric

$$\sum_{t=1}^l \sum_{m=1}^{N_R} \left| r_t^m - \sqrt{\frac{\rho}{N_T}} \sum_{n=1}^{N_T} \alpha_{m,n} \cdot c_t^n \right|^2 \quad (2.1)$$

over all codewords and decides in favor of the codeword that minimizes this metric [5]. Assuming that the code word  $\mathbf{c} = c_1^1 c_1^2 \cdots c_1^{N_T} c_2^1 c_2^2 \cdots c_2^{N_T} \cdots c_l^1 c_l^2 \cdots c_l^{N_T}$  is transmitted, an error occurs when the maximum-likelihood receiver decides in favor of another code word  $\mathbf{e} = e_1^1 e_1^2 \cdots e_1^{N_T} e_2^1 e_2^2 \cdots e_2^{N_T} \cdots e_l^1 e_l^2 \cdots e_l^{N_T}$ . With the CSI available to the receiver, the probability of transmitting  $c$  and deciding in favor of  $e$  by the decoder, which is referred to as pairwise error probability, can be bounded by [13]

$$\begin{aligned} \Pr(\mathbf{c} \rightarrow \mathbf{e} | \alpha_{m,n}, m = 1, 2, \dots, N_R, n = 1, 2, \dots, N_T) \\ \leq \exp(-d^2(\mathbf{c}, \mathbf{e})E_s/4N_0) \end{aligned} \quad (2.2)$$

where  $E_s$  is the symbol energy,  $N_0/2$  is the noise variance per dimension, and

$$d^2(\mathbf{c}, \mathbf{e}) = \sum_{m=1}^{N_R} \sum_{t=1}^l \left| \sum_{n=1}^{N_T} \alpha_{m,n} (c_t^n - e_t^n) \right|^2 \quad (2.3)$$

where  $l$  is the number of symbols in a frame. Setting  $\Omega_m = (\alpha_{m,1}, \alpha_{m,2}, \dots, \alpha_{m,N_T})$ , after some mathematical manipulations, Equation (2.3) can be rewritten as

$$d^2(\mathbf{c}, \mathbf{e}) = \sum_{m=1}^{N_R} \Omega_m A \Omega_m^* \quad (2.4)$$

where

$$A_{m,n} = \sum_{t=1}^l (c_t^m - e_t^m) \overline{(c_t^n - e_t^n)} \quad (2.5)$$

Thus, the pairwise error probability in Equation (2.2) can be expressed as

$$\begin{aligned} \Pr(\mathbf{c} \rightarrow \mathbf{e} | \alpha_{m,n}, m = 1, 2, \dots, N_R, n = 1, 2, \dots, N_T) \\ \leq \prod_{m=1}^{N_R} \exp(-\Omega_m A \Omega_m^* E_s/4N_0) \end{aligned} \quad (2.6)$$

It is apparent that matrix  $\mathbf{A}$  is function of codewords  $\mathbf{c}$  and  $\mathbf{e}$ . Since  $\mathbf{A}$  is

Hermitian, there exists a unitary matrix  $\mathbf{V}$  and a real diagonal matrix  $\mathbf{D}_A$  such that  $\mathbf{VAV}^H = \mathbf{D}_A$  [13]. Furthermore, the diagonal elements of  $\mathbf{D}_A$  are eigenvalues  $\lambda_n, n = 1, 2, \dots, N_T$  of  $\mathbf{A}$ , counting multiplicities. By construction, a difference matrix between codewords  $\mathbf{c}$  and  $\mathbf{e}$  can be expressed as

$$\mathbf{B}(\mathbf{c}, \mathbf{e}) = \begin{pmatrix} e_1^1 - c_1^1 & e_2^1 - c_2^1 & \cdots & e_l^1 - c_l^1 \\ e_1^2 - c_1^2 & e_2^2 - c_2^2 & \cdots & e_l^2 - c_l^2 \\ \vdots & \vdots & \ddots & \vdots \\ e_1^{N_T} - c_1^{N_T} & e_2^{N_T} - c_2^{N_T} & \cdots & e_l^{N_T} - c_l^{N_T} \end{pmatrix} \quad (2.7)$$

Clearly matrix  $\mathbf{B}$  is a square root of matrix  $\mathbf{A}$ , i.e.  $\mathbf{A} = \mathbf{B}\mathbf{B}^H$ . The eigenvalues of matrix  $\mathbf{A}(\mathbf{c}, \mathbf{e})$  are non-negative real numbers.

Next assume that the elements in the channel matrix  $\mathbf{H}$  are complex Gaussian random variables with mean  $E\{\alpha_{m,n}\}$ . Let  $\mathbf{K}^m = (E\{\alpha_{m,1}\}, E\{\alpha_{m,2}\}, \dots, E\{\alpha_{m,N_T}\})$  be the mean vector. In a Rician fading channel, the mean  $E\{\alpha_{m,n}\}$  does not equal to zero. Let  $(\tilde{\alpha}_{1,n}, \tilde{\alpha}_{2,n}, \dots, \tilde{\alpha}_{m,N_T}) = \Omega_m V^*$ , then we have the relationship

$$\Omega_m A(\mathbf{c}, \mathbf{e}) \Omega_m^* = \sum_{i=1}^{N_T} \lambda_i |\tilde{\alpha}_{m,n}|^2 \quad (2.8)$$

Since  $V$  is unitary and  $\tilde{\alpha}_{m,n}$  are independent complex Gaussian random variable,  $|\tilde{\alpha}_{m,n}|$  are independent Rician distributed random variable with probability density function

$$p(|\tilde{\alpha}_{m,n}|) = 2|\tilde{\alpha}_{m,n}| \exp(-|\tilde{\alpha}_{m,n}|^2 - K_{m,n}) I_0(2|\tilde{\alpha}_{m,n}| \sqrt{K_{m,n}}) \quad (2.9)$$

for  $|\tilde{\alpha}_{m,n}| \geq 0$ , where  $I_0$  is the zero order modified Bessel function of the first kind. Thus to compute an upper bound on the probability of bit error we simply average

$$\prod_{n=1}^{N_R} \exp(-(E_s/4N_0) \sum_{n=1}^{N_T} |\tilde{\alpha}_{m,n}|^2) \quad (2.10)$$

with respect to independent Rician distribution  $|\tilde{\alpha}_{m,n}|$ . After some mathematical

manipulation, we get the pairwise error probability bound under Rician channel as [13]

$$\Pr(\mathbf{c} \rightarrow \mathbf{e}) \leq \prod_{m=1}^{N_R} \left( \prod_{n=1}^{N_T} \frac{1}{1 + \frac{E_s}{4N_0} \lambda_n} \exp \left( -\frac{K_{m,n} \frac{E_s}{4N_0} \lambda_n}{1 + \frac{E_s}{4N_0} \lambda_n} \right) \right) \quad (2.11)$$

When the mean of channel coefficients  $E\{\alpha_{m,n}\}$  equal to zero for all  $m$  and  $n$ , the Rician fading channel becomes the Rayleigh fading channel. The inequality expressed by Equation (2.11) can be written as the following equation and we get the upper bound of the pairwise error probability under the Rayleigh fading channel as

$$\Pr(\mathbf{c} \rightarrow \mathbf{e}) \leq \left( \frac{1}{\prod_{i=1}^{N_T} (1 + \lambda_i E_s / 4N_0)} \right)^{N_R} \quad (2.12)$$

Let  $r$  denote the rank of matrix  $\mathbf{A}$ . Then the kernel of  $\mathbf{A}$  has dimension  $N_T - r$  and exactly  $N_T - r$  eigenvalues of  $\mathbf{A}$  are zero. If the non-zero eigenvalues of matrix  $\mathbf{A}$  are  $\lambda_1, \lambda_2, \dots, \lambda_r$ , then the pairwise error probability can be simplified to [13]

$$\Pr(\mathbf{c} \rightarrow \mathbf{e}) \leq \left( \prod_{i=1}^r \lambda_i \right)^{-N_R} (E_s / 4N_0)^{-rN_R} \quad (2.13)$$

So a diversity gain of  $rN_R$  and a coding gain of  $(\lambda_1 \lambda_2 \dots \lambda_r)^{1/r}$  is achieved. It is clear that the ranks of matrices  $\mathbf{A}(\mathbf{c}, \mathbf{e})$  and  $\mathbf{B}(\mathbf{c}, \mathbf{e})$  are the same, which provides a link between the rank of matrix  $\mathbf{B}$  and the diversity order of the space time code.

As explained before in Equation (1.21) the diversity gain is the power of the SNR in the denominator of the expression for the pairwise error probability as specified in Equation (2.13). The coding gain is an approximate measure of the gain compared to an uncoded system operating with the same diversity gain. From the analysis above, we arrive at the following design criteria [13]:

The Rank Criterion: In order to achieve the maximum diversity  $N_T N_R$ , the matrix  $\mathbf{B}(\mathbf{c}, \mathbf{e})$  has to be full rank for any codewords  $\mathbf{c}$  and  $\mathbf{e}$  in the code book. If matrix  $\mathbf{B}(\mathbf{c}, \mathbf{e})$  has minimum rank  $r$  over the set of two tuples of distinct codewords, then a

diversity of  $rN_R$  is achieved.

The Determinant Criterion: Assume that a diversity order of  $rN_R$  is achieved. The minimum of the  $r$ th root of the product of all non-zero eigenvalues of matrix  $\mathbf{A}(\mathbf{c}, \mathbf{e})$  over all possible pairs of distinct code words  $\mathbf{c}$  and  $\mathbf{e}$  corresponds to the coding gain, where  $r$  is the rank of matrix  $\mathbf{A}(\mathbf{c}, \mathbf{e})$ . When a diversity gain of  $rN_R$  is achieved, then the minimum of the determinant of  $\mathbf{A}(\mathbf{c}, \mathbf{e})$  taken over all pairs of codewords  $\mathbf{c}$  and  $\mathbf{e}$  must be maximized.

One of the promising means to achieve high diversity gain and spectral efficiency in the MIMO wireless communication system is to use space-time coding technique [5], [13], [14]. Space-time trellis and block codes are two major classes of space-time codes. The orthogonal space time block codes satisfy the Rank Criterion and achieve full diversity. The space time trellis codes that satisfy Rank Criterion, also satisfy Determinant Criterion, and achieve both diversity and coding gain at the price of higher complexity than the space time block codes.

## 2.2 Space-Time Trellis Code

We proceed to design trellis codes for wireless communication systems that employ  $N_T$  transmit and  $N_R$  receive antennas, commonly known as space time trellis codes, using the criteria in the previous section. We assume that a four state trellis is used whose trellis diagram is shown in Figure 2.1 [13]. In this example of a space-time trellis code, the number of transmit antennas  $N_T = 2$  and the number of receive antennas  $N_R$  can be any integer. The encoding starts with the initial state  $S_0$ . The information symbols, generated from information bits, determine state transitions, and the two encoded symbols to be transmitted from the two transmit antennas simultaneously are shown in Figure 2.1. For instance, if the incoming sequence of symbols from 4-PSK modulation is  $2, 1, 2, 3, 0, 0, 1, 3, 2, \dots$ , then the next state is  $S_2$  because the first symbol is 2. The two symbols 02 will be the symbols transmitted from antenna 1 and 2, respectively, according to the trellis diagram. The second

input symbol is 1 so the third state is 1. The transition on the trellis is from  $S_2$  to  $S_1$ , and the symbols 21 are transmitted from antenna 1 and 2 on the second symbol slot, respectively. The encoding process keeps on going like this and finally the sequence of signal transmitted by the first antenna is 0, 2, 1, 2, 3, 0, 0, 1, 3,  $\dots$ , and the signal sequence transmitted from the second antenna is 2, 1, 2, 3, 0, 0, 1, 3, 2,  $\dots$ .

Once all of the information symbols are encoded, the trellis is terminated to complete each frame of symbols. We observe that two bits of information are transmitted per use of the channel, thus resulting in a spectral efficiency of 2 bits/sec/Hz. In general, to obtain a spectral efficiency of  $\xi$  bits/sec/Hz, we need to use a trellis with  $2^\xi$  branches emanating from each state.

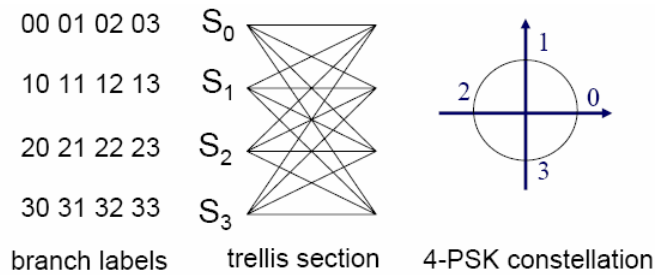


Figure 2.1: A Four-State Space-Time Trellis Code,  $N_T=2$

This process is a simple extension of trellis-coded modulation. Instead of using a trellis which determines only a single symbol to be transmitted for each trellis section, each branch is associated with multiple symbols that are to be transmitted from the multiple antennas.

The maximum likelihood decoding of the space time trellis code is accomplished

by implementing Equation (2.1), where we assume that the CSI, i.e. the values of  $\alpha_{m,n}$  for  $1 \leq m \leq N_R$  and  $1 \leq n \leq N_T$  are known at the receiver. By the way of construction, the space time trellis codes are paths through the code trellis. Therefore, the minimization of the decision rule in Equation (2.1) is equivalent to the process of finding a path through the space time code trellis with the minimum Euclidean distance from the received signal sequence. Also, observing that the metric is additive at each time step, it is clear that one can use the well known Viterbi algorithm for efficient decoding.

In particular, at time  $t = 0$ , we assume that the encoder is in state 0. We extend the paths emanating from this state, and record the value of the path metric computed using

$$\sum_{m=1}^{N_R} \left| r_1^m - \sqrt{\frac{\rho}{N_T}} \sum_{n=1}^{N_T} \alpha_{m,n} \cdot c_1^n \right|^2 \quad (2.14)$$

At time  $t$ , we have one path through the trellis for each state of the encoder together with corresponding value of the accumulated path metric for each state. To extend each of these paths by one more step, for each state, at time  $t+1$ , all paths that merge with that particular state are considered as candidates. The possible path metrics are computed by adding

$$\sum_{m=1}^{N_R} \left| r_{t+1}^m - \sqrt{\frac{\rho}{N_T}} \sum_{n=1}^{N_T} \alpha_{m,n} \cdot c_{t+1}^n \right|^2 \quad (2.15)$$

to the current path metrics, and all of these extensions except the one with the minimum accumulated path metric are discarded, and the time index is incremented by one more step. Typically the trellis is terminated in the final steps back to the state  $S_0$ . Therefore for these steps, only extensions of the paths that lead to trellis termination are considered, and at the end of the frame, the path through the trellis that is closest to the received signal sequence is declared as the maximum likelihood codeword.

Space-time trellis codes of 8 state and 16 state using 4-PSK modulation, which

achieves 2 bits/sec/Hz, for  $N_T = 2$  transmit antennas are presented in [13]. A space time trellis code using 8-PSK modulation to achieve a higher spectral efficiency is also proposed in [13].

At a given diversity gain and data rate, the trellis code constructed for space time applications here performs better than the block coded modulation designed for space time application at the price of higher complexity. When the number of transmit antennas is fixed, the decoding complexity of a space-time trellis code, measured by the number of states in the trellis in the decoder, increases exponentially with transmission rate. With CSI available at the receiver, the complexity of the maximum likelihood decoding algorithm, i.e. the Viterbi algorithm, of the space-time trellis codes proposed in [13] increases exponentially with the number of states in the trellis, making their implementation challenging in practice. In this scenario, it is more appropriate to use other space time coding techniques, such as the block coded modulation designed for space time application, which are known as space time block codes (STBC).

## 2.3 Space-Time Block Code

Space-time block codes take advantage of multiple transmit and receive antennas to achieve the promised capacity gain [15], [5]. At the receiver, maximum likelihood decoding is achieved using a simple method by decoupling the signals transmitted from different antennas rather than joint detection. The use of orthogonal structure of STBC permits maximum likelihood decoding to be implemented with linear processing at the receiver, resulting in a less complex receiver structure preferable in practical wireless communication systems. The STBC schemes are found to be attractive solutions in industrial applications. STBC techniques as a means of achieving the potential capacity gain in MIMO systems have been adopted by the third generation wireless industry standard, such as the 3GPP HSPA MIMO [16], [17] and LTE MIMO [18], [19]; and the 3GPP2 UMB MIMO [20]. The STBC has also been used

in the IEEE 802.11n standard for wireless LANs [21].

In addressing the challenge of decoding complexity, a remarkable scheme for two transmit antenna MIMO system is proposed [15], which is widely referred to as the Alamouti scheme. It is a simple transmit diversity scheme, which encodes two symbols at a time in two symbol periods. Let us consider symbols  $s_1$  and  $s_2$ . During the first symbol time slot,  $s_1$  is transmitted by the first antenna and  $s_2$  is transmitted by the second antenna. In the second time slot,  $-s_2^*$  is transmitted from the first antenna, while  $s_1^*$  is transmitted from the second antenna. This encoding process is illustrated in Figure 2.2.

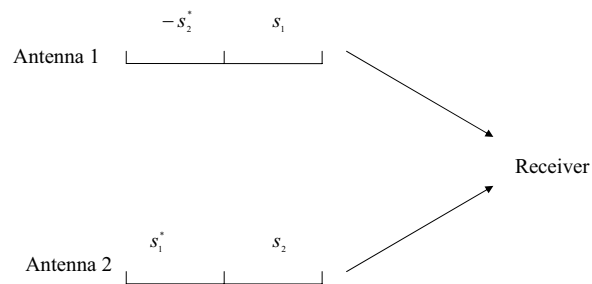


Figure 2.2: The Alamouti Scheme

This STBC, like any other STBC, is usually represented by its transmission matrix

and is specified as

$$G_{c2} = \begin{pmatrix} s_1 & s_2 \\ -s_2^* & s_1^* \end{pmatrix} \quad (2.16)$$

where columns 1 and 2 represent the signals transmitted by antennas 1 and 2, respectively. The signals on rows 1 and 2 specify the signals transmitted by the two antennas in time slot 1 and 2, respectively. The symbols are the modulation symbols used by the transmitter, selected from a constellation, for instance BPSK or QPSK modulation. Since two symbols are transmitted in two symbol time slots, the overall transmission rate is 1, which is also called full rate.

From Equation (2.16) it can be easily verified that  $D_{c2} = G_{c2}^H G_{c2} = (\sum_{i=1}^2 |s_i|^2) \mathbf{I}_2$ , where  $\mathbf{I}_2$  is the  $2 \times 2$  identity matrix. When a STBC satisfies this property, it is called an orthogonal STBC.

At the receiver, the maximum likelihood detection algorithm amounts to minimizing the decision metric expressed as [15], [5]

$$\sum_{m=1}^{N_R} \left( \left| r_1^m - \sqrt{\frac{\rho}{N_T}} (\alpha_{m,1} s_1 + \alpha_{m,2} s_2) \right|^2 + \left| r_2^m + \sqrt{\frac{\rho}{N_T}} (\alpha_{m,1} s_2^* - \alpha_{m,2} s_1^*) \right|^2 \right) \quad (2.17)$$

over all possible values of symbols  $s_1$  and  $s_2$ . Since this STBC is orthogonal, minimizing the maximum likelihood decision metric given by Equation (2.17) is equivalent to minimizing [5]

$$\left| \left[ \sum_{m=1}^{N_R} \sqrt{\frac{\rho}{N_T}} (r_1^m \alpha_{m,1}^* + (r_2^m)^* \alpha_{m,2}) \right] - s_1 \right|^2 + \frac{\rho}{N_T} \left( -1 + \sum_{m=1}^{N_R} \sum_{n=1}^2 |\alpha_{m,n}|^2 \right) |s_1|^2 \quad (2.18)$$

for detecting  $s_1$  and

$$\left| \left[ \sum_{m=1}^{N_R} \sqrt{\frac{\rho}{N_T}} (r_1^m \alpha_{m,2}^* - (r_2^m)^* \alpha_{m,1}) \right] - s_2 \right|^2 + \frac{\rho}{N_T} \left( -1 + \sum_{m=1}^{N_R} \sum_{n=1}^2 |\alpha_{m,n}|^2 \right) |s_2|^2 \quad (2.19)$$

for decoding  $s_2$ . This is a simple decoding algorithm because there is no cross product

terms of  $s_1$  and  $s_2$  in the decision metric and symbols  $s_1$  and  $s_2$  can be decoded individually.

To design STBC for MIMO system with more than two transmit antennas, we can use the theory of orthogonal designs and the theory of generalized orthogonal designs as proposed in [5]. Design of STBC based on the theory of orthogonal design can be carried out for both real and complex constellations [5].

### 2.3.1 STBCs from Real Orthogonal Designs

A real orthogonal design of size  $N_T$  is an  $N_T \times N_T$  orthogonal matrix with entries the indeterminates  $\pm x_1, \pm x_2, \dots, \pm x_{N_T}$  [5], where the values of  $x_n, n = 1, 2, \dots, N_T$  are real numbers and they are chosen from real modulation symbols, such as PAM modulation. An example of the real orthogonal design is  $2 \times 2$  design given by

$$\begin{pmatrix} x_1 & x_2 \\ -x_2 & x_1 \end{pmatrix} \quad (2.20)$$

It can be shown that a real orthogonal design exists if and only if  $N_T = 2, 4$ , or  $8$ . To expand the set of dimensions  $N_T$  for which there exists an orthogonal design of size  $N_T$ , we introduce generalized real orthogonal designs.

A generalized orthogonal design  $G$  of size  $N_T$  is a  $p \times N_T$  matrix with entries  $0, \pm x_1, \pm x_2, \dots, \pm x_k$  such that  $G^T G = D$ , where  $D$  is a diagonal matrix with diagonal  $D_{ii}, i = 1, 2, \dots, N_T$  of the form  $l_1^i x_1^2 + l_2^i x_2^2 + \dots + l_k^i x_k^2$  and coefficients  $l_1^i, l_2^i, \dots, l_k^i$  are strictly positive integers [5].

Let us consider transmission of a generalized real orthogonal design using a real signal constellation  $A$  of size  $2^b$ . At time slot 1,  $kb$  bits arrive at the encoder and select constellation symbols  $x_1, x_2, \dots, x_k$ . The encoder populates the transmission matrix and at time slots  $t = 1, 2, \dots, p$ . Signals  $G_{t1}, G_{t2}, \dots, G_{tN_T}$  are transmitted simultaneously by antennas  $1, 2, \dots, N_T$ . Clearly  $b$  bits are transmitted per  $p$  transmissions. The rate  $R$  of the resulting STBC, whose transmission matrix given by

the matrix  $G$ , is defined to be  $k/p$ . An example of the STBC from generalized real orthogonal designs for a MIMO system with  $N_T = 3$  is specified by [5]

$$\begin{pmatrix} x_1 & x_2 & x_3 \\ -x_2 & x_1 & -x_4 \\ -x_3 & x_4 & x_1 \\ -x_4 & -x_3 & x_2 \end{pmatrix} \quad (2.21)$$

### 2.3.2 STBC from Complex Orthogonal Designs

The Alamouti scheme given by Equation (2.16) for two transmit antennas is a STBC from complex orthogonal designs with symbols selected from a complex constellation such as QPSK. In particular, a complex orthogonal design  $o_c$  of size  $N_T$  is defined as an orthogonal matrix with entries the indeterminates  $\pm s_1, \pm s_2, \dots, \pm s_n$ , their complex conjugates  $\pm s_1^*, \pm s_2^*, \dots, \pm s_n^*$ , or multiples of these indeterminates by  $\pm j$ , where  $j = \sqrt{-1}$  [5].

It is shown that [5] STBCs from complex orthogonal designs only exists for  $N_T = 2$ . This means that the Alamouti scheme is unique in this sense.

When a complex signal constellation  $S$  of size  $2^b$  is used and  $b$  represents the number of bits mapped to a symbol, the theory of generalized complex orthogonal designs is used to construct a STBC [5], [14]. Let  $G_c$  be a  $p \times N_T$  matrix whose elements belong to the set  $\{0, \pm s_1, \pm s_1^*, \dots, \pm s_k, \pm s_k^*\}$ , their product by  $j = \sqrt{-1}$  or linear combination of these terms, where  $s_i \in S$ ,  $1 \leq i \leq k$ , are symbols in the complex signal constellation and  $k$  is the number of non-zero elements in each column of matrix  $G_c$ . The columns of matrix  $G_c$  represent the signals transmitted on the antennas,  $n = 1, 2, \dots, N_T$ , and the rows in matrix  $G_c$  are the signals transmitted in symbol periods,  $t = 1, 2, \dots, p$ . If  $D_c = G_c^H G_c$  is diagonal with diagonal elements of the form  $[D_c]_{n,n} = (d_1^n |s_1|^2 + d_2^n |s_2|^2 + \dots + d_k^n |s_k|^2)$  and the coefficients  $d_1^n, d_2^n, \dots, d_k^n$  are all strictly positive real,  $G_c$  is referred to as a generalized complex orthogonal design of size  $N_T$  [5].

At the transmitter, the encoding process can be described as follows. At time slot 1,  $kb$  bits arrive at the encoder and select constellation symbols  $s_1, s_2, \dots, s_k$ , where  $b$  represents the number of bits mapped to a symbol. The encoder populates matrix  $G_c$  with elements  $s_i, i = 1, \dots, k$ . At symbol periods  $t = 1, 2, \dots, p$ , the  $N_T$  elements on each row of matrix  $G_c$  are transmitted by antennas  $1, 2, \dots, N_T$  simultaneously. Thus  $k$  symbols, i.e.  $kb$  bits are transmitted by  $p$  symbol periods. The rate of the STBC is defined as  $R = k/p$  [5]. It is shown [13] that for a STBC from complex orthogonal designs we have code rate  $R \leq 1$ . When the code rate of a STBC is equal to 1, the STBC is referred to as a full rate STBC. For instance the STBC specified in Equation (2.16) [15] is a full rate code for two transmit antenna MIMO system. The encoding process, i.e. the formation of matrix  $G_c$  only requires linear processing.

It is shown in [5] that the metric expressed in Equation (2.1) is the sum of  $k$  components each involving one variable  $s_i$ , for  $i = 1, 2, \dots, k$  when the orthogonal STBC is used. Indeed, if the metric in Equation (2.1) is expanded, the cross terms involving  $s_{m,n_1} s_{m,n_2}^*$  or  $\alpha_{m,n_1} \alpha_{m,n_2}^*$ ,  $1 \leq n_1 \neq n_2 \leq N_T$  are canceled out since the  $n_1$ th and the  $n_2$ th columns of  $G_c$  are orthogonal. Thus it can be implemented using linear processing at the receiver and the computational complexity of the receiver using maximum likelihood decoding is lower when the STBC used is orthogonal. The STBC proposed in [5] is orthogonal and can be decoded using linear processing at the receiver. The possibility of low complexity decoding facilitates their practical implementation.

A STBC is said to achieve full diversity when the matrix  $\mathbf{B}$  defined by Equation (2.7) has full rank over all possible distinct pairs of codewords  $\mathbf{c}, \mathbf{e}$  and the full diversity of a STBC system is  $N_T N_R$  [5]. If matrix  $\mathbf{B}$  has minimum rank  $r$  over all distinct pairs of codewords  $c$  and  $e$ , then the STBC achieves the diversity order of  $r N_R$  [5]. The negative of the slope on the BER versus SNR curve of this STBC is  $r$ . This provides an analytical means to evaluate the diversity order of a STBC in addition to the method defined by Equation (1.21). This method does not require lengthy Monte Carlo simulation to calculate BER of the STBC in a wireless MIMO system.

It is shown in [5] that transmission using an orthogonal design STBC provides full diversity.

To design a STBC from complex orthogonal designs, it is desirable to maximize the rank  $r$  of the matrix  $\mathbf{B}$ , which is suggested by the rank criteria or diversity criteria of STBC design [5]. In order to achieve maximum diversity, the matrix  $\mathbf{B}$  should be full rank over all possible pairs of possible code words  $\mathbf{c}$  and  $\mathbf{e}$ .

The STBC scheme for two transmit antennas given in Equation (2.16) [15] was later generalized to more than two transmit antennas in [5] using generalized complex orthogonal design. The STBC given in Equation (2.16) [15] is a complex orthogonal STBC and achieves full diversity with a code rate equal to one; thus achieving full rate. It turns out that the complex orthogonal STBC schemes that achieve full diversity all have rates lower than 1 when there are three or more transmit antennas [5].

Using the generalized complex orthogonal design, an orthogonal STBC for three transmit antennas was proposed originally in [5]. Applying unitary operations and changing variables, an equivalent STBC that is a slightly modified version of the original STBC is given by [22]

$$G_{c3} = \begin{pmatrix} s_1 & -s_2^* & -s_3^* \\ s_2 & s_1^* & 0 \\ s_3 & 0 & s_1^* \\ 0 & s_3 & -s_2 \end{pmatrix} \quad (2.22)$$

The corresponding matrix  $D_{c3} = G_{c3}^H G_{c3} = (\sum_{i=1}^3 |s_i|^2) \mathbf{I}_3$  is diagonal. This STBC is orthogonal but the code rate is  $R = 3/4$ . The zeros in the transmission matrix  $G_{c3}$  represent that there is no transmitted signal from that particular antenna during that symbol period.

Along the same thought, an orthogonal STBC for four transmit antennas was proposed originally in [5]. Applying unitary operations and changing variables, an equivalent STBC that is slightly modified version of the original STBC is given by

[22]

$$G_{c4} = \begin{pmatrix} s_1 & s_2 & s_3 & 0 \\ -s_2^* & s_1^* & 0 & s_3 \\ -s_3^* & 0 & s_1^* & -s_2 \\ 0 & -s_3^* & s_2^* & s_1 \end{pmatrix} \quad (2.23)$$

The corresponding matrix  $D_{c4} = G_{c4}^H G_{c4} = (\sum_{i=1}^4 |s_i|^2) \mathbf{I}_4$  is diagonal. This STBC is orthogonal but the code rate is  $R = 3/4$ . The zeros in the transmission matrix  $G_{c4}$  represent that there is no transmitted signal from that particular antenna during that symbol period.

For any number of transmit antennas, there exists STBC from generalized complex orthogonal design with linear processing that achieves code rate  $R = 1/2$  [5], which sets the lower bound for the achievable code rate. It is shown in [23] that the rate of STBC from generalized complex orthogonal designs with linear processing is less than 1 when the number of transmit antennas is greater than 2. It is desirable to construct STBCs from generalized complex orthogonal design that have high rate  $R$  when there are more than two transmit antennas, so the resources provided by a MIMO system can be fully utilized.

## 2.4 High Rate STBC from Complex Designs

A full rate STBC for four transmit antennas,  $N_T = 4$ , was proposed in [24], based on the STBC given in Equation (2.16). If we consider the following STBC for  $N_T = k = p = 4$  [24]

$$G_{qo4} = \begin{pmatrix} \mathring{A}_{12} & \mathring{A}_{34} \\ -\mathring{A}_{34}^* & \mathring{A}_{12}^* \end{pmatrix} = \begin{pmatrix} s_1 & s_2 & s_3 & s_4 \\ -s_2^* & s_1^* & -s_4^* & s_3^* \\ -s_3^* & -s_4^* & s_1^* & s_2^* \\ s_4 & -s_3 & -s_2 & s_1 \end{pmatrix} \quad (2.24)$$

It is easy to see that the minimum rank of matrix  $\mathbf{A}$  for this STBC given in Equation (2.24), where  $\mathbf{A} = \mathbf{B}\mathbf{B}^H$  and  $\mathbf{B}$  is given by Equation (2.7), is  $r = 2$ . Therefore a diversity order of 2 is achieved while the rate of the STBC is one [24]. The maximum diversity that a MIMO system with four transmit and one receive antenna can provide is 4. Now if we define  $\nu_i, i = 1, 2, 3, 4$  as the  $i$ th column of  $G_{qo4}$ , it is easy to see that [24]

$$\langle \nu_1, \nu_2 \rangle = \langle \nu_1, \nu_3 \rangle = \langle \nu_2, \nu_4 \rangle = \langle \nu_3, \nu_4 \rangle = 0 \quad (2.25)$$

where  $\langle \nu_m, \nu_n \rangle = \sum_{l=1}^4 (\nu_m)_l (\nu_n)_l^*$  is the inner product of vectors  $\nu_m$  and  $\nu_n$ . Therefore the subspace created by  $\nu_1$  and  $\nu_4$  is orthogonal to the subspace created by  $\nu_2$  and  $\nu_3$ . Using this orthogonality, the maximum likelihood decision metric given in Equation (2.1) can be calculated as the sum of two terms  $f_{14}(s_1, s_4) + f_{23}(s_2, s_3)$  [24], where  $f_{14}$  is independent of  $s_2$  and  $s_3$ , and  $f_{23}$  is independent of  $s_1$  and  $s_4$ . Thus, the minimization of metric given by Equation (2.1) is equivalent to minimizing these two terms independently. In other words, the decoder can first find  $(s_1, s_4)$  that minimizes  $f_{14}(s_1, s_4)$  among all possible  $(s_1, s_4)$  pairs. In parallel, the decoder selects the pair  $(s_2, s_3)$  that minimizes  $f_{23}(s_2, s_3)$ . The complexity of the decoder is reduced without sacrificing the performance.

We can verify that matrix  $D_{qo4} = G_{qo4}^H G_{qo4}$  is not diagonal. So this STBC is not an orthogonal STBC. But the subspace created by certain columns is orthogonal to the subspace created by other columns and hence this STBC is called a Quasi-Orthogonal STBC. Since this code detects the symbols in pairs, the complexity of its decoder is higher than the complexity of the decoder of the orthogonal STBC with  $N_T = 4$ .

In a later work [25], a quasi-orthogonal STBC based on a constellation rotation method to improve the performance is proposed. The transmission matrix of the

proposed STBC is specified by

$$G(s) = \begin{pmatrix} s_1 & s_2 & s_3 & s_4 \\ s_2^* & -s_1^* & s_4^* & -s_3^* \\ s_3 & -s_4 & -s_1 & s_2 \\ s_4^* & s_3^* & -s_2^* & -s_1^* \end{pmatrix} \quad (2.26)$$

The quasi-orthogonal STBCs specified in Equation (2.24) and (2.26) belong to the same family of quasi-orthogonal STBCs. The constellation rotation proposed in [25] applies to this family of quasi-orthogonal STBCs. It is shown [25] that symbols  $s_1$  and  $s_3$  form pairs, and so do symbols  $s_2$  and  $s_4$ . The decision metric for pair  $(s_1, s_3)$  can be minimized independently from the decision metric for pair  $(s_2, s_4)$ . Let us look at the received signal due to the  $(s_1, s_3)$  pair. At the  $m$ th receive antenna, one can write the part of the receive signal due to  $(s_1, s_3)$  as [25]

$$\begin{bmatrix} r_1 \\ r_2^* \\ r_3 \\ r_4^* \end{bmatrix} = \sqrt{\frac{\rho}{N_T}} \check{H} \begin{bmatrix} s_1 \\ s_3 \end{bmatrix} + \begin{bmatrix} \eta_1 \\ \eta_2^* \\ \eta_3 \\ \eta_4^* \end{bmatrix} \quad (2.27)$$

where  $\check{H}$  is the partial channel related to  $(s_1, s_3)$ . A  $2 \times 2$  equivalent channel is fully determined by  $\check{H}^H \check{H}$ . Solving this further, we obtain the following two equations

$$\tilde{r}_1 = \sqrt{\frac{\rho}{N_T}} \sqrt{\frac{\acute{r}_m + \acute{a}_m/j}{2}} (s_1 + js_3) + \bar{\eta}_1 \quad (2.28)$$

$$\tilde{r}_2 = \sqrt{\frac{\rho}{N_T}} \sqrt{\frac{\acute{r}_m - \acute{a}_m/j}{2}} (s_1 - js_3) + \bar{\eta}_2 \quad (2.29)$$

where  $\acute{r}_m = \sum_{n=1}^4 |\alpha_{m,n}|^2$  and  $\acute{a}_m = 2j \text{Im}(\alpha_{m,1}^* \alpha_{m,3} + \alpha_{m,4}^* \alpha_{m,2})$ . Note that in Equations (2.28) and (2.29), if the symbols  $s_1$  and  $s_3$  are drawn from constellations  $\mathring{A}_1$  and  $\mathring{A}_2$  of order  $P_1$  and  $P_2$ , respectively, then the constellations  $\mathbb{B}_1$  and  $\mathbb{B}_2$  for the

received “symbols”  $s_1 + js_3$  and  $s_1 - js_3$ , respectively, will be each of maximum order  $P_1P_2$ . Let  $d_{\mathbb{B}_1}(s_1, s_3)$  and  $d_{\mathbb{B}_2}(s_1, s_3)$  denote the minimum distance of  $\mathbb{B}_1$  and  $\mathbb{B}_2$  from given pair  $(s_1, s_3)$  to all other pairs of symbols. Our goal is to maximize the minimum distance of the two  $d_{\mathbb{B}_1}(s_1, s_3)$  and  $d_{\mathbb{B}_2}(s_1, s_3)$ . One way to achieve this is by rotating the constellation  $\mathring{A}_2$  around itself by a fixed angle  $\phi$ . Please note that the rotation does not change the minimum distance of the constellation  $\mathring{A}_2$ , but it changes the minimum distances of  $\mathbb{B}_1$  and  $\mathbb{B}_2$ . Since the equivalent channel as seen by the pair  $(s_1, s_3)$  is similar to the one seen by  $(s_2, s_4)$ , we apply the same rotation technique for the pair  $(s_2, s_4)$ . This constellation rotation technique results in a 6 dB gain in SNR at BER of  $10^{-6}$  for transmission spectral efficiency of 2 bit/sec/Hz. This scheme is applicable to MIMO systems with four transmit antennas  $N_T = 4$ .

When a different base code is used, a similar constellation rotation technique can generate a new STBC scheme [26], where the constellation phase rotations are introduced and the resulting code achieves full diversity for a special PSK based constellation. The performance of this code matches the performance of the code in [25]. Again, this STBC is designed for four transmit antennas.

In the works of [25], [26], the rotation angles are chosen based on the minimum Euclidean distance criterion. An angle rotation criterion based on the diversity criterion is proposed in [27], [28]. The basic idea of the quasi-orthogonal STBC is to use the orthogonal STBC as building blocks to construct a high dimensional quasi-orthogonal STBC, which has the same code rate as the constituent orthogonal STBC. Assume  $G_{N_T}(s_1, s_2, \dots, s_k)$  is a  $p \times N_T$  orthogonal STBC from complex designs using complex variables  $s_1, s_2, \dots, s_k$ , where  $p$  corresponds to the time dimension, i.e. the number of symbol periods to finish a STBC encoding, and  $N_T$  corresponds to the space dimension, i.e. the number of transmit antennas. Then a quasi-orthogonal design  $G_{2N_T}(s_1, s_2, \dots, s_{2k})$  of size  $2p \times 2N_T$  in complex variables  $s_1, s_2, \dots, s_{2k}$  can be constructed as

$$Q_{2N_T} = \begin{bmatrix} \mathring{A}_1 & \mathring{A}_2 \\ \mathring{A}_2 & \mathring{A}_1 \end{bmatrix} \quad (2.30)$$

where  $\dot{A}_1 = G_{N_T}(s_1, s_2, \dots, s_k)$  and  $\dot{A}_2 = G_{N_T}(s_{k+1}, s_{k+2}, \dots, s_{2k})$ . For any possible two codewords  $\mathbf{c}$  and  $\mathbf{e}$ , the difference matrix  $\mathbf{B}$  can be calculated according to Equation (2.7) and can be expressed as  $\mathbf{B} = Q_{2N_T}(\Delta s_1, \dots, \Delta s_{2k})$ , where  $\Delta s_i = s_i - \tilde{s}_i, i = 1, 2, \dots, 2k$ . Based on the quasi-orthogonal structure, the determinant of matrix  $\mathbf{B}$  can be found by [27]

$$\det(\mathbf{B}) = \left( \sum_1^k |\Delta s_i - \Delta s_{i+k}|^2 \right)^{N_T} \left( \sum_1^k |\Delta s_i + \Delta s_{i+k}|^2 \right)^{N_T} \quad (2.31)$$

From Equation (2.31), it is easy to see that if symbols  $s_i$  and  $s_{i+k}, i = 1, 2, \dots, k$ , are drawn from the same signal constellation, then the value of  $\det(\mathbf{B})$  will equal to zero when some pairs of code words  $\mathbf{c}$  and  $\mathbf{e}$  are chosen. Thus the quasi-orthogonal STBC can not achieve full diversity. It was proposed [25], [28] that symbols  $s_i, i = 1, 2, \dots, k$ , be taken from the symbol constellation  $\Omega$  and symbols  $s_{i+k}, i = 1, 2, \dots, k$ , from the rotated signal constellation  $e^{j\Theta}\Omega$ , where  $\Theta$  is the angle rotation, so that the determinant of matrix  $\mathbf{B}$  is not zero over all possible codeword pairs  $\mathbf{c}$  and  $\mathbf{e}$ , and full diversity can be achieved. In [28], the angle of rotation  $\Theta$  based on the diversity criterion is optimized and it is concluded that the optimal angle minimizes

$$|\det(B)|^{1/2N_T} \quad (2.32)$$

over all possible pairs of code words  $\mathbf{c}$  and  $\mathbf{e}$ .

It is desirable to increase the rate  $R$  of the STBC when it achieves full diversity. When these STBCs with special modulation symbol constellation are designed, they start with the diversity criterion that suggests to maximize the rank of matrix  $\mathbf{B}$  specified in Equation (2.7). At the receiver, the decoding algorithm detects the symbols in pairs, which leads to higher complexity compared to the decoder of the orthogonal STBC. Although some of these STBCs for a MIMO system with four transmit antennas achieves full diversity full rate, none of these STBCs are orthogonal. In our work, we look at the conditions to satisfy the orthogonality criterion and propose a

family of new STBCs with a new modulation scheme for MIMO system with three and four transmit antennas.

# Chapter 3

## A New Family of Space-Time Block Codes

As discussed in Chapter 2 the code rates of the complex orthogonal STBCs are less than one when the number of transmit antennas is greater than two. The Alamouti STBC discussed earlier is the only orthogonal STBC that has rate equal to one and it is designed for two transmit antenna MIMO systems. To increase the rate of STBCs when the number of transmit antennas  $N_T > 2$ , quasi-orthogonal STBCs that reach rate one for four transmit antennas were proposed. Unfortunately, the quasi-orthogonal STBCs do not achieve full diversity. Later, constellation rotation of the modulation signal was used to improve the diversity gain of quasi-orthogonal STBCs and full diversity quasi-orthogonal STBCs were designed using this technique. The design criterion for the signal constellation rotation technique is optimizing the diversity order. The quasi-orthogonal STBCs and the corresponding signal constellations are designed for a MIMO system with four transmit antennas.

In this Chapter, we design orthogonal STBCs and define a new modulation scheme, “triple QPSK” to improve the performance of a new full rate STBC for a three transmit antenna MIMO system. This STBC, whose modulation method is “triple QPSK”, is simulated using Monte Carlo simulation, and the resulting BER is found. An upper

bound of the probability of bit error is derived using the union bound analysis. This STBC has rate  $R = 1$ , is orthogonal when the transmitted symbols are generated using the proposed “triple QPSK” modulation, and achieves full diversity gain for three transmit antennas. The quasi-orthogonal STBC has rate  $R = 1$  but does not achieve full diversity. The decoder of the new STBC employs a maximum likelihood detection algorithm and detects the transmitted symbols in pairs by taking advantage of the encoding structure of the “triple QPSK” modulation that has memory. The memory depth of the “triple QPSK” is 2, which is the same as the length of the pair of symbols detected jointly. The decoding complexity of this code is comparable to the decoding complexity of the quasi-orthogonal STBCs in [24], [25], and [28], whose decoding algorithms at the receiver detect symbols in pairs and the decision metrics contain product terms of two symbols that makes the computation more complex. In the decision metric of the proposed STBC, there are only single symbol terms and no product terms of two symbols because the STBC is orthogonal using the “triple QPSK” modulation. The decoding complexity of this proposed STBC using the “triple QPSK” modulation is slightly higher than the decoder complexity of the orthogonal STBC from complex design for  $N_T = 3$  given in Equation (2.22).

This work is extended to design STBCs for four transmit antennas. We propose a new STBC for four transmit antennas that takes advantage of the “triple QPSK” modulation to achieve full rate, full diversity, and orthogonality. One of the key contributors to the fact that these STBCs from complex orthogonal designs for the number of transmit antennas,  $N_T = 3$  and 4, achieve full rate and full diversity is using the proposed “triple QPSK” modulation, which has memory. Throughout the following discussion in this chapter it is assumed that perfect channel state information,  $\mathbf{H}$ , is available at the receiver.

### 3.1 New STBC for Three Transmit Antennas

To increase the code rate of the orthogonal STBC for three transmit antennas given by Equation (2.22), we transmit a fourth symbol  $s_4$  (or its complex conjugate) on the transmit antennas during the silent periods. Thus, we propose a new STBC and the transmission matrix of the new STBC is given by

$$\mathbf{G}_{cn} = \begin{pmatrix} s_1 & -s_2^* & -s_3^* \\ s_2 & s_1^* & s_4^* \\ s_3 & -s_4^* & s_1^* \\ s_4 & s_3^* & -s_2^* \end{pmatrix} \quad (3.1)$$

It is apparent that the zeros in the transmission matrix given by Equation (2.22) have been replaced by the 4th symbol  $s_4$  or its complex conjugate  $s_4^*$  in the new STBC specified by Equation (3.1). The number of non-zero elements in any column in the transmission matrix given in Equation (3.1),  $k = 4$ . The time it takes to transmit this STBC is four symbol periods and  $p = 4$ . Thus the rate of this proposed STBC  $R = k/p = 1$ . Let us check the orthogonality criteria  $\mathbf{D}_{cn} = \mathbf{G}_{cn}^H \mathbf{G}_{cn}$  for this STBC. It is easy to see that

$$\begin{aligned} D_{cn} &= \mathbf{G}_{cn}^H \mathbf{G}_{cn} \\ &= \begin{pmatrix} \sum_{i=1}^4 |s_i|^2 & 0 & 0 \\ 0 & \sum_{i=1}^4 |s_i|^2 & d_{23} \\ 0 & d_{32} & \sum_{i=1}^4 |s_i|^2 \end{pmatrix} \end{aligned} \quad (3.2)$$

where  $d_{23} = d_{32}^* = s_2 s_3^* + s_1 s_4^* - s_4 s_1^* - s_3 s_2^*$ . There are two non-zero off diagonal terms in matrix  $\mathbf{D}_{cn}$  and they are complex conjugate of each other. Thus if one of the non-zero off diagonal term is made to be zero under certain conditions, the other one will be made equal to zero at the same time. By computer search, the transmission matrix specified by Equation (3.1) has the minimum number of non-zero off diagonal

terms in its corresponding  $\mathbf{D}_{cn}$  matrix given by Equation (3.2) and it is adopted. The non-zero off diagonal terms in matrix  $\mathbf{D}_{cn}$  introduce coupling effects between the symbols transmitted on different antennas during different symbol periods. The STBC from complex design  $G_{cn}$  can be orthogonal when  $\mathbf{D}_{cn}$  is diagonal and  $d_{23} = 0$ . To make the matrix  $\mathbf{D}_{cn}$  diagonal, we set the non-trivial off-diagonal terms equal to zero, which results in

$$s_2s_3^* + s_1s_4^* - s_4s_1^* - s_3s_2^* = 0 \quad (3.3)$$

Let  $s_i = Re[s_i] + jIm[s_i], i = 1, 2, 3, 4$ , where  $Re[ ]$  represents the real part of a complex variable and  $Im[ ]$  stands for the imaginary part of a complex variable. One solution to equation (3.3) is of the form

$$Re[s_1] + jIm[s_1] = \gamma_1(Re[s_4] + jIm[s_4]) \quad (3.4)$$

$$Re[s_2] + jIm[s_2] = \gamma_2(Re[s_3] + jIm[s_3]) \quad (3.5)$$

where  $\gamma_1$  and  $\gamma_2$  are scalar constants, and  $\gamma_1, \gamma_2 \notin \{0, 1\}$ . This is a sufficient condition for equation (3.3) to hold. The complex signal constellation that satisfies this condition has the property,  $s_1$  is scalar proportional to  $s_4$  and  $s_2$  is scalar proportional to  $s_3$ .

None of the commonly used modulation schemes have a constellation whose symbols satisfy Equations (3.4) and (3.5). We propose a new modulation scheme, called “triple QPSK”, whose signal constellation is shown in Figure 3.1. Using the “triple QPSK” modulation, the proposed STBC satisfies the orthogonality criterion, i.e.  $\mathbf{D}_{cn} = \mathbf{G}_{cn}^H \mathbf{G}_{cn}$  is diagonal. There are 12 points in the “triple QPSK” constellation. Four of them are on the inner circle with amplitude 1, the second four signals are on the second circle with amplitude  $R_2$ , and the third four signals are on the third circle with amplitude  $R_3$ . Six of the signals have real parts equal to their imaginary parts, which belong to group 1 and the other six signals whose real parts equal to the negative of their imaginary parts, which belong to group 2.

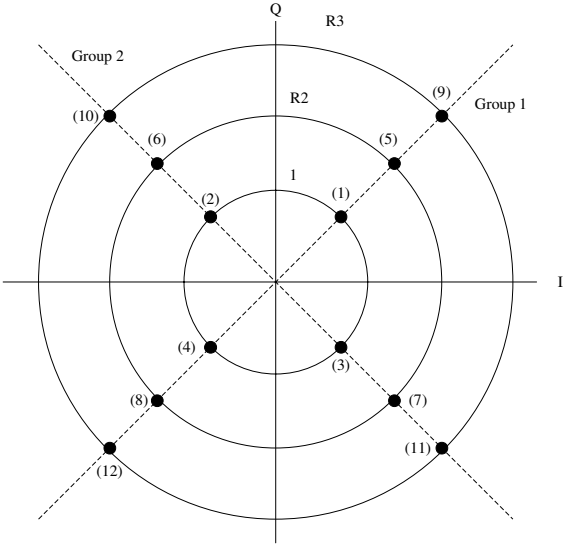


Figure 3.1: Signal Constellation of the “triple QPSK”

The modulator takes 8 data bits and generates 4 symbols at a time. So the “triple QPSK” carries 2 bits per symbol. The first two bits are mapped into one of the symbols on the inner circle according to regular QPSK modulation rule with Gray mapping and  $s_1$  is generated. The second two bits are similarly mapped into one of the symbols on the inner circle according to regular QPSK modulation rule with Gray mapping and  $s_2$  is generated. The third two bits are used to generate  $s_3$ . If  $s_2$  belong to group 1, the third two bits are mapped into one of the four symbols in group 1

Table 3.1: Mapping Rule of “triple QPSK” Modulation

| Symbol Index | Bits | Symbol Index | Bits |
|--------------|------|--------------|------|
| 1            | 00   | 7            | 10   |
| 2            | 01   | 8            | 11   |
| 3            | 10   | 9            | 10   |
| 4            | 11   | 10           | 00   |
| 5            | 00   | 11           | 11   |
| 6            | 01   | 12           | 01   |

that has radius of either  $R_2$  or  $R_3$  and  $s_3$  is generated. If  $s_2$  belongs to group 2, the third two bits are mapped into one of the four symbols in group 2 that has radius of either  $R_2$  or  $R_3$  and  $s_3$  is generated. In a similar fashion,  $s_4$  is generated from the fourth two bits using  $s_1$  as a group divider. If  $s_1$  belongs to group 1, the fourth two bits are mapped into one of the four symbols in group 1 that has radius of either  $R_2$  or  $R_3$  and  $s_4$  is generated. If  $s_1$  falls into group 2, the fourth two bits are mapped into one of the four symbols in group 2 that has radius of either  $R_2$  or  $R_3$  and  $s_4$  is generated.

The number in a pair of parenthesis on the signal constellation shown in Figure 3.1 is the index of the symbols in the “triple QPSK” modulation. The mapping rules of the “triple QPSK” modulation is given in Table 3.1.

It is clear that the transmit symbols generated by the “triple QPSK” modulation satisfy Equations (3.4) and (3.5), hence the matrix  $\mathbf{D}_{cn}$  given in Equation (3.2) is diagonal if the symbols are generated by the “triple-QPSK” modulation. The orthogonality criterion is satisfied. By checking the ranks of all possible matrices  $\mathbf{A} = \mathbf{B}\mathbf{B}^H$ , where matrix  $\mathbf{B}$  is given by Equation (2.7), we have concluded that all possible matrices  $\mathbf{A}$  have full rank, thus the full diversity condition is met. The transmission matrix of the new STBC expressed in Equation (3.1) is orthogonal and achieves full diversity gain when the “triple QPSK” modulation is used. It should be noted that this proposed STBC for three transmit antennas does not belong to the

quasi-orthogonal STBC even when the “triple QPSK” is not used, because its transmission matrix is not a square matrix and is not constructed based on an existing orthogonal STBC with lower dimension transmission matrix.

It is observed that the symbol  $s_4$  depends partially on the pervious symbol  $s_1$  according to the “triple QPSK”. So does  $s_3$  depends partially on the previous symbol  $s_2$ . Thus there is memory in the “triple QPSK” modulation and the depth of the memory is two symbols long.

The symbols generated by the “triple QPSK” modulation come in pairs where the first symbol is selected from the inner circle and the second symbol is chosen from the outer circles with radius  $R_2$  or  $R_3$ . The resulting sequence of symbols has half the symbols from the outer circles, whose radius is  $R_2$  or  $R_3$ , and the other half from the inner unit circle over a sufficiently long period of time. Thus, the symbol energy of the “triple QPSK” is related to the symbol energy of the QPSK modulation by

$$E_{s,\text{tripleQPSK}} = (0.5 + 0.25 \cdot (R_2^2 + R_3^2))E_{s,\text{QPSK}} \quad (3.6)$$

We need to consider this energy difference in our simulations and analysis.

To find the optimal values of  $R_2$  and  $R_3$ , we check the required  $E_b/N_0$  for the BER to be  $10^{-4}$  when  $R_2$  and  $R_3$  vary. The results are plotted in Figure 3.2. Based on this, the optimal values are found to be  $R_2 = 0.55$  and  $R_3 = 1.6$ . Since the BER versus SNR curves are monotonic and they all have the same diversity order, i.e. slope, the optimal values of  $R_2$  and  $R_3$  are independent of the BER value.

Having gone through the STBC encoding using the STBC specified in Equation (3.1) and the model given in Equation (1.7), the signal at the receiver from symbol periods 1 to 4 can be expressed as

$$\mathbf{r}_3 = \mathbf{G}_{cn} \mathbf{h}_3^T + \mathbf{n}_3 \quad (3.7)$$

where  $\mathbf{r}_3 = (r_1^m \ r_2^m \ r_3^m \ r_4^m)^T$  is the received signal vector,  $\mathbf{G}_{cn}$  is given by Equation

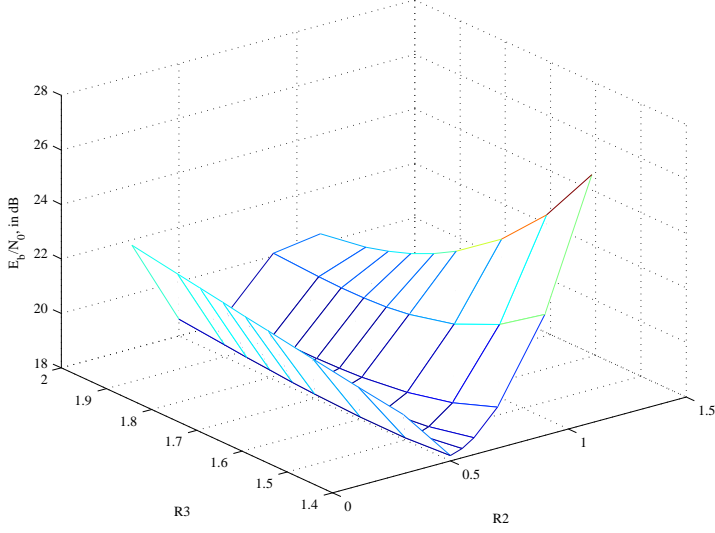


Figure 3.2: BER of the New STBC with  $R_2$  and  $R_3$

(3.1),  $\mathbf{h}_3 = (\alpha_{m1} \ \alpha_{m2} \ \alpha_{m3})$  is the channel coefficients vector,  $\mathbf{n}_3 = (n_1 \ n_2 \ n_3 \ n_4)^T$  is the complex AWGN vector, and  $()^T$  represents the matrix transpose operation. Substituting the received signal into the maximum likelihood decision metric given by Equation (2.1) and simplifying, we derive  $M_i(s_i)$ , the decision metrics for  $s_i$ ,  $1 \leq i \leq 4$  as

$$M_1(s_1) = \sum_{n=1}^3 |\alpha_{mn}|^2 |s_1|^2 - (r_1^{m*} \alpha_{m1} + \alpha_{m2}^* r_2^m + \alpha_{m3}^* r_3^m) s_1 - (r_1^m \alpha_{m1}^* + \alpha_{m2} r_2^{m*} + \alpha_{m3} r_3^{m*}) s_1^* \quad (3.8)$$

$$M_2(s_2) = \sum_{n=1}^3 |\alpha_{mn}|^2 |s_2|^2 - (\alpha_{m1} r_2^{m*} - \alpha_{m2}^* r_1^m - \alpha_{m3}^* r_4^m) s_2 - (\alpha_{m1}^* r_2^m - \alpha_{m2} r_1^{m*} - \alpha_{m3} r_4^{m*}) s_2^* \quad (3.9)$$

$$M_3(s_3) = \sum_{n=1}^3 |\alpha_{mn}|^2 |s_3|^2 - (\alpha_{m1} r_3^{m*} + \alpha_{m2}^* r_4^m - \alpha_{m3}^* r_1^m) s_3 - (\alpha_{m1}^* r_3^m + \alpha_{m2} r_4^{m*} - \alpha_{m3} r_1^{m*}) s_3^* \quad (3.10)$$

$$M_4(s_4) = \sum_{n=1}^3 |\alpha_{mn}|^2 |s_4|^2 - (\alpha_{m1} r_4^{m*} - \alpha_{m2}^* r_3^m + \alpha_{m3}^* r_2^m) s_4 - (\alpha_{m1}^* r_4^m - \alpha_{m2} r_3^{m*} + \alpha_{m3} r_2^{m*}) s_4^* \quad (3.11)$$

In the “triple QPSK” modulation, symbol  $s_3$  depends on  $s_2$  as well as the third two bits and symbols  $s_4$  depends on  $s_1$  as well as the fourth two bits. So the symbols  $s_1$  and  $s_4$  can be detected in pairs; so can  $s_2$  and  $s_3$ . The decision rule can be expressed as

$$\operatorname{argmin}_{(s_1, s_2, s_3, s_4)} \left\{ \sum_{i=1}^4 M_i(s_i) \right\}$$

which is equivalent to a sum of uncorrelated two parts.

$$\operatorname{argmin}_{(s_1, s_4)} \{M_1(s_1) + M_4(s_4)\} + \operatorname{argmin}_{(s_2, s_3)} \{M_2(s_2) + M_3(s_3)\} \quad (3.12)$$

These two parts of the decision metric can be minimized independently without sacrificing the performance, which leads to the minimization of the whole decision metric. When computing the sum of  $M_1(s_1)$  and  $M_4(s_4)$ , we have to use the trellis diagram of the “triple QPSK”. The same calculation also applies to finding the decision metric of the  $(s_2, s_3)$  sequence. The trellis diagram of the “triple QPSK” is illustrated in Figure 3.3, which has memory length of 2.

## 3.2 Performance of the New STBC for Three Transmit Antennas

We have simulated the BER of a wireless communication system with three transmit antennas using the orthogonal STBC, whose transmission matrix is given by Equation (2.22) at different SNRs using Monte Carlo simulation. The single transmit and single receive antenna case is also simulated as a reference. We have also simulated the system with three transmit antennas using the new full rate STBC, with the transmission matrix given by Equation (3.1). The newly proposed “triple QPSK”

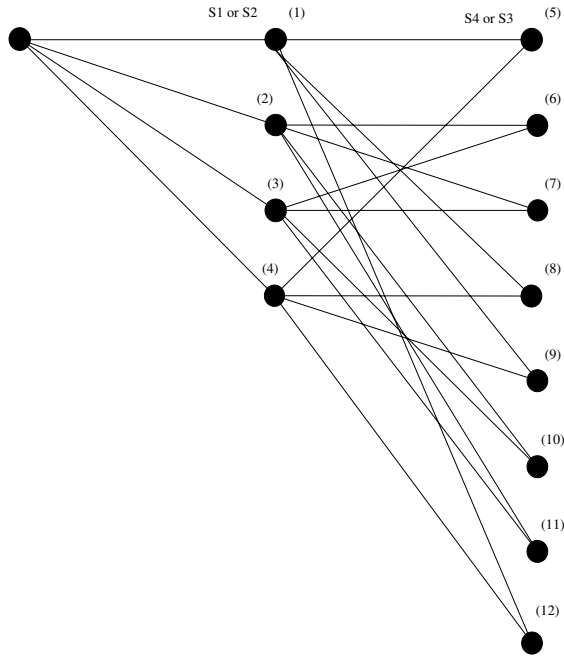


Figure 3.3: Trellis Diagram of the “triple QPSK” Modulation

modulation is used in order to achieve orthogonality. We have used the optimal values of  $R_2$  and  $R_3$  in our simulations. Every symbol of the “triple QPSK” represents 2 data bits. Since the code rate of the new STBC is 1, the spectral efficiency of it using the “triple QPSK” is 2 bit/s/Hz. In the simulation of the orthogonal STBC, QPSK modulation is used, in which each symbol represents 2 data bits. Since the code rate of the orthogonal STBC is  $3/4$ , its spectral efficiency is 1.5 bit/s/Hz. In all of the results presented, the number of receive antennas is one. The proposed

STBC and the “triple QPSK” modulation can be applied when there are more than one receive antennas in the system. There are received signals at all of the receive antennas specified by Equation (1.10). The maximum likelihood decoding algorithm given in Equation (2.1) includes the scenario when  $N_R > 1$ .

One parameter in the Monte Carlo simulation of BER of the wireless communication system is the number of bits transmitted from the transmitter to the receiver. This number of bits used in the simulation is usually determined by the BER level and the confidence interval required in the simulation. The detailed derivation and information on the confidence interval is described in Appendix A. A general that the number of bits should be on the order of  $10/P_e$  is given in Appendix A to reach 90% of confidence interval. In all of the simulations in this dissertation the number of bits at least on the order of  $100/P_e$  is used.

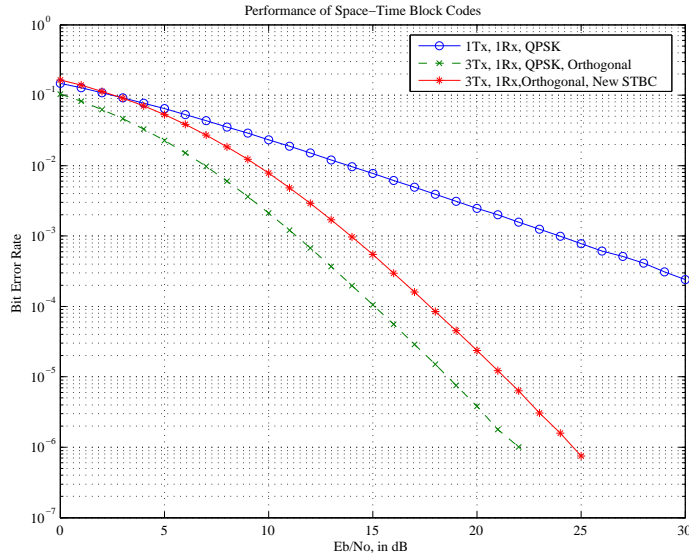


Figure 3.4: BER of Orthogonal STBC and New STBC,  $N_T=3$

The BER versus  $E_b/N_0$  curves are plotted in Figure 3.4. As it is shown in this figure, in the region where SNR is greater than 5 dB, the BER of the new STBC is significantly lower than the BER of the single transmit and single receive antenna

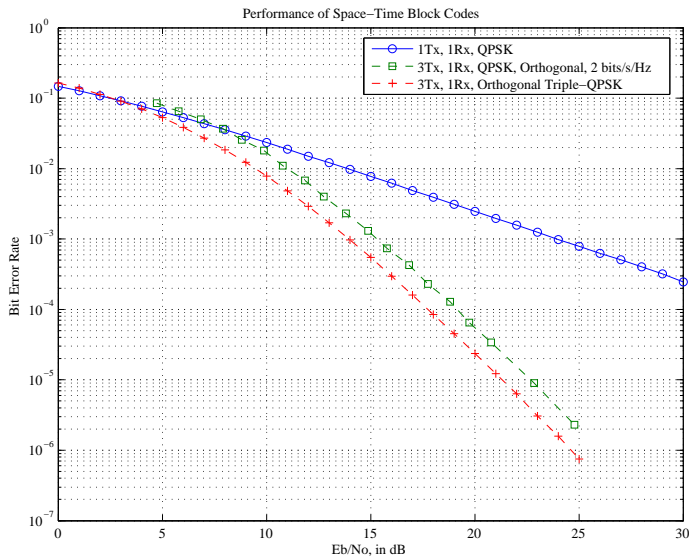


Figure 3.5: BER of New STBC and Orthogonal STBC with Same Rate,  $N_T=3$

system, as expected. At high SNR region, the slope of BER vs. SNR curve of the new STBC is 3, which is the maximum diversity gain a three transmit and one receive antenna system can provide. As it is observed from the plots, the slope of the BER vs.  $E_b/N_0$  curve of the new STBC is the same as the slope of the BER vs.  $E_b/N_0$  curve of the orthogonal STBC, which is known to have full diversity. Thus, the new STBC using the “triple QPSK” achieves full diversity gain over the single transmit and single receive antenna system, as expected.

In Figure 3.4, at equal  $E_b/N_0$ , the BER of the new STBC is higher than the BER of the orthogonal STBC. At BER of  $10^{-3}$ , the required  $E_b/N_0$  for the new STBC is 3 dB higher than that of the orthogonal STBC. This is the price paid to achieve higher spectral efficiency by 33%. In applications where spectral efficiency is desired more than power efficiency, the proposed STBC using the “triple QPSK” modulation is a good choice.

It is interesting to compare the BER versus  $E_b/N_0$  curves when the two STBCs have the same spectral efficiency. The BER performance of an orthogonal STBC

with spectral efficiency of 2 bit/s/Hz is studied in [29] and the resulting BER versus  $E_b/N_0$  curve is plotted in Figure 3.5. In the simulation in [29], a rate 1/2 STBC with 16-QAM modulation is used. At equal BER, the required  $E_b/N_0$  of the new STBC is lower than the required  $E_b/N_0$  of the orthogonal STBC in [29]. At BER value of  $10^{-3}$ , the required  $E_b/N_0$  for the new STBC is 1.4 dB lower than the required  $E_b/N_0$  for the orthogonal STBC in [29], at equal data rates. This is a considerable reduction in the required signal power. In applications where the range of communication is emphasized, the proposed STBC using the “triple QPSK” offers considerably better performance. The BER versus SNR performance curve is influenced by both the coding and modulation schemes.

To find out the probability of error, we consider the pairwise error probability given by Equation (2.13).

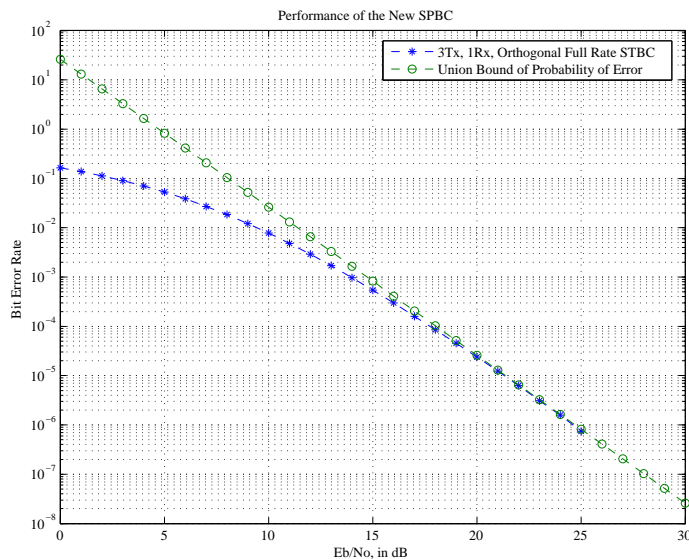


Figure 3.6: Performance of the New Full Rate STBC,  $N_T=3$

Using the union bound analysis, an upper bound of the probability of bit error

can be calculated by

$$P^{(e)} = \sum_{\mathbf{c}} P_{\mathbf{c}} \cdot P_c^{(e)} \leq \sum_{\mathbf{c}} P_{\mathbf{c}} \sum_{\mathbf{e}} \omega_{\mathbf{c} \oplus \mathbf{e}} \cdot P(c \rightarrow e) \quad (3.13)$$

where  $P_{\mathbf{c}}$  is the probability that code  $\mathbf{c}$  is transmitted, which is uniformly distributed by assumption,  $P_c^{(e)}$  is the sum of all of the possible pairwise error probability weighted by the number of bits that are different between code  $\mathbf{c}$  and any other code  $\mathbf{e}$  when code  $\mathbf{c}$  is transmitted, and  $\omega_{\mathbf{c} \oplus \mathbf{e}}$  is the Hamming distance between code  $\mathbf{c}$  and  $\mathbf{e}$ .

The upper bound of the probability of a bit error is plotted in Figure 3.6. For comparison, the BER vs.  $E_b/N_0$  obtained from Monte Carlo simulation is also plotted in Figure 3.6. As seen in Figure 3.6, the upper bound of the probability of bit error is loose at low signal to noise ratio but becomes tighter in middle to high signal to noise ratios. The looseness of the union bound at the low SNR region is expected.

The upper bound on the bit error probability also indicates that the new STBC using “triple QPSK” modulation achieves full diversity gain over single transmit single receive antenna system when used over Rayleigh fading channels. The slope of the bit error probability versus SNR curve is 3, i.e. the maximum diversity available to a MIMO system with three transmit and one receive antenna. To analytically verify the diversity achieved by this new STBC with “triple-QPSK” modulation, we have constructed the matrix  $\mathbf{A} = \mathbf{B}\mathbf{B}^H$ , where matrix  $\mathbf{B}$  is given by Equation (2.7), using all possible code combinations of  $\mathbf{c}$  and  $\mathbf{e}$ . By checking the rank of matrix  $\mathbf{A}$  for all cases we have shown that this scheme achieves maximum diversity.

### 3.3 New STBC for Four Transmit Antennas

The quasi-orthogonal STBCs have rate 1 and this allows them to fully utilize the resources available in a MIMO system. These codes are primarily designed for four transmit antennas although they can be expanded for any  $2^i$  number of transmit antennas, where  $i$  is a positive integer greater than one. The rules on constructing

the transmission matrix of quasi-orthogonal STBCs are developed and their properties are analyzed in [24], [30]. One property that is particularly helpful here is how to change the position of the symbols in the transmission matrix so that the non-zero off diagonal terms in the product of the Hermitian transpose of the transmission matrix and the transmission matrix itself, can be placed in the desired off diagonal locations. We also would like to take advantage of the proposed “triple QPSK” modulation to transfer some of the quasi-orthogonal STBCs to orthogonal STBCs. To this end, we would like the non-zero off diagonal terms to have the same expression in terms of symbols as those studied in the previous sections. The expression of the non-zero off diagonal terms, in terms of the transmission symbols, can also be changed to what we want by using computer search. Based on these rules and the order of symbols  $s_i$ ,  $1 \leq i \leq 4$ , we need in our “triple-QPSK” modulation proposed in the previous sections, we propose the following quasi-orthogonal STBC

$$\mathbf{G}_{qon} = \begin{pmatrix} s_1 & s_4 & s_3 & s_2 \\ -s_4 & s_1 & -s_2 & s_3 \\ -s_3^* & s_2^* & s_1^* & -s_4^* \\ -s_2^* & -s_3^* & s_4^* & s_1^* \end{pmatrix} \quad (3.14)$$

To check whether this STBC is orthogonal or not, we consider the product matrix

$$\begin{aligned} \mathbf{D}_{qon} &= \mathbf{G}_{qon}^H \mathbf{G}_{qon} \\ &= \begin{pmatrix} d & g & 0 & 0 \\ -g & d & 0 & 0 \\ 0 & 0 & d & g \\ 0 & 0 & -g & d \end{pmatrix} \end{aligned} \quad (3.15)$$

where  $d = \sum_{i=1}^4 |s_i|^2$  and  $g = s_1 s_4^* - s_4 s_1^* + s_2 s_3^* - s_3 s_2^*$ . The non-zero off diagonal term  $g$  has the same expression as the non-zero off diagonal term  $d_{23}$  in previous sections and the term  $g$  can be made zero when the “triple QPSK” modulation is used to generate

the symbols. The non-zero off-diagonal terms in matrix  $\mathbf{D}_{qon}$  introduce coupling effects between the symbols transmitted on different antennas during different symbol periods. To make the matrix  $\mathbf{D}_{qon}$  diagonal, we modulate the data and generate the symbols  $s_i, i = 1, 2, 3, 4$  using the proposed “triple-QPSK” modulation. As it is shown previously, the off-diagonal terms  $g$  equals to zero when the “triple-QPSK” modulation is used.

From Equations (1.7) and (3.14), the received signal can be expressed as

$$\mathbf{r}_4 = \mathbf{G}_{qno}\mathbf{h}_4^T + \mathbf{n}_4 \quad (3.16)$$

where  $\mathbf{r}_4 = (r_1^m \ r_2^m \ r_3^m \ r_4^m)^T$  is the received signal vector,  $\mathbf{G}_{qno}$  is given in Equation (3.14),  $\mathbf{h}_4 = (\alpha_{m1} \ \alpha_{m2} \ \alpha_{m3} \ \alpha_{m4})$  is the channel coefficients vector, and  $\mathbf{n}_4 = (n_1 \ n_2 \ n_3 \ n_4)^T$  is the complex AWGN vector. The ML decision metrics,  $M_i(s_i)$ , are

$$M_i(s_i) = \sum_{n=1}^4 |\alpha_{mn}|^2 |s_i|^2 - \psi_i s_i - \psi_i^* s_i^* \quad (3.17)$$

where  $\psi_i, i = 1, 2, 3, 4$  are given by

$$\psi_1 = \alpha_{m1} r_1^{m*} + \alpha_{m2} r_2^{m*} + \alpha_{m3}^* r_3^m + \alpha_{m4}^* r_4^m \quad (3.18)$$

$$\psi_2 = \alpha_{m1}^* r_4^m - \alpha_{m2}^* r_3^m + \alpha_{m3} r_2^{m*} - \alpha_{m4} r_1^{m*} \quad (3.19)$$

$$\psi_3 = \alpha_{m1}^* r_3^m + \alpha_{m2}^* r_4^m - \alpha_{m3} r_1^{m*} - \alpha_{m4} r_2^{m*} \quad (3.20)$$

$$\psi_4 = \alpha_{m1} r_2^{m*} - \alpha_{m2} r_1^{m*} - \alpha_{m3}^* r_4^m + \alpha_{m4}^* r_3^m \quad (3.21)$$

In the “triple QPSK” modulation, symbol  $s_3$  depends on  $s_2$  as well as the third two bits and symbols  $s_4$  depends on  $s_1$  as well as the fourth two bits. Therefore, symbols  $s_1$  and  $s_4$  can be detected in pairs; as can  $s_2$  and  $s_3$ . The decision rule can

be expressed as

$$\operatorname{argmin}_{(s_1, s_2, s_3, s_4)} \left\{ \sum_{i=1}^4 M_i(s_i) \right\}$$

which is equivalent to a sum of two uncorrelated parts.

$$\operatorname{argmin}_{(s_1, s_4)} \{M_1(s_1) + M_4(s_4)\} + \operatorname{argmin}_{(s_2, s_3)} \{M_2(s_2) + M_3(s_3)\} \quad (3.22)$$

These two parts in the decision metric can be minimized independently, which will result in the minimization of the decision metric and the performance of the maximum likelihood detection rule will not be sacrificed. As it is the case in the three transmit antenna scenario, we have to use the trellis diagram of the “triple QPSK” modulation, illustrated in Figure 3.3, when the decision metrics of  $(s_1, s_4)$  and  $(s_2, s_3)$  are calculated.

### 3.4 Performance of the New STBC for Four Transmit Antennas

We have simulated the performance of the proposed STBC for four transmit antennas using “triple-QPSK” modulation over a Rayleigh fading channel. We go through the optimization process to choose the values of  $R_2$  and  $R_3$  that make the required  $E_b/N_0$  the lowest to achieve BER at  $10^{-4}$  on the BER versus  $E_b/N_0$  curve. The optimal values are  $R_2 = 0.55$  and  $R_3 = 1.6$ , equal to the optimal values of  $R_2$  and  $R_3$  respectively for three transmit antennas. The optimal values for  $R_2$  and  $R_3$  are used in our simulations. The BER at different SNRs is obtained using Monte Carlo simulation. The quasi-orthogonal STBC [24] specified by Equation (2.24) is also simulated. We have also simulated the orthogonal STBC with four transmit antennas given in Equation (2.23) [5] as well as the single transmit-receive antenna case for reference. Regular QPSK modulation scheme with Gray mapping is used in the quasi-orthogonal STBC, orthogonal STBC, and single antenna systems. The

quasi static Rayleigh channel model with CSI available at the receiver is used for simulations. In all cases it is assumed that there exists a single receive antenna. The extension of the system that have more than one receive antennas is straight forward. The system model is given by Equation (1.10) and the maximum likelihood detection algorithm is specified by Equation (2.1).

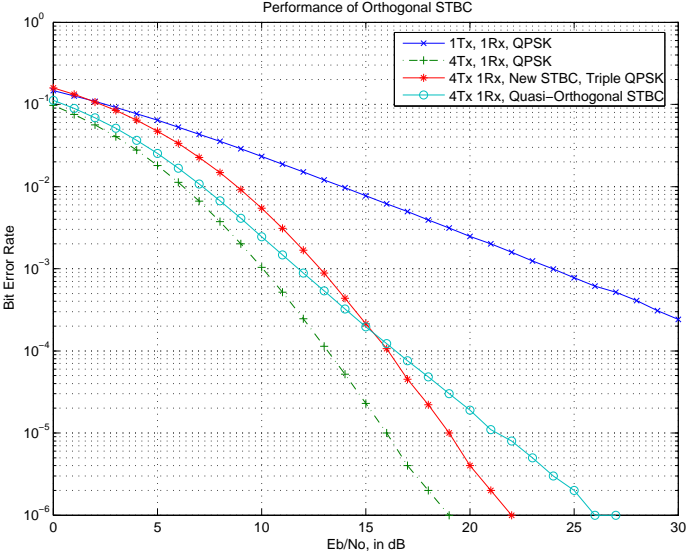


Figure 3.7: BER of Quasi-Orthogonal STBC and New STBC,  $N_T = 4$

The BER vs.  $E_b/N_0$  curves are illustrated in Figure 3.7. The BER of the proposed scheme is higher than the BER of the quasi-orthogonal STBC when  $E_b/N_0$  is less than 15 dB, however, at higher SNR's the BER of the proposed scheme becomes lower than the BER of the quasi-orthogonal STBC. The proposed scheme achieves diversity of 4, which is full diversity for a MIMO system with  $N_T = 4$  and  $N_R = 1$ , compared to the quasi-orthogonal STBC that has diversity of 2 [24]. This is the reason why the proposed scheme has a better performance than the quasi-orthogonal STBC at high SNR's.

It is noticed that the proposed scheme achieves the same full diversity of order 4 as the orthogonal STBC does. But the required  $E_b/N_0$  to reach BER of  $10^{-3}$  is about

3 dB higher in the proposed scheme. This is the price to achieve the 33% higher spectral efficiency in the proposed scheme. The proposed STBC provides a high rate alternative in system design for MIMO system with four transmit antennas.

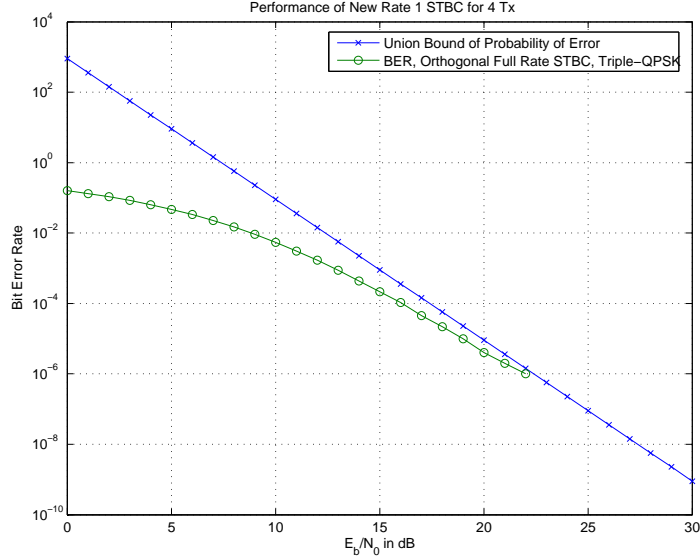


Figure 3.8: Performance of the New Full Rate STBC,  $N_T = 4$

Using the formula specified by Equation (3.13), the results of the upper bound of probability of bit error are calculated and plotted in Figure 3.8. For comparison, the BER vs.  $E_b/N_0$  from simulation is also plotted in the same figure. As it is seen, the upper bound of the probability of bit error is loose in low  $E_b/N_0$  region but matches the BER results obtained from simulation very well in the moderate to high  $E_b/N_0$  region.

The upper bound of the bit error probability also indicates that this new STBC using the “triple-QPSK” achieves full diversity gain over single transmit single receive antenna system under the Rayleigh fading channel. The slope of the probability of bit error versus SNR curve is 4, which is the maximum diversity available to a MIMO system with four transmit and one receive antenna. We have also constructed matrix  $\mathbf{A}$ , where  $\mathbf{A} = \mathbf{B}^H \mathbf{B}$ , and matrix  $\mathbf{B}$  is given in Equation (2.7), for all of the possible

pairs of code words  $\mathbf{c}$  and  $\mathbf{e}$  in the STBC codebook. In all cases the rank of  $\mathbf{A}$  is 4 indicating that this STBC using the “triple-QPSK” achieves full diversity.

# Chapter 4

## Performance of Space-Time Block Codes with Imperfect Channel Information

So far, we have assumed that the CSI is perfectly known to the receiver although not known to the transmitter in the MIMO system. In practical MIMO wireless communication systems, the receiver usually does not have the information of the CSI and estimates the CSI through the known signals from the transmitter such as pilot signals or training symbols. The estimated CSI, which is not perfect and is noisy, is what the receiver uses to detect the symbols. This may result in the performance degradation of the STBCs we studied in the last Chapter. Thus, in this Chapter we consider modeling of the estimation error of the CSI and its effects on the performance of the STBCs.

### 4.1 Performance of STBC with Noisy CSI

In wireless communication systems, normally there is a channel estimator in the receiver and the channel estimator extracts from the received signal an estimate of

the fading channel coefficients during each data frame. One method for channel estimation is to turn off all transmit antennas except transmit antenna  $n$  and to send a pilot signal on antenna  $n$  [31]. By this method channel coefficients  $\alpha_{m,n}$  are estimated for  $1 \leq m \leq N_R$ . This procedure can be repeated for  $1 \leq n \leq N_T$  until all of the channel coefficients  $\alpha_{m,n}, m = 1, 2, \dots, N_R, n = 1, 2, \dots, N_T$  are estimated. An alternative method to estimate channel coefficients is to use orthogonal signal sequences, e.g., the Walsh sequences, for pilot signals one sent from each transmit antenna.

No matter what method is used to estimate channel coefficients, the channel estimator generates channel estimates  $\hat{\alpha}_{m,n}$  for channel coefficients  $\alpha_{m,n}, m = 1, 2, \dots, N_R, n = 1, 2, \dots, N_T$ , which are usually not their exact value. The channel coefficients  $\alpha_{m,n}, m = 1, 2, \dots, N_R, n = 1, 2, \dots, N_T$  are modeled as complex Gaussian random variables with zero mean and unit variance. We can assume that  $\hat{\alpha}_{m,n}$  is a zero mean complex Gaussian random variable dependent only on  $\alpha_{m,n}$  with correlation coefficient  $\mu$  [31]. In general we may assume that

$$\hat{\alpha}_{m,n} = \alpha_{m,n} + \epsilon_{m,n} \quad (4.1)$$

where  $\epsilon_{m,n}$  is the channel estimation error. It is reasonable to assume that  $\epsilon_{m,n}$  is a complex Gaussian random variable with mean zero and variance  $\sigma_\epsilon^2$ . We can also assume that  $\epsilon_{m,n}$  is independent of  $\alpha_{m,n}$ . The correlation coefficient  $\mu$  between  $\hat{\alpha}_{m,n}$  and  $\alpha_{m,n}$  has a simple expression in terms of  $\sigma_\epsilon^2$  given by

$$\mu = \frac{1}{\sqrt{1 + \sigma_\epsilon^2}} \quad (4.2)$$

Generally speaking,  $\sigma_\epsilon^2$  is a small real positive number at reasonable SNR values and this makes  $\mu$  close to one.

During each frame, the estimate of the channel coefficients,  $\hat{\alpha}_{m,n}$ , rather than the

channel coefficients themselves are available to the receiver and these values are being used for signal detection. Let us examine the pairwise error probability when the channel estimate  $\hat{\alpha}_{m,n}$  is used at the detector. Assume that a code word  $\mathbf{c} = c_1^1 c_1^2 \cdots c_1^{N_T} c_2^1 c_2^2 \cdots c_2^{N_T} \cdots c_l^1 c_l^2 \cdots c_l^{N_T}$  is transmitted. The probability that the maximum likelihood receiver decides in favor of another code  $\mathbf{e} = e_1^1 e_1^2 \cdots e_1^{N_T} e_2^1 e_2^2 \cdots e_2^{N_T} \cdots e_l^1 e_l^2 \cdots e_l^{N_T}$  is given by [31]

$$P(\mathbf{c} \rightarrow \mathbf{e} | \hat{\alpha}_{m,n}, m = 1, 2, \dots, N_R, n = 1, 2, \dots, N_T) \leq \exp \left( -\mu^2 d^2(c, e) \frac{E_s}{4N_0 + 4N_T(1 - |\mu|^2)E_s} \right) \quad (4.3)$$

where  $N_0/2$  is the noise variance per dimension and

$$d^2(\mathbf{c}, \mathbf{e}) = \sum_{m=1}^{N_R} \sum_{t=1}^l \left| \sum_{n=1}^{N_T} \left( \hat{\alpha}_{m,n} / \sqrt{2\sigma} \right) (c_t^n - e_t^n) \right|^2 \quad (4.4)$$

where  $2\sigma^2$  is the variance of  $\hat{\alpha}_{m,n}$ . Although this pairwise error probability is derived for the STBC using modulation that has signal constellation with equal energy [31], we can apply this pairwise error probability to our STBC with the ‘‘triple QPSK’’ modulation through the relationship in the signal constellation energy specified in Equation (3.6). After some manipulation [31], the pairwise error probability can be bounded as

$$P(\mathbf{c} \rightarrow \mathbf{e}) \leq \left( \prod_{i=1}^r \lambda_i \right)^{-N_R} \left( \frac{|\mu|^2 (E_s / 4N_0)}{1 + N_T(1 - |\mu|^2)(E_s / N_0)} \right)^{-rN_R} \quad (4.5)$$

where  $\lambda_i, i = 1, 2, \dots, r$  are eigenvalues of matrix  $\mathbf{A} = \mathbf{B}\mathbf{B}^H$ , where matrix  $\mathbf{B}$  is given in Equation (2.7), and  $r$  is the rank of matrix  $\mathbf{A}$ . The matrix rank is given by  $r = N_T$  when matrix  $\mathbf{A}$  is full rank. It is obvious that the design criteria of maximizing the rank of matrix  $\mathbf{A}$  is still valid in the presence of channel estimation error. An upper bound for the bit error probability when there is channel estimation error can be found by using Equation (4.5) in Equation (3.13).

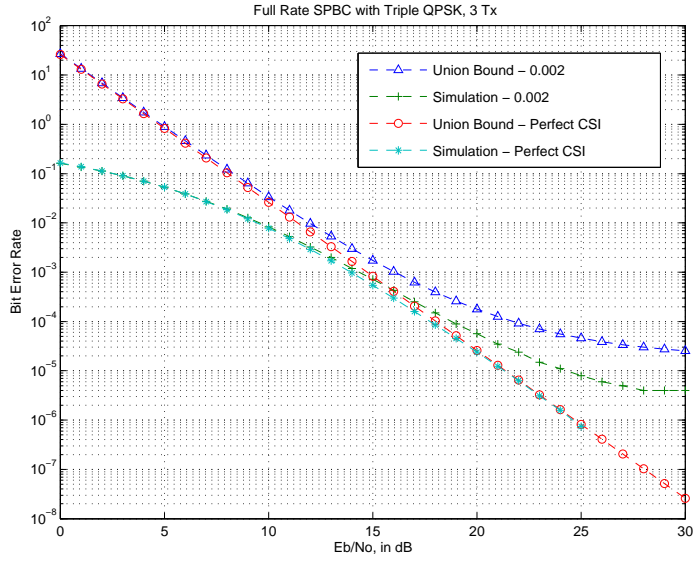


Figure 4.1: Performance of the New STBC with Noisy CSI  $\sigma_\epsilon^2 = 0.2\%$ ,  $N_T=3$

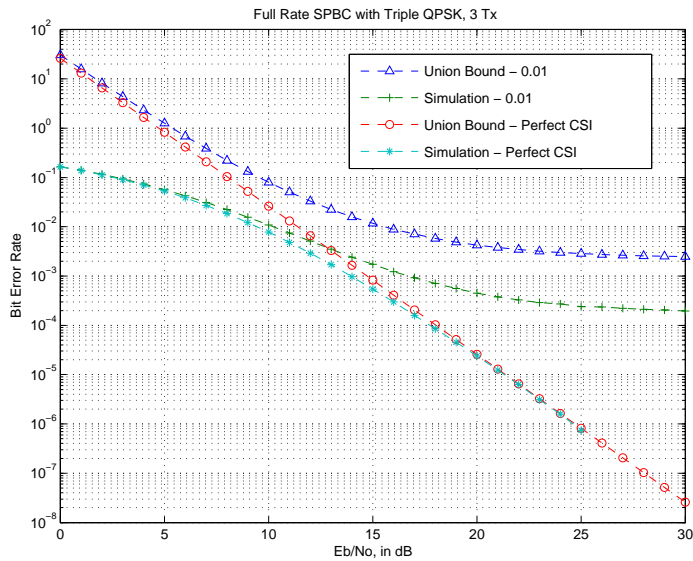


Figure 4.2: Performance of the New STBC with Noisy CSI  $\sigma_\epsilon^2 = 1\%$ ,  $N_T=3$

We have simulated the new STBC with the “triple QPSK” modulation using channel estimates at the receiver. The channel estimates are modeled by Equation (4.1).

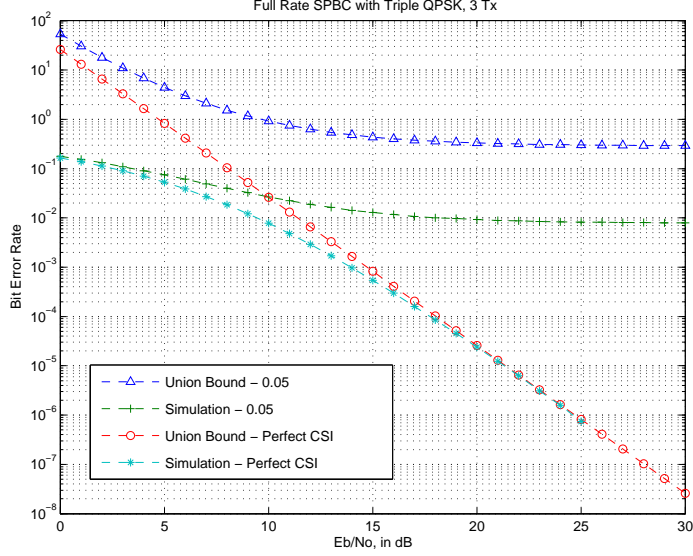


Figure 4.3: Performance of the New STBC with Noisy CSI  $\sigma_\epsilon^2 = 5\%$ ,  $N_T=3$

In this simulation, the channel is still a quasi-static fading channel so the CSI,  $\alpha_{m,n}$ , and the channel estimate,  $\hat{\alpha}_{m,n}$ , stays constant during one frame period. The CSI and its estimate change independently from frame to frame. The BER is calculated via Monte Carlo simulation and the upper bound on the bit error probability is calculated using Equation (4.5) and (3.13).

The variance of the channel estimation error  $\sigma_\epsilon^2$  is used to model the accuracy of the channel estimation. In this study, the variance of channel estimation error is selected to be  $\sigma_\epsilon^2 = 0.2\%, 1\%, 5\%$ . Because the variance of the channel coefficients is 1, the variance of the channel estimation error correspond to  $\sigma_\epsilon^2 = -27dB, -20dB, -13dB$  respectively. For three transmit antennas  $N_T = 3$ , the BER and the probability of bit error bound versus  $E_b/N_0$  are given in Figures 4.1 - 4.3. The BER and the upper bound of the probability of bit error versus SNR, which is first presented in Figures 3.6, are also plotted in Figures 4.1 - 4.3 for comparison. Both the BER and the bit error probability bound decrease as  $E_b/N_0$  increases, but they reach an error floor at high  $E_b/N_0$  due to the presence of the channel estimation error. The diversity

order achieved by the STBCs with perfect CSI at the receiver is compromised by the channel estimation error. At the equal  $E_b/N_0$  value, the BER and the probability of bit error bound increase when the channel estimation error,  $\sigma_\epsilon^2$  increases. At BER equal to  $10^{-3}$  level, the SNR loss is 0.5 dB when  $\sigma_\epsilon^2 = -27dB$  and the SNR loss is 2.7 dB when  $\sigma_\epsilon^2 = -20dB$ .

There is a gap between the analytical upper bound of the probability of bit error and the BER obtained from simulation. As the error in channel estimation,  $\sigma_\epsilon^2$  increases, this gap also increases. Since the correlation coefficient  $\mu$  decreases when the channel estimation error,  $\sigma_\epsilon^2$ , increases, the pairwise error probability specified in Equation (4.5) will also increase. These effects lead to the upper bound of the bit error probability to increase further.

For the STBC with four transmit antennas,  $N_T = 4$ , the BER and the upper bound of the probability of bit error versus  $E_b/N_0$  are shown in Figure 4.4 and Figure 4.5 for channel estimation error  $\sigma_\epsilon^2 = 0.2\%$  and  $\sigma_\epsilon^2 = 1\%$  respectively. The upper bound of the probability of bit error and the BER versus SNR when perfect CSI is available are also plotted in Figure 4.4 and 4.5 for comparison. The BER performance is affected by the channel estimation error and reaches an error floor at high  $E_b/N_0$ . At BER equal to  $10^{-3}$  level, the SNR loss is 0.3 dB when  $\sigma_\epsilon^2 = -27dB$  and the SNR loss is 2.0 dB when  $\sigma_\epsilon^2 = -20dB$ . At BER value of  $10^{-3}$ , the SNR loss when  $N_T = 4$  is smaller than the SNR loss when  $N_T = 3$  due to noisy CSI.

## 4.2 Performance of Alamouti STBC with Noisy CSI using QPSK

A low complexity linear combining scheme is presented in [15] and it is shown that this linear combining scheme is equivalent to the maximum-likelihood symbol detection when the channel is quasi-static and CSI is known at the receiver. This linear

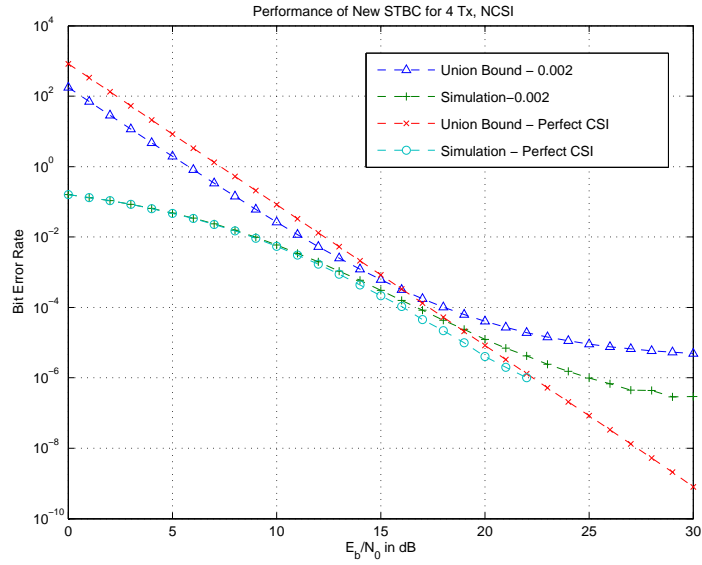


Figure 4.4: Performance of the New STBC with Noisy CSI  $\sigma_\epsilon^2 = 0.2\%$ ,  $N_T=4$

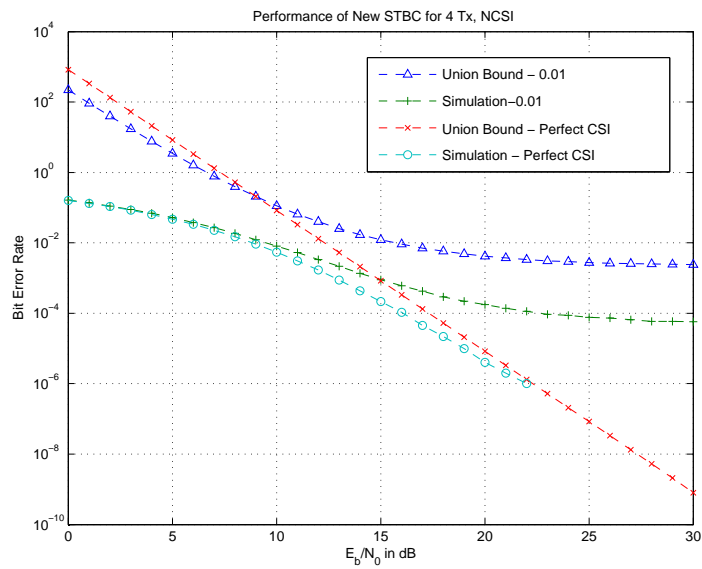


Figure 4.5: Performance of the New STBC with Noisy CSI  $\sigma_\epsilon^2 = 1\%$ ,  $N_T=4$

combining scheme can achieve the same performance as the maximum ratio combining of the diversity branches and the maximum likelihood (ML) space-time decoder.

In this work we focus on the space-time block coding scheme introduced in [15]. In all analysis that indicate the performance gain of STBC, it is assumed that CSI is available at the receiver.

In actual wireless communication systems, the channels are not quasi-static and this makes it hard for the linear combining scheme to eliminate interference completely even when perfect CSI [32], [33] is available, resulting in performance degradation of linear combining schemes. It is suggested that an interference suppression technique combined with ML detection algorithm to be used when channel is not quasi-static [32], [34]. In practical wireless systems, CSI usually is known neither at the receiver nor at the transmitter. In this scenario, the CSI can be estimated through transmission of pilot signals resulting in some error in estimation of CSI at the receiver due to channel impairments such as time-varying channel fading, spatial correlation of transmit antennas and noise on the pilot channel. The error in estimation of CSI results in performance degradation of the coherent linear combining detection scheme proposed in the Alamouti scheme [35], [36] and [37]. It is shown that the linear combining scheme can not completely cancel the interference from the other symbols if imperfect channel estimates are used at the receiver [33]-[38].

The analytical performance of a zero-forcing and a decision-feedback detector assuming perfect CSI for the non-quasi-static fading channel model was derived in [34]. Analysis of the performance of STBC assuming noisy CSI using a quasi-static channel model were given in [33] - [38]. Analysis on the performance of space-time codes over spatially correlated Rayleigh fading channels were presented in [35] - [37]. However, these studies have focused on each of the factors affecting the performance of the Alamouti scheme individually. Factors, such as noisy CSI, Doppler frequency shift, spatial correlation of transmit antennas and quasi-static assumption of channel characteristics, have a close relationship. It is desirable to consider them all in the performance analysis of the space time block codes.

An analysis of the space-time transmit diversity (STTD) system over a rapidly fading Rayleigh channel with imperfect channel state information is presented in

[39], [40]. This analysis takes into account imperfect CSI, the Doppler frequency shift, spatial correlation and the time-varying fading channel. In [39], [40] the STBC scheme originally proposed in [15] is considered under the assumption that a BPSK modulation is used. In this work, we extend the analysis of the STTD system with imperfect CSI under rapid Rayleigh fading channel assuming that the STBC scheme proposed in [15] is used with QPSK modulation. Since we are interested in the space time block codes from complex designs, complex modulation schemes will be used and investigated.

### 4.2.1 System Model

The system we investigate is the downlink DS-CDMA wireless communication system using the QPSK modulation. There are two transmit antennas at the base station and one receive antenna at the mobile station. The data sequences transmitted from the two transmit antennas are space-time encoded according to the STBC scheme proposed in [15]. Two distinct pilot sequences are transmitted from the two antennas. The spreading gains on the pilot and data channels are assumed to be the same and the symbol period is denoted by  $\tau$ .

The signal constellation of the QPSK modulation take values in the set  $\{\frac{1}{2}(\pm 1 \pm j)\}$  and the pilot symbols are selected from the set  $\{\frac{1}{2}(\pm 1 + j)\}$ . To facilitate the analysis, we rotate the coordinate system by  $\pi/4$  and form the new coordinate denoted by  $I$  and  $Q$  [41]. In the  $I$  and  $Q$  coordinates, the values of the data symbols are in the set  $\{\pm 1, \pm j\}$  and the pilot symbols take value from the set  $\{1, j\}$ .

The channels are assumed to be time-varying Rayleigh fading channels. Let the channel coefficient between the transmit antennas I and II and the receive antenna during symbol period  $k'$  be denoted by  $\alpha_{k'}$  and  $\beta_{k'}$ , respectively. Since the channel is assumed to be Rayleigh fading,  $\alpha_{k'}$  and  $\beta_{k'}$  are circularly symmetric zero mean complex Gaussian random variables. The autocorrelation functions of  $\alpha_{k'}$  and  $\beta_{k'}$ , assumed to be identical, can be expressed as  $\frac{1}{2}E[\alpha_{k'}\alpha_{k'-m'}^*] = \frac{1}{2}E[\beta_{k'}\beta_{k'-m'}^*] =$

Table 4.1: Modified STBC for 2 Tx Antennas

| Symbol Time | Antenna I | Antenna II |
|-------------|-----------|------------|
| 1           | $s_1$     | $-s_2^*$   |
| 2           | $s_2$     | $s_1^*$    |

$\sigma_c^2 R(m'\tau)$ , where  $R(0)$  is normalized to unity. The cross-correlation between  $\alpha_{k'}$  and  $\beta_{k'}$  is given as  $\frac{1}{2}E[\alpha_{k'}\beta_{k'-m'}^*] = \rho'\sigma_c^2 R(m'\tau)$ , where  $\rho'$  represents the spatial correlation between the two transmit antennas. The channel coefficients are assumed to be constant during one symbol period  $\tau$ .

The transmitted sequence is space-time encoded by the modified STBC scheme for two transmit antennas [16], [17], [21], which was originally proposed in [15]. The modified STBC encoding scheme is given in Table 4.1 which is the scheme used in industry [16], [17], [21]. Since two symbols are processed by the STBC encoder at a time, we can consider only two symbol periods of the transmission and detection process without loss of generality.

## 4.2.2 Performance Analysis of STBC

We denote the transmitted energy per pilot and data symbols by  $E_{p'}$  and  $E_s$ , respectively. Then, the transmitted energy per pilot and data symbols per transmit antenna will be  $E_{p'}/2$  and  $E_s/2$ , respectively. The baseband representation of the received data signals can be expressed as

$$\begin{aligned} \mathbf{r}_{s,k'} &= \begin{bmatrix} r_{s,2k'+1} \\ r_{s,2k'+2}^* \end{bmatrix} \\ &= \sqrt{\frac{E_s}{2}} \begin{bmatrix} \alpha_{2k'+1} & -\beta_{2k'+1} \\ \beta_{2k'+2}^* & \alpha_{2k'+2}^* \end{bmatrix} \begin{bmatrix} s_{2k'+1} \\ s_{2k'+2}^* \end{bmatrix} + \begin{bmatrix} n_{s,2k'+1} \\ n_{s,2k'+2}^* \end{bmatrix} \end{aligned} \quad (4.6)$$

where the subscript  $k'$  denotes symbol time index, the subscript  $s$  indicates the data channel,  $r_{s,k'}$  represents the received data signal during the symbol time index  $k'$  and the  $n_{s,k'}$  represents the zero mean circular symmetric complex Gaussian noise with variance  $\sigma_s^2$  on the data channel.

On the pilot channel, the pilot signal is used to estimate the channel coefficients using an FIR filter with  $(2M + 1)$  taps. The received pilot signals on channels I and II can be written in a vector form as,  $\mathbf{r}_{p',k'}^1 = [r_{p',k'-M}^1, \dots, r_{p',k'}^1, \dots, r_{p',k'+M}^1]^T$  and  $\mathbf{r}_{p',k'}^2 = [r_{p',k'-M}^2, \dots, r_{p',k'}^2, \dots, r_{p',k'+M}^2]^T$ , respectively, where the  $T$  denotes the matrix transpose operation and the individual element can be expressed as

$$r_{p',k'}^1 = \sqrt{\frac{E_{p'}}{2}} \alpha_{k'} + n_{p',k'}^1 \quad (4.7)$$

$$r_{p',k'}^2 = \sqrt{\frac{E_{p'}}{2}} \beta_{k'} + n_{p',k'}^2 \quad (4.8)$$

where  $n_{p',k'}^1$  and  $n_{p',k'}^2$  are the zero mean circular symmetric complex Gaussian random variables with variance  $\sigma_{p'}^2$  denoting the noise on pilot channel I and II, respectively. The received pilot signals are sent to an FIR filter with  $(2M + 1)$  taps to generate the estimates of the channel coefficients. The resulting estimates are

$$\hat{\alpha}_{k'} = \mathbf{h}^H \cdot \mathbf{r}_{p',k'}^1 \quad \hat{\beta}_{k'} = \mathbf{h}^H \cdot \mathbf{r}_{p',k'}^2 \quad (4.9)$$

where  $\mathbf{h} = [h_M \cdots h_0 \cdots h_{-M}]^T$  represent the filter coefficients and  $()^H$  represents the Hermitian transpose of a matrix. This framework is general enough that the value of  $\mathbf{h}$  can be obtained from any linear estimation algorithm. In this work, a Wiener filter with  $(2M + 1)$  taps is employed to estimate the channel coefficients. Applying the Wiener filter design results [42],

$$\frac{1}{2} E [\mathbf{r}_{p',k'}^1 (\mathbf{r}_{p',k'}^1)^H] \mathbf{h} = \frac{1}{2} E \left[ \sqrt{\frac{E_{p'}}{2}} \alpha_{k'}^* \mathbf{r}_{p',k'}^1 \right] \quad (4.10)$$

$$\frac{1}{2}E [\mathbf{r}_{p',k'}^2(\mathbf{r}_{p',k'}^2)^H] \mathbf{h} = \frac{1}{2}E \left[ \sqrt{\frac{E_{p'}}{2}} \beta_{k'}^* \mathbf{r}_{p',k'}^2 \right] \quad (4.11)$$

the filter coefficients can be found as

$$\mathbf{h} = \sqrt{\frac{2}{E_{p'}}} \left( \mathbf{D}_0 + \frac{2}{\bar{\gamma}_{p'}} \mathbf{I}_{2M+1} \right)^{-1} \mathbf{w}_0 \quad (4.12)$$

where  $\bar{\gamma}_{p'} = E_{p'}\sigma_c^2/\sigma_p^2$  is the SNR on the pilot channel,  $\mathbf{I}_{2M+1}$  is the identity matrix, matrix  $\mathbf{D}_0$  is derived from the square matrix  $\mathbf{D}_e$  of dimension  $2M+1$ , whose elements are  $D_e(m', n') = R((e+m'-n')\tau)$ , and  $\mathbf{w}_0$  is derived from  $\mathbf{w}_e$ , which is the  $(M+1)^{th}$  column of  $\mathbf{D}_e$  when  $e = 0$ .

The linear combining scheme generates the decision statistics for the detection of data symbols by employing the estimates of the CSI [15], and this process during symbol time index 1 and 2 can be described as

$$\begin{aligned} \begin{bmatrix} z_1 \\ z_2^* \end{bmatrix} &= \begin{bmatrix} \hat{\alpha}_1^* & \hat{\beta}_2 \\ -\hat{\beta}_1^* & \hat{\alpha}_2 \end{bmatrix} \mathbf{r}_{s,1} \\ &= \frac{E_s}{2} \mathbf{G} \begin{bmatrix} s_1 \\ s_2^* \end{bmatrix} + \begin{bmatrix} \tilde{n}_{s,1} \\ \tilde{n}_{s,2} \end{bmatrix} \end{aligned} \quad (4.13)$$

where  $z_1$  and  $z_2$  are the decision statistics generated from the linear combining schemes for the first and second data symbols, respectively, the noise terms are  $\tilde{n}_{s,1} = \hat{\alpha}_1^* n_{s,1} + \hat{\beta}_2 n_{s,2}^*$ ,  $\tilde{n}_{s,2} = \hat{\beta}_1^* n_{s,1} + \hat{\alpha}_2 n_{s,2}^*$  and the composite channel gain  $\mathbf{G}$  can be expressed as

$$\mathbf{G} = \begin{bmatrix} \alpha_1 \hat{\alpha}_1^* + \beta_2^* \hat{\beta}_2 & \alpha_2^* \hat{\beta}_2 - \beta_1 \hat{\alpha}_1^* \\ \beta_2^* \hat{\alpha}_2 - \alpha_1 \hat{\beta}_1^* & \beta_1 \hat{\beta}_1^* + \alpha_2^* \hat{\alpha}_2 \end{bmatrix} \quad (4.14)$$

Clearly if perfect CSI is available and the channel is quasi-static then we have  $\hat{\alpha}_1 = \hat{\alpha}_2 = \alpha_1 = \alpha_2$  and  $\hat{\beta}_1 = \hat{\beta}_2 = \beta_1 = \beta_2$  [15]. In this case, the interference from

other symbols can be completely eliminated and Equation (4.14) becomes

$$\mathbf{G} = \begin{bmatrix} |\alpha_1|^2 + |\beta_1|^2 & 0 \\ 0 & |\alpha_1|^2 + |\beta_1|^2 \end{bmatrix} \quad (4.15)$$

In practice, perfect CSI is not available at the receiver and the quasi-static channel condition is not always met. To find the error probability under these assumptions, we first note that the error probability for the first and second symbols are equal, therefore we focus on the error probability for the first symbol. The error probability of the Alamouti scheme using the QPSK modulation can be expressed as

$$P_s = \frac{1}{4}(P_{s,s_2=1} + P_{s,s_2=-1} + P_{s,s_2=j} + P_{s,s_2=-j}) \quad (4.16)$$

where  $P_{s,s_2=a}$  denotes the probability of symbol error given that  $s_2 = a$  and  $a = 1, -1, j, \text{ or } -j$ . From Equation (4.13), the decision statistics generated by the linear combiner corresponding to the first symbol is  $z_1 = \hat{\alpha}_1^* r_{s,1} + \hat{\beta}_2 r_{s,2}^*$ . The real part of  $z_1$  can be written in the quadratic form  $\text{Re}[z_1] = \mathbf{x}^H \mathbf{Q} \mathbf{x}$ , where

$$\mathbf{x} = \begin{bmatrix} r_{s,1} & r_{s,2} & \hat{\alpha}_1 & \hat{\beta}_2 \end{bmatrix}^T \quad (4.17)$$

$$\mathbf{Q} = \frac{1}{2} \begin{pmatrix} \mathbf{0}_2 & \mathbf{I}_2 \\ \mathbf{I}_2 & \mathbf{0}_2 \end{pmatrix} \quad (4.18)$$

Without loss of generality, we assume that  $s_1 = 1$ . The decision criterion is  $\text{Re}[z_1] : 0$  and  $\text{Im}[z_1] : 0$  for QPSK [41]. Then the probability of bit error for the real component can be expressed as [41]

$$P_b = Pr[\mathbf{x}^H \mathbf{Q} \mathbf{x} < 0] \quad (4.19)$$

The probability of bit error for the imaginary component is the same as that for the real component [41]. Thus we only need to calculate the probability of bit error of the

real component when calculating the probability of bit error for QPSK modulation [41]. Because  $\mathbf{x}$  is a zero mean correlated complex Gaussian random vector, the characteristic function of  $\mathbf{x}^H \mathbf{Q} \mathbf{x}$  can be found by [43]

$$\Phi_z(s) = | \mathbf{I}_{m'} - 2s \mathbf{\Sigma} \mathbf{Q} |^{-1} \quad (4.20)$$

where  $\mathbf{\Sigma}$  is the covariance matrix of  $\mathbf{x}$  and  $\mathbf{\Sigma} = \frac{1}{2} E [\mathbf{x} \mathbf{x}^H]$  because the mean of  $\mathbf{x}$  is zero. This equation can be expanded as

$$\mathbf{\Sigma} = \frac{1}{2} E \left( \begin{bmatrix} r_{s,1} \\ r_{s,2} \\ \hat{\alpha}_1 \\ \hat{\beta}_2 \end{bmatrix} \begin{bmatrix} r_{s,1} & r_{s,2} & \hat{\alpha}_1 & \hat{\beta}_2 \end{bmatrix}^* \right) \quad (4.21)$$

After some mathematical manipulations,  $\mathbf{\Sigma}$  can be expressed as

$$\mathbf{\Sigma} = \begin{pmatrix} \mathbf{A}_{11} & \mathbf{A}_{12} \\ \mathbf{A}_{12}^H & \mathbf{A}_{22} \end{pmatrix} \quad (4.22)$$

where

$$\mathbf{A}_{11} = E_s \sigma_c^2 \begin{bmatrix} (1 - \rho'a) + \bar{\gamma}_s^{-1} & 0 \\ 0 & (1 + \rho'a) + \bar{\gamma}_s^{-1} \end{bmatrix} \quad (4.23)$$

$$\mathbf{A}_{12} = \frac{\sqrt{E_s E_{p'} \sigma_c^2}}{2} \begin{bmatrix} \mathbf{w}_0^H \mathbf{h} (1 - \rho'a) & \mathbf{w}_1^H \mathbf{h} (\rho' - a) \\ \mathbf{w}_{-1}^H \mathbf{h} (\rho' + a) & \mathbf{w}_0^H \mathbf{h} (1 + \rho'a) \end{bmatrix} \quad (4.24)$$

$$\mathbf{A}_{22} = \frac{E_{p'} \sigma_c^2}{2} \begin{bmatrix} a_{22} & \rho' \mathbf{h}^h \mathbf{D}_{-1} \mathbf{h} \\ \rho' \mathbf{h}^H \mathbf{D}_1 \mathbf{h} & a_{22} \end{bmatrix} \quad (4.25)$$

where  $\bar{\gamma}_s = E_s \sigma_c^2 / \sigma_c^2$  is the average SNR of the data channel and  $a_{22} = \mathbf{h}^H (\mathbf{D}_0 + 2\bar{\gamma}_{p'}^{-1} \mathbf{I}_{2M+1}) \mathbf{h}$ .

Knowing the covariance matrix  $\mathbf{\Sigma}$ , the bit error probability  $P_b$  can be evaluated by using the eigenvalues of  $2\mathbf{\Sigma}\mathbf{Q}$  [1]. The resulting expression is

$$P_b = P[z < 0] = \int_{\varepsilon-j\infty}^{\varepsilon+j\infty} \frac{j\Phi_z(s)}{2\pi s} ds \quad (4.26)$$

From the residue theorem, this integration can be calculated by

$$P_b = -\text{Res} \left[ \frac{\Phi_z(s)}{s} \text{ at LHP poles} \right] \quad (4.27)$$

and the residue at an  $n^{\text{th}}$  order pole can be calculated by

$$\text{Res}[f(s) \text{ at } a] = \lim_{s \rightarrow a} \frac{p^{(n-1)}(s)}{(n-1)!} \quad (4.28)$$

where  $p(s) = (s - a)^n f(s)$  and  $p^{(n)}(s)$  denotes the  $n^{\text{th}}$  derivative of  $p(s)$ . When the Wiener filter is used for channel estimation, the filter coefficient calculated from Equation (4.12) can be substituted into Equation (4.23) and the sub-matrices within the covariance matrix become

$$\mathbf{A}_{11} = E_s \sigma_c^2 \left( 1 - \frac{1}{2}(a + a^*)\rho' + \bar{\gamma}_s^{-1} \right) \mathbf{I}_2 \quad (4.29)$$

$$\mathbf{A}_{12} = \frac{\sigma_c^2}{2} \sqrt{\frac{E_s}{2}} \begin{bmatrix} \varepsilon_0 & \varepsilon_1(-a^*) \\ \varepsilon_1^* a & \varepsilon_0 \end{bmatrix} \quad (4.30)$$

$$\mathbf{A}_{22} = \sigma_c^2 \frac{\varepsilon_0}{2} \mathbf{I}_2 \quad (4.31)$$

where

$$\begin{aligned} \varepsilon_0 &= \mathbf{w}_0^H (\mathbf{D}_0/2 + \bar{\gamma}_{p'}^{-1} \mathbf{I}_{2M+1})^{-1} \mathbf{w}_0 \\ \varepsilon_1 &= \mathbf{w}_1^H (\mathbf{D}_0/2 + \bar{\gamma}_{p'}^{-1} \mathbf{I}_{2M+1})^{-1} \mathbf{w}_0 \end{aligned} \quad (4.32)$$

Focusing on the special case when there is no spatial correlation between the two

transmit channels and  $\rho' = 0$ , the covariance matrix is simplified to

$$\Sigma = \sigma_c^2 \begin{bmatrix} E_s(1 + \bar{\gamma}_s^{-1})\mathbf{I}_2 & \sqrt{\frac{E_s}{8}} \begin{bmatrix} \varepsilon_0 & -\varepsilon_1 a^* \\ \varepsilon_1^* a & \varepsilon_0 \end{bmatrix} \\ \sqrt{\frac{E_s}{8}} \begin{bmatrix} \varepsilon_0 & \varepsilon_1 a^* \\ -\varepsilon_1^* a & \varepsilon_0 \end{bmatrix} & \frac{\varepsilon_0}{2}\mathbf{I}_2 \end{bmatrix} \quad (4.33)$$

We now can find the eigenvalues of  $2\Sigma\mathbf{Q}$ . It turns out that  $2\Sigma\mathbf{Q}$  has two eigenvalues each of order 2 given by

$$\begin{aligned} \lambda_1 &= \sigma_c^2 \sqrt{\frac{E_s}{8}} \varepsilon_0 (1 + \Upsilon) \\ \lambda_2 &= \sigma_c^2 \sqrt{\frac{E_s}{8}} \varepsilon_0 (1 - \Upsilon) \end{aligned} \quad (4.34)$$

where

$$\Upsilon = \left( \frac{4(1 + \bar{\gamma}_s^{-1})}{\varepsilon_0} - \left( \frac{|\varepsilon_1|}{\varepsilon_0} \right)^2 \right)^{-1/2} \quad (4.35)$$

From Equations (4.32) and (4.35), it can be shown that the poles of the characteristic function of  $\mathbf{x}^H \mathbf{Q} \mathbf{x}$  given by Equation (4.20) are  $1/\lambda_1$  and  $1/\lambda_2$ . The pole on the left half plane is  $1/\lambda_1$  and the pole  $1/\lambda_2$  is on the right half plane. Using the fact that the residue is invariant to the scaling of the poles [39], the probability of bit error can be calculated as

$$\begin{aligned} P_b &= \lim_{s \rightarrow \frac{\sigma_c^2 \varepsilon_0}{\lambda_2}} \frac{d}{ds} \left( \frac{\left( s - \frac{\sigma_c^2 \varepsilon_0}{\lambda_2} \right)^2}{s \left( 1 - \frac{s \lambda_1}{\sigma_c^2 \varepsilon_0} \right)^2 \left( 1 - \frac{s \lambda_2}{\sigma_c^2 \varepsilon_0} \right)^2} \right) \\ &= \frac{1}{4} (2 + \Upsilon) (1 - \Upsilon)^2 \end{aligned} \quad (4.36)$$

### 4.2.3 Performance Results

In this section, we present some results to illustrate the effect of Doppler frequency shift and imperfect CSI on the performance of the wireless communication system using STBC. We consider a Rayleigh fading channel model that was originally presented in [3]. The autocorrelation function of the fading channel is the zeroth-order Bessel function of the first kind  $J_0(2\pi f_d\tau)$ , which is derived from the Jakes' power spectral density [3], where  $f_d$  denotes the maximum Doppler frequency.

The probability of bit error is shown in Figure 4.6. The STBC used is the Alamouti scheme with two transmit and one receive antennas. The bit error probability plots are generated using the analytical results given by Equation (4.36). Similar to the channel conditions evaluated in [39], we consider three fading channels that have  $f_d\tau = 0.0005, 0.03$  and  $0.05$ . The data SNRs are fixed at 10 dB and 30 dB. The fading of the channel becomes more severe as the product of  $f_d\tau$  increases. It is observed that the performance of wireless communication system using STBC degrades as the channel fading increases.

As it is expected, the performance of the wireless communications using STBC improves as the pilot SNR increases. The STBC system achieves more diversity gain when more reliable CSI is available at the receiver. The STBC performs better when the data SNR increases.

At high pilot SNR region, the probability of bit error exhibits an error floor. It shows that the channel estimates can no longer be improved beyond certain SNR value on the pilot channel. The error floor is determined by the SNR on the data channel and the normalized Doppler frequency of the channel  $f_d\tau$ .

The probability of bit error versus data SNR is plotted in Figure 4.7. The normalized Doppler frequency  $f_d\tau = 0.0005$ . There are three levels of pilot SNR, i.e. 0, 10, and 20 dB. At every pilot SNR level, the probability of bit error decreases when data SNR increases. There are error floors at high data SNR region on every pilot SNR levels, which are caused by pilot SNR and the channel estimation error. When the

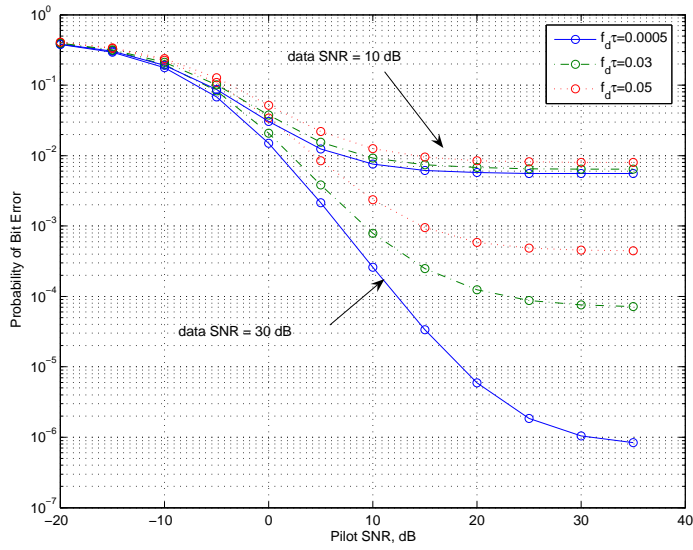


Figure 4.6:  $P_b$  affected by Channel Profile, Pilot SNR and Data SNR

pilot SNR increases, there is less noise in the channel estimates and the error floor is lower at high data SNR.

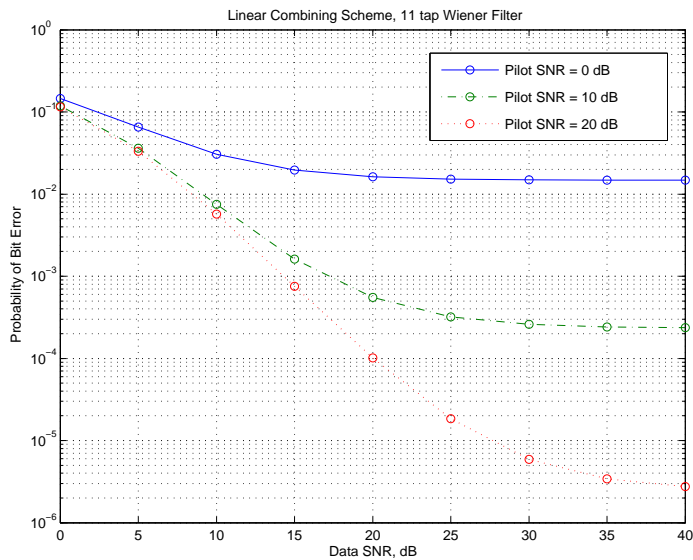


Figure 4.7:  $P_b$  affected by Pilot SNR and Data SNR

When the pilot SNR is 20 dB, the probability of bit error versus data SNR is illustrated in Figure 4.8. The normalized Doppler frequencies of the channel are  $f_d\tau = 0.0005$ , 0.03 and 0.05 respectively. At high data SNR, there are error floors at every  $f_d\tau$  levels and the error floors are determined by the normalized Doppler frequencies.

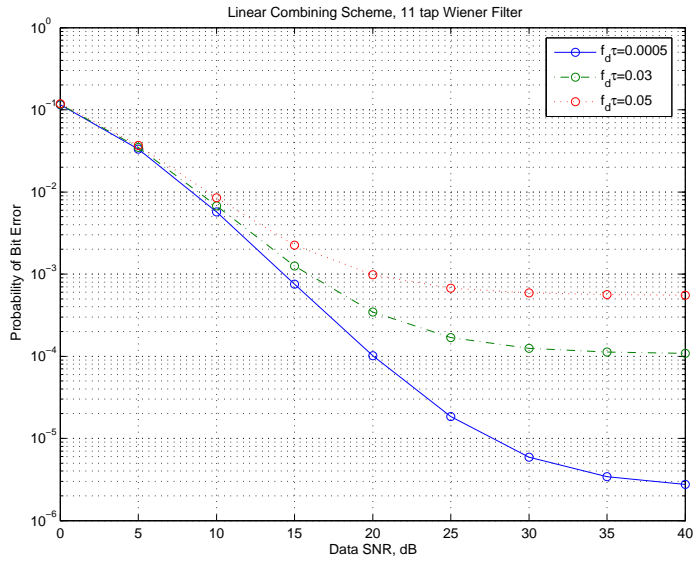


Figure 4.8:  $P_b$  affected by Channel Profile and Data SNR

## Chapter 5

# A New Family of Differentially Encoded Space Time Block Codes

The STBC scheme has a remarkable performance and achieves significant diversity gain over fading channel when the CSI is perfectly available at the receiver. Unfortunately, the performance of the STBC is very sensitive to the channel estimation error as the results presented in the last chapter suggest. In practical wireless communication systems, it is sometimes difficult to have an accurate estimate of the CSI, for instance, when either the channel fading rate or the number of transmit antennas increases. In an effort to increase channel capacity or to increase the system diversity gain, it is accepted practice to increase the number of transmit antennas. But increasing the number of transmit antennas increases the required training period and reduces the available time to transmit data before the channel coefficients change [44]. In very fast fading scenario, for example when a train travels at a velocity of 500 km/hour, it may be impractical to learn even a single element in the channel coefficient matrix  $\mathbf{H}$  [44]. Therefore, a communication strategy that does not require the CSI is attractive in cases when estimation of the CSI can not be done accurately.

In single transmit and single receive antenna wireless communication systems, a differential encoding and decoding technique can be used to cope with the situation

where no CSI is available. The differential encoder can be described as [1]

$$b_{out,i} = b_{out,i-1} \oplus b_{in,i} \quad (5.1)$$

where  $b_{in,i}$  is the current input binary bit to the encoder,  $b_{out,i-1}$  is the previous output from the encoder,  $b_{out,i}$  is the current output from the encoder, and  $\oplus$  stands for modulo-2 addition. In essence, the difference between the current input bit and the previous output of the differential encoder determines the output from the differential encoder. At the decoder, the differentially encoded bits can be recovered by using

$$\hat{b}_i = b_{out,i-1} \oplus b_{out,i} \quad (5.2)$$

Where  $\hat{b}_i$  is the detected bit,  $b_{out,i}$  and  $b_{out,i-1}$  are two received bits. It is obvious that the recovered bit depends only on the difference between  $b_{out,i}$  and  $b_{out,i-1}$ . When the differentially encoded signal is demodulated, the received signal in any time interval is compared to the detected signal from the previous time interval [1] and there is no need of the CSI at the receiver for detection purpose. One drawback to the differential encoding and decoding technique is that there is loss in SNR on the BER versus SNR curve compared to the coherent detection method, which requires the channel coefficients. But the benefit outweighs its drawback in case where the channel coefficients are not available.

To realize the capacity gain unveiled by the study in [45], a new class of capacity approaching modulation schemes, unitary space time modulation that is designed for flat Rayleigh fading channel is proposed in [44] when the CSI is available neither at the transmitter nor at the receiver. One important characteristic of the unitary space time modulation is that the signals transmitted on different antennas are mutually orthogonal. The differential unitary space time modulation is proposed in [46] and [47]. The transmitted signal matrix at each time block is the matrix product of the previously transmitted signal matrix and the current data matrix with unitary

modulation. It is also shown in [46] and [47] that a constellation of unitary matrices that achieves full diversity for MIMO systems with CSI available at the receiver can also achieve full diversity in MIMO systems without CSI at the receiver if differential encoding is employed. But there is a certain SNR loss on the performance curve of the BER versus SNR. The signal constellations proposed in [46] and [47] form groups under matrix multiplication that allow easy implementation at the transmitter. However, the design of signal constellations that do not form groups is not covered in those works.

To use the group differential space time block code, the group property is defined in a way that is related to differential encoding and decoding [47]. Let  $\nu$  be a set of  $L$  distinct unitary matrices,  $\nu = (V_1, V_2, \dots, V_L)$ . We recall that  $\nu$  has group property or it forms a group if the product of any two elements in  $\nu$  is also an element in  $\nu$ , which is described as

$$V_{i1}V_{i2} = V_{i3} \tag{5.3}$$

where  $V_{i1}, V_{i2}, V_{i3} \in \nu$ , and  $i1, i2$ , and  $i3$  are integers [47].

A differential detection scheme for a two transmit antenna MIMO system based on the Alamouti STBC [15] given by Equation (2.16) is proposed in [48]. This scheme applies to the STBC with PSK modulation and it can be considered as a differential unitary space time modulation. The data matrix does not have the group property in general. In [49], a general differential STBC scheme for any number of transmit antennas is proposed based on generalized complex orthogonal designs. The modulation scheme used in [49] is also PSK. It is worth mentioning that all of these differential schemes for STBCs require that the modulation scheme have a single amplitude.

In this chapter, we will apply a modified differential encoding and decoding technique to STBC in MIMO wireless communication systems. In particular we apply this method to the proposed STBC with the “triple QPSK” modulation. We show that the proposed STBCs with the “triple QPSK” modulation can be used when neither the transmitter nor the receiver has access to the CSI, with marginal degradation in

performance compared with coherent demodulation when the CSI is available to the receiver but not to the transmitter.

## 5.1 Differential STBC for Three Transmit Antennas

A differential transmission for the STBC from complex orthogonal design that was originally proposed in [5] was modified in [50] by using a differential non-coherent decoder. This scheme applies to the complex orthogonal STBCs and requires that the transmission matrix of the STBC be a square matrix similar to the matrices specified in Equations (2.16) and (2.23). It applies directly to the STBC with two and four transmission antennas, whose transmission matrices are given by Equations (2.16) and (2.23), respectively. The differential scheme proposed in [48] is based on the Alamouti STBC and can be regarded as a special case of this general approach. The differential scheme in [50] is applied to design a differential scheme for the quasi-orthogonal STBC in [51].

Unlike other differential detection schemes for STBC, the differential scheme for STBC proposed in [50] does not require the modulation scheme to use a single amplitude signal constellation, but it does require that the STBC to be orthogonal for the differential encoding and decoding algorithm to work. These properties make it attractive to be applied to the orthogonal full-rate, full-diversity STBCs with the “triple QPSK” modulation, which has multiple amplitudes in its signal constellation that are orthogonal when using the “triple QPSK” modulation.

Once again, we consider the MIMO system we have been investigating that has  $N_T$  transmit and  $N_R$  receive antennas. The system can be modeled as

$$\mathbf{Y} = \sqrt{\frac{\rho}{N_T}} \mathbf{S} \mathbf{H}^T + \mathbf{W} \quad (5.4)$$

where  $\mathbf{Y}$  is a  $l \times N_R$  matrix of received signal,  $\rho$  is the SNR at each receive antenna,  $\mathbf{S}$

is the  $l \times N_T$  transmitted signal matrix,  $\mathbf{H}$  is the  $N_R \times N_T$  channel matrix, and  $\mathbf{W}$  is the  $l \times N_R$  additive noise matrix.  $l$  is the number of symbols in the transmitted block after STBC encoding. The elements of matrix  $\mathbf{W}$  are independent complex Gaussian random variable with zero mean and unit variance.

In differential encoding and decoding of the STBC, although the channel coefficients  $\mathbf{H}$  are known neither to the transmitter nor to the receiver, it is assumed that they remain unchanged during an entire frame duration, which consists of  $l$  symbol periods. From equation (5.4), it is clear that  $E\{\mathbf{Y}|\mathbf{S}\} = 0$  and [45]

$$E\{\mathbf{Y}\mathbf{Y}^H|\mathbf{S}\} = \mathbf{I}_l + \rho\mathbf{S}\mathbf{S}^H \quad (5.5)$$

Thus, without channel coefficients  $\mathbf{H}$  and conditioned on  $\mathbf{S}$ , each column of the received signal  $\mathbf{Y}$  is complex Gaussian distributed random vector with mean zero and covariance matrix  $\mathbf{I}_l + \rho\mathbf{S}\mathbf{S}^H$ . The conditional probability density function of the received signal can be expressed as [50]

$$p(\mathbf{Y}|\mathbf{S}) = \frac{\exp\{-tr[(\mathbf{I} + \rho\mathbf{S}\mathbf{S}^H)^{-1}\mathbf{Y}\mathbf{Y}^H]\}}{\pi^{TM} \det^M(\mathbf{I} + \rho\mathbf{S}\mathbf{S}^H)} \quad (5.6)$$

where  $tr$  denotes the trace of a matrix and  $\det$  stands for the determinant of a matrix. It is important to note that  $p(\mathbf{Y}|\mathbf{S})$  will not change if matrix  $\mathbf{S}$  is right multiplied by any  $N_T \times N_T$  unitary matrix  $\mathbf{\Phi}$  in Equation (5.6). This means that matrices  $\mathbf{S}$  and  $\mathbf{S}\mathbf{\Phi}$  are indistinguishable for non-coherent detection.

As we discussed in chapter 3, a STBC can be described by its transmission matrix, which is  $p \times N_T$  in dimension, and can be regarded as a mapping from the set of modulation symbols  $s_i$ , where index  $i = 1, \dots, k$ , to transmission matrix  $\mathbf{G}_c$ , where  $k$  is the number of non-zero elements in the columns of matrix  $\mathbf{G}_c$ . The elements in  $\mathbf{G}_c$  are transmitted by  $N_T$  antennas over  $p$  symbol periods. The orthogonality criteria of the STBC from complex orthogonal designs guarantees that the following condition

holds

$$\mathbf{G}_c^H \mathbf{G}_c = \left( \sum_{i=1}^k |s_i|^2 \right) \mathbf{I}_{N_T} = a^2 \mathbf{I}_{N_T} \quad (5.7)$$

When the transmission matrix of a STBC is a square matrix, i.e., when  $p = N_T$ , we have  $\mathbf{G}_c^H \mathbf{G}_c = \mathbf{G}_c \mathbf{G}_c^H$ . We define  $a$  as the amplitude of matrix  $\mathbf{G}_c$ . The STBCs from the complex orthogonal design given in Equation (2.16) for two transmit antennas and Equation (2.23) for four transmit antennas have square transmission matrices. At this point, we consider the STBC with square transmission matrix  $\mathbf{G}_c$ .

Let us define matrix  $\mathbf{V}$  to be

$$\mathbf{V} = \frac{1}{\sqrt{k}} \mathbf{G}_c \quad (5.8)$$

where matrix  $\mathbf{G}_c$  is a transmission matrix of a STBC from complex orthogonal design and  $k$  is the number of non-zero elements in each column of matrix  $\mathbf{G}_c$ . For matrix  $\mathbf{V}$ , we have

$$\mathbf{V} \mathbf{V}^H = a^2 \mathbf{I}_{N_T} \quad (5.9)$$

where  $a = \sqrt{\frac{1}{k} \sum_{i=1}^k |s_i|^2}$  is the amplitude of matrix  $\mathbf{V}$ . It can be easily verified that the amplitude  $a$  of matrix  $\mathbf{V}$  is equal to 1 for all  $\mathbf{V}$  if the modulation symbols  $s_i, i = 1, \dots, k$  are generated from a modulation scheme that has a single amplitude constellation such as PSK. Otherwise, the amplitude  $a$  will take some discrete values and be the average of these values.

At the transmitter of the differentially encoded STBC system, an identity matrix which contains no information is sent to initialize the transmission; thus we can write  $\mathbf{S}_0 = \mathbf{I}_{N_T}$ . After initialization, the data matrices are differentially encoded and transmitted. At the  $t$  time block, the transmitted matrix is a  $p \times p$  square matrix, which can be written as

$$\mathbf{S}_t = \mathbf{V}_t \tilde{\mathbf{S}}_{t-1} \quad (5.10)$$

where matrix  $\mathbf{V}_t$  is determined by using Equation (5.8) and matrix  $\tilde{\mathbf{S}}_{t-1}$  is the normalized version of  $\mathbf{S}_{t-1}$ , defined as

$$\tilde{\mathbf{S}}_{t-1} = \frac{1}{a_{t-1}} \mathbf{S}_{t-1} \quad (5.11)$$

where  $a_{t-1}$  is the amplitude of matrix  $\mathbf{S}_{t-1}$ . It can be verified that  $\tilde{\mathbf{S}}_{t-1} \tilde{\mathbf{S}}_{t-1}^H = \mathbf{I}_{N_T}$ , i.e.,  $\tilde{\mathbf{S}}_{t-1}$  is a unitary matrix.

To decode the differentially encoded STBC, the receiver takes two consecutively received signal matrices and their signal structure can be expressed as

$$\mathbf{Y}_{t-1} = \sqrt{\frac{\rho}{N_T}} \mathbf{S}_{t-1} \mathbf{H}^T + \mathbf{W}_{t-1} \quad (5.12)$$

$$\mathbf{Y}_t = \sqrt{\frac{\rho}{N_T}} \mathbf{S}_t \mathbf{H}^T + \mathbf{W}_t \quad (5.13)$$

If we substitute Equation (5.10) into Equation (5.13) and apply Equation (5.12), we can obtain the following equation

$$\mathbf{Y}_t = a_{t-1}^{-1} \mathbf{V}_t \mathbf{Y}_{t-1} - a_{t-1}^{-1} \mathbf{V}_t \mathbf{W}_{t-1} + \mathbf{W}_t \quad (5.14)$$

Because the noise matrices have identically independent distributed elements and the noise matrices are independent at different time blocks, the above equation can be rewritten as [50]

$$\mathbf{Y}_t = a_{t-1}^{-1} \mathbf{V}_t \mathbf{Y}_{t-1} + \sqrt{1 + a_{t-1}^{-2} a_t^2} \mathbf{W}'_t \quad (5.15)$$

where  $\mathbf{W}'_t$  is a  $N_T \times N_R$  equivalent noise matrix whose elements are independent identically complex Gaussian distributed random variables with zero mean and unit variance. The first term in Equation (5.15) can be treated as the signal part while the second term can be viewed as the noise part of the received signal block at the  $t$  block. We can gain further insight into Equation (5.15) by viewing  $a_{t-1}^{-1}$  as the known channel coefficient matrix for the system transmitting signal block  $\mathbf{V}_t$  with

noise variance  $1 + a_{t-1}^{-2}a_t^2$ . If the dependence of the equivalent noise variance on the transmitted signal is ignored, we can find the following near optimal differential decoding rule [50]

$$(\hat{\mathbf{V}}_t)_{no} = \arg \min_{\mathbf{V}} \|\mathbf{Y}_t - a_{t-1}^{-1} \mathbf{V} \mathbf{Y}_{t-1}\|^2 \quad (5.16)$$

Because the amplitude of the previous symbol  $a_{t-1}$  is estimated from the last detected symbol and is not known at the receiver, in [50], the differential decoding rule specified in Equation (5.16) is called near optimal rule and we use this term for consistency. In [50], there is an optimal differential decoding rule and it requires perfect knowledge of the amplitude of the previous symbol  $a_{t-1}$ . The knowledge of  $a_{t-1}$  is not generally available at the receiver in practical wireless communication systems so we do not investigate the optimal differential rule here. Based on the results presented in [50], the SNR loss due to the near optimal differential decoding compared to the optimal differential decoding rule is less than 0.1 dB, which is very small. The near optimal differential decoding rule is selected as the method of differential decoding in this dissertation. Taking advantage of the orthogonal structure of the STBC from complex orthogonal designs, it has been shown [5] that the data symbols  $s_i, i = 1, \dots, k$  can be decoupled and detected individually from Equation (5.16). As a consequence, this near optimal differential detection algorithm has linear complexity [50].

Since the transmission matrix,  $\mathbf{G}_{c4}$  specified in Equation (2.23) for STBC from complex orthogonal design of four transmit antennas is an orthogonal square matrix, we can apply the differential encoding and decoding algorithm outlined from Equation (5.8) to Equation (5.16), and have a differential STBC from complex orthogonal design for a MIMO system with four transmit antennas. Since in matrix  $\mathbf{G}_{c4}$  any column is orthogonal to all other columns, we can take the first three columns to

form a matrix  $\mathbf{G}_{c32}$  of  $4 \times 3$  dimension given by

$$\mathbf{G}_{c32} = \begin{pmatrix} s_1 & s_2 & s_3 \\ -s_2^* & s_1^* & 0 \\ -s_3^* & 0 & s_1^* \\ 0 & -s_3^* & s_2^* \end{pmatrix} \quad (5.17)$$

It is apparent that the columns of  $\mathbf{G}_{c32}$  are orthogonal and  $\mathbf{G}_{c32}^H \mathbf{G}_{c32} = (\sum_{i=1}^3 |s_i|^2) \mathbf{I}_3$ . For a three transmit antenna MIMO system, the STBC whose transmission matrix is specified by Equation (5.17) has the same performance in diversity and multiplexing gain as the STBC whose transmission matrix is specified by Equation (2.22).

Using the fact that the three columns of matrix  $\mathbf{G}_{c32}$  are the first three columns of matrix  $\mathbf{G}_{c4}$ , which is a transmission matrix of a STBC from complex orthogonal design for four transmit antennas, we can differentially encode the STBC from complex orthogonal design for three transmit antennas whose transmission matrix is  $\mathbf{G}_{c32}$  in the following way. At first, we differentially encode the STBC whose transmission matrix is  $\mathbf{G}_{c4}$  using the procedures specified from Equation (5.8) to Equation (5.11). We only transmit the first three columns of  $\mathbf{S}_t$  when the differentially encoded signal block  $\mathbf{S}_t$  is sent. The fourth column is discarded, which is similar to puncturing the four column matrix, and this process can be called ‘‘Space Puncturing’’ or ‘‘Antenna Puncturing’’. Thus, the received signal block  $\mathbf{Y}_t$  that is given by Equation (5.13) contains information in the first three columns of matrix  $\mathbf{S}_t$  only.

The receiver will differentially detect the STBC using the near optimal decoding rule given in Equation (5.16). An important fact to notice is that the transmission matrix  $\mathbf{G}_c$ , which is used in the near optimal differential decoding algorithm specified by Equation (5.8) to calculate matrix  $\mathbf{V}_t$ , is the  $4 \times 4$  matrix  $\mathbf{G}_{c4}$  rather than the  $4 \times 3$  matrix  $\mathbf{G}_{c32}$ , and the matrix  $\mathbf{V}_t$  is a  $4 \times 4$  square matrix.

So we have a differential encoding and decoding scheme for a STBC from complex orthogonal design for three transmit antennas. The performance of this algorithm

is investigated by using Monte Carlo simulation. In our simulations we have selected three transmit antennas and one receive antenna in the MIMO system. The channel coefficient matrix  $\mathbf{H}$  stays constant during a frame duration and changes independently from frame to frame. The channel coefficient is available neither to the receiver nor to the transmitter.

The symbol error rate plots versus SNR with both differential detection and coherent detection are shown in Figure 5.1, where QPSK modulation is used. The slope of the symbol error rate versus SNR curve on a log-log scale with differential detection is the same as that of the symbol error rate versus SNR curve with coherent detection. This confirms that the differential STBC from complex orthogonal design achieves the same diversity gain as the coherent STBC achieves. At symbol error rate of  $10^{-3}$ , the SNR loss due to non-coherent detection is about 3 dB. The differential scheme for STBC from complex orthogonal design achieves the maximum diversity gain that this system can provide. However to achieve the same symbol error rate, the required SNR in the differential detection is higher than the required SNR in the coherent detection system.

In Figure 5.2, the symbol error rate versus SNR curves of STBC with coherent and differential detection are plotted when 16-QAM modulation is used. The differential STBC achieves full diversity gain that a three transmit and one receive antenna MIMO system can provide. The SNR penalty of the differential detection scheme compared with the coherent detection is about 3.5 dB at symbol error rate of  $10^{-3}$ . The result shows that the proposed differential encoding and decoding scheme for STBC from complex orthogonal design for three transmit antenna applies to modulations that have multiple amplitudes in their signal constellation. Thus we can apply this differential detection scheme to our new STBC using the “triple QPSK” modulation, which has three levels of amplitude in its signal constellation.

The symbol error rate versus SNR plots for differential STBCs with two, three, and four transmit antennas are illustrated in Figure 5.3. In all cases there exist one receive antenna and the modulation used is 16-QAM for all of cases. The transmission

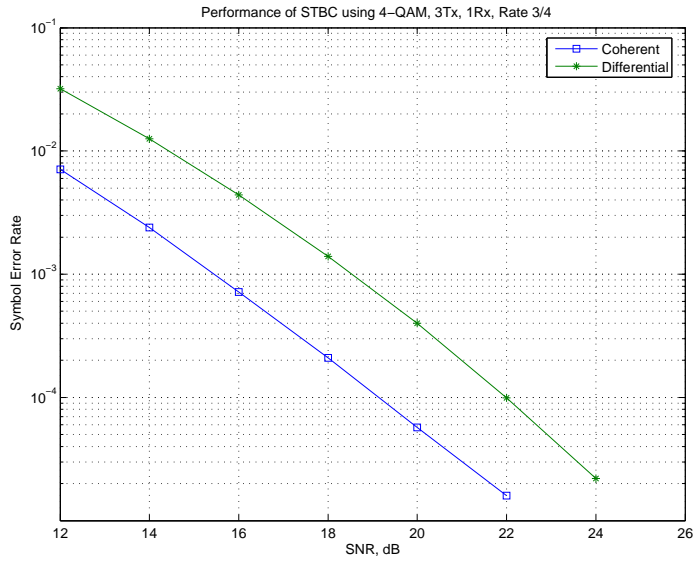


Figure 5.1: Performance of the STBC Using Differential Detection, QPSK With Three Transmit Antennas

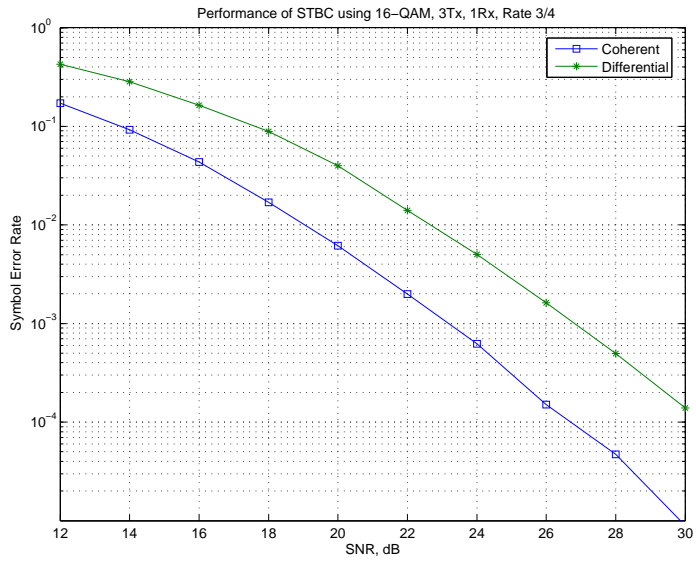


Figure 5.2: Performance of the STBC with Differential Detection, 16-QAM,  $N_T=3$

matrices of complex orthogonal STBCs for two, three, and four transmit antennas

are given in Equations (2.16), (2.22), and (2.23) respectively. The channel matrix  $\mathbf{H}$  is complex Gaussian that stays constant during one frame period and changes independently from one frame to the next frame. The symbol error rate decreases when the SNR increases. The slope of the symbol error rate versus SNR curve, i.e. the diversity order, increases when the number of transmit antenna increases. All of them achieve the maximum diversity order their MIMO system can provide respectively. Thus this differential encoding and decoding algorithm can be applied to MIMO systems with two, three and four transmit antennas with no penalty in diversity gain.

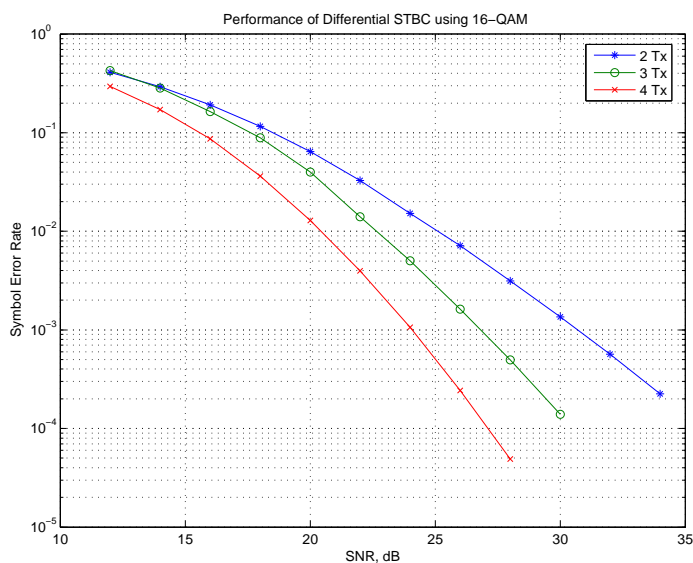


Figure 5.3: Performance of the Differential STBC with 16-QAM,  $N_T = 2,3,4$

## 5.2 Differential Detection for New STBC with “triple-QPSK”

We can apply the differential detection scheme for the STBC from complex orthogonal designs for three transmit antennas to our new STBC using the “triple OPSK”

modulation. The transmission matrix,  $\mathbf{G}_{qon}$  of our STBC for four transmit antennas given in Equation (3.14) is a square matrix. When the “triple QPSK” modulation is used, it can be shown that

$$\mathbf{G}_{qon}^H \mathbf{G}_{qon} = \left( \sum_{i=1}^4 |s_i|^2 \right) \mathbf{I}_4 \quad (5.18)$$

Hence the orthogonality criteria is satisfied and the columns of matrix  $\mathbf{G}_{qon}$  are orthogonal. We take the first three columns of matrix  $\mathbf{G}_{qon}$  and form a  $4 \times 3$  matrix  $\mathbf{G}_{cn2}$  as

$$\mathbf{G}_{cn2} = \begin{pmatrix} s_1 & s_4 & s_3 \\ -s_4 & s_1 & -s_2 \\ -s_3^* & s_2^* & s_1^* \\ -s_2^* & -s_3^* & s_4^* \end{pmatrix} \quad (5.19)$$

If the “triple QPSK” modulation is used to generate the symbols, we can easily verify that

$$\mathbf{G}_{cn2}^H \mathbf{G}_{cn2} = \left( \sum_{i=1}^4 |s_i|^2 \right) \mathbf{I}_3 \quad (5.20)$$

The STBC for three transmit antennas, whose transmission matrix is  $\mathbf{G}_{cn2}$ , is a complex orthogonal design when the “triple QPSK” modulation is used. We can apply the differential detection for STBC from complex orthogonal design for three transmit antennas that we just proposed to this new STBC using the “triple QPSK” modulation with three transmit antennas. This differential encoding and decoding scheme uses the “Space Puncturing” technique. The performance of this algorithm, which is given by Equations (5.8) to (5.16) together with the “Space Puncturing”, is studied using Monte Carlo simulation. The channel coefficients are available to neither the receiver nor the transmitter, and stay constant over a frame period.

The symbol error rate versus SNR plot of the differential detection scheme for the new STBC for three transmit antennas using the “triple QPSK” modulation is shown in Figure 5.4. The symbol error rate versus SNR curve of the coherent detection is also

plotted for reference. The new STBC for three transmit antennas using the “triple QPSK” with differential detection scheme achieves full diversity gain that a three transmit antenna and one receive antenna MIMO system can provide. Compared with the coherent detection method, the differential detection suffers an SNR loss of about 6 dB at a symbol error rate of  $10^{-3}$ . This is the loss due to the fact that the CSI is not used in the detection and the fourth column of symbols is not transmitted, which is part of the encoding and decoding procedure.

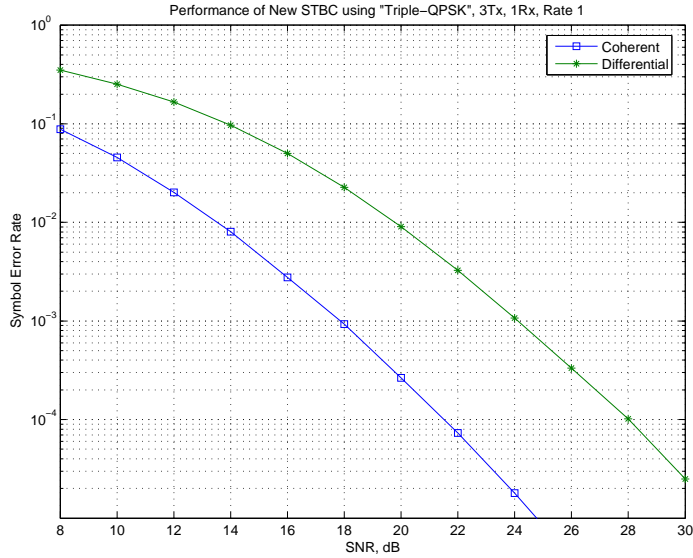


Figure 5.4: Performance of the New STBC using “triple QPSK” with Differential Detection,  $N_T=3$

For the new STBC using the “triple QPSK” modulation for four transmit antennas whose transmission matrix is  $\mathbf{G}_{qon}$  given by Equation (3.14), the differential detection scheme can be applied by following the procedures laid out by Equations (5.8) to (5.16). We investigate the performance of this case using Monte Carlo simulation. There are four transmit and one receive antenna in the MIMO system. The channel coefficients are not used in the encoding and the decoding process. The random complex Gaussian channel coefficients stay constant during a frame period and change independently from frame to frame.

The performance of the new STBC using the “triple QPSK” modulation for four transmit antennas with differential detection is given in Figure 5.5. The symbol error rate versus SNR plots are shown in Figure 5.5. This differential scheme for the new STBC using the “triple QPSK” modulation achieves full diversity that a MIMO system with four transmit antenna and one receive antenna can provide. The SNR required for the differential scheme to reach a certain symbol error rate is higher than the SNR required to achieve the same symbol error rate for the coherent scheme. This SNR loss is about 5 dB at symbol error rate of  $10^{-3}$ . This is due to the fact that the CSI is not used in the encoding and decoding process in the differential scheme. Since there are four transmit antennas and the fourth column in the transmission matrix  $\mathbf{G}_{qon}$  is transmitted, this SNR loss is smaller than the SNR loss in the differential scheme for three transmit antennas.

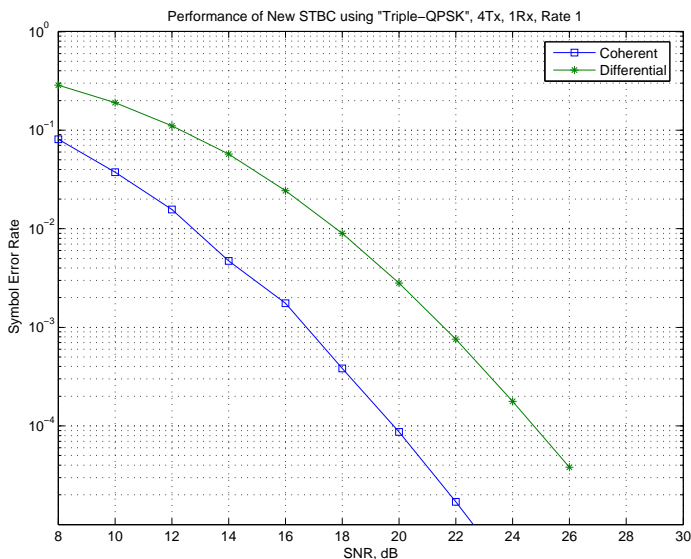


Figure 5.5: Performance of the New STBC using “triple QPSK” with Differential Detection,  $N_T=4$

At a symbol error rate of  $10^{-3}$ , in Figure 5.5, the SNR loss due to differential encoding and decoding is 5 dB, where all four columns of transmission matrix are transmitted; while in Figure 5.4, the SNR loss due to differential encoding and decoding

is 6 dB, where there is “Space Puncturing” and only the first three columns are transmitted. Therefore the SNR loss due to “Space Puncturing” is about 1 dB at a symbol error rate of  $10^{-3}$ .

# Chapter 6

## Concluding Remarks

In this dissertation, we proposed a family of full rate STBCs from complex orthogonal designs that achieve full diversity when used with the proposed “triple QPSK” modulation. These STBCs are designed for MIMO systems that have three and four transmit antennas. Although one receive antenna is used throughout the analysis, these STBCs can be easily expanded to MIMO systems that have more than one receive antennas. The performance of the proposed schemes is evaluated using Monte Carlo simulation. An upper bound of the probability of bit error is also developed for this scheme. Both the simulation results and analytical results show that the new scheme achieves the full diversity that the MIMO system can provide while transmitting at full rate. This is a 33% code rate increase over the conventional orthogonal STBCs whose rates are  $3/4$  when there are three and four transmit antennas.

The proposed “triple QPSK” modulation has a memory of depth two symbols. Our results showed that the orthogonal STBCs from complex orthogonal designs can achieve full rate, full diversity for three and four transmit antennas by employing a modulation scheme with short memory. At the receiver, the maximum likelihood detection algorithm is used to detect the symbols and the memory effect that is inherent to the “triple QPSK” modulation is utilized for joint decoding of the symbols. The decoder goes through the trellis of the “triple QPSK” modulation and decodes

the symbols in pair.

The new full rate STBCs for three and four transmit antennas, and the “triple QPSK” modulation are derived from the orthogonality criterion, which is different from the diversity criterion used to derive high rate STBCs and associated signal constellations in the existing research works.

Throughout this dissertation, it is assumed that there is no knowledge of the CSI at the transmitter, which is normally the situation in practical wireless communication systems. In the first part of our study, the CSI is assumed to be perfectly known to the receiver. More often, this is not the case in practical wireless communication systems. Usually, the receiver needs to estimate the CSI through a pilot signal or a training sequence. Regardless of the method used for channel estimation, there is a certain amount of error in the estimate of CSI. We studied the performance of the proposed scheme when there is error in the CSI estimates at the receiver. The results show that the scheme is very sensitive to errors in the estimates of CSI. The STBCs using the “triple QPSK” modulation have an error floor at high SNR region when there is more than 0.2% estimation error in the CSI at the receiver.

In some scenarios such as in channels whose fading rate is high or in MIMO system with a large number of transmit antennas, it is impossible to estimate the channel state information. Thus, we apply a differential encoding and decoding scheme to the orthogonal STBCs from complex orthogonal design. The CSI is required neither at the receiver nor at the transmitter in this case. The proposed differential detection algorithm applies to modulation schemes whose signal constellation has multiple amplitudes, such as 16-QAM. We propose a differential encoding and decoding scheme for orthogonal STBC from complex orthogonal design for three transmit antennas, whose transmission matrix is not a square matrix, using the “Space Puncturing” technique. The differential STBC from complex orthogonal design achieves full diversity but suffers from a certain amount of SNR loss compared with the coherent STBC from complex orthogonal design when there are three transmit antennas.

The differential encoding and decoding algorithms for three and four transmit

antennas require that the STBCs to be orthogonal. Since the new STBCs proposed in this dissertation are orthogonal when the “triple QPSK” modulation is used, these differential detection schemes can be applied to the proposed scheme for three and four transmit antenna MIMO systems. The resulting differential STBCs using the “triple QPSK” modulation are orthogonal, and achieve full rate and full diversity for three and four transmit antennas. They all suffer a certain amount of SNR loss compared with their coherent counterparts while no CSI is needed at either the transmitter or the receiver.

High rate STBC systems have attracted a lot of interest since they are required to build high throughput wireless communication systems. The techniques studied in this work can be applied to future research in this area. Research on high rate STBCs for MIMO systems with a large number of transmit and receive antennas, such as 8 or 16 transmit and receive antennas, is an active topic, since such systems can provide large diversity and multiplexing gain. The STBCs for a large number of transmit and receive antennas can be derived from the STBCs for two or three transmit antennas by grouping their transmission matrices together. The proposed STBCs for three and four transmit antennas can be grouped with the Alamouti STBC for two transmit antennas to form orthogonal full-rate, full-diversity STBCs for six, seven, eight or sixteen transmit antennas. The proposed “triple QPSK” modulation or any other appropriate modulation can be used to help achieve this goal.

Modified modulations and modified signal constellations are proven techniques to achieve high rate, high diversity and multiplexing gain for the STBCs in MIMO systems. In addition to achieving high diversity gain, which is presented in this research and the surveyed literatures, modified modulation schemes can help achieve high multiplexing gain by jointly detecting the STBC data streams using all of the receive antennas together. In this dissertation, the STBCs and the “triple QPSK” modulation scheme were initially derived in a MIMO system, where there is multiple transmit and one receive antenna. Then they were applied to the MIMO systems with multiple transmit and receive antennas. We can explore derivatives of the “triple

QPSK” modulation designed for high rate STBCs multiple transmit and receive antennas that achieve orthogonality and full diversity while obtaining multiplexing gain as well. The signal constellation of the “triple QPSK” consists of conventional QPSK constellation and scaled versions of the constellation of QPSK. We can investigate whether rotated constellations of QPSK can be added to further enhance the performance of the STBCs.

The proposed new STBCs and the “triple QPSK” modulation can be applied to research in cooperative network communication, where the nodes in the network share their resources and forward each other’s packets to the destination at the physical layer. The relay channel can mimic the MIMO system even when the cooperating nodes can individually support single antenna and it can exploit the spatial diversity that physically separated nodes provide. Both diversity gain and multiplexing gain can be achieved in the relay channel. We can investigate the diversity and multiplexing gain achieved in the relay channel when the proposed STBCs and the “triple QPSK” are used.

The proposed STBCs using the “triple QPSK” modulation can be adopted to the multiuser MIMO system. When there are multiple users in the wireless communication network with MIMO, the techniques can be radically different from those in the single user MIMO system as these techniques imply the use of spatial sharing of the channel by the users. In spatial multiple access, the resulting multi-user interference is handled by the multiple antennas that provide both per-link diversity and give degrees of freedom necessary to spatially separate the users. The downlink is a broadcasting channel and is the most challenging case. Information theory reveals that the optimum transmit strategy for the multi-user MIMO broadcasting channel involves a theoretical pre-interference cancellation technique known as dirty paper coding combined with an implicit user scheduling and power loading algorithm. In future research, the pre-coding, feedback, and scheduling strategies on the downlink of the multi-user MIMO network employing the proposed STBCs with the “triple QPSK” modulation can be investigated. On the uplink, which is a multiple access

channel, the generalization of the single user MIMO schemes to the multi-user MIMO case can be explored using the proposed STBCs along with the “triple QPSK” modulation. The multi-user MIMO system allows a joint optimization of antenna selection techniques with resource allocation protocols. It exhibits robustness to multipath fading channel, allows compact antenna spacing at the base-station, and yields diversity and multiplexing gain even without multiple antennas at the mobile terminals. However, the base-station needs the CSI of the mobile channel to realize these gains, which may limit its practical application to time division duplex or low mobility settings. To circumvent this issue and reduce the feedback load, the multi-user MIMO can be combined with opportunistic scheduling, which may open the range of application of the multi-user MIMO to more diverse environments. The proposed differential encoding and decoding technique can be applied to the multi-user MIMO system as well, since it does not require CSI at either the transmitter or the receiver.

# Appendix A

## Confidence Intervals

One of the parameters used to evaluate the performance of the communication systems is the bit error rate (BER) or the probability of bit error. There are a number of ways to arrive at an estimate of the BER and the Monte Carlo simulation method is often used to estimate the BER. We consider a communication system that transmits information using binary signal 0 and 1. The decision process at the receiver can be described in terms of the probability density functions  $f_0(v; t)$  and  $f_1(v; t)$ , of the input at the sampling instant  $t$ , given that 0 or 1 was sent respectively [52]. We denote the threshold value as  $V_T$ . If the received signal is above  $V_T$ , then the receiver declares that 1 was sent and vice versa. An error occurs when 1 was sent and the received signal is below  $V_T$  or when 0 was sent and the received signal is above  $V_T$ . The probability of these occurrences is

$$\Pr[\text{error}|\text{one}] \triangleq p_1 = \int_{-\infty}^{V_T} f_1(v)dv \quad (\text{A.1})$$

$$\Pr[\text{error}|\text{zero}] \triangleq p_0 = \int_{V_T}^{\infty} f_0(v)dv \quad (\text{A.2})$$

Let us suppose for the moment that a 0 is sent, so Equation (A.2) applies and can be rewritten as [52]

$$p_0 = \int_{-\infty}^{\infty} h_0(v) f_0(v) dv \quad (\text{A.3})$$

where  $h_0(v) = 1$  for  $v \geq V_T$  and  $h_0(v) = 0$  for  $v < V_T$ . Then Equation (A.3) is equivalent to

$$p_0 = E[h_0(v)] \quad (\text{A.4})$$

A natural estimator  $\hat{p}_0$  of the expectation  $p$  in Equation (A.4) is the sample mean

$$\hat{p}_0 = \frac{1}{N} \sum_{i=1}^N h_0(v_i) \quad (\text{A.5})$$

where  $v_i \triangleq v(t_i)$ , and the  $t_i$  are the symbol spaced instants at which the decisions are made. Clearly,  $h_0(v)$  is an error detector and the summation in Equation (A.5) is an error counter. This shows a suitable empirical basis for estimating the BER is the observation of error occurrences, and in our context this defines the Monte Carlo method [52]. Extending Equation (A.5) to all types of symbols, if  $N$  bits are transmitted through the communication system, out of which  $\varphi$  are observed to be in error, a simple and natural unbiased estimator of the BER is the simple mean [52]

$$\hat{p} = \varphi/N \quad (\text{A.6})$$

In the limit  $N \rightarrow \infty$  the estimate  $\hat{p}$  will converge to the true value  $p$ . For finite  $N$  we quantify the reliability of the estimator in terms of confidence intervals. We seek two numbers  $h_1$  and  $h_2$ , functions of  $\hat{p}$ , such that with given probability,  $h_2 \leq p \leq h_1$ , and the confidence interval,  $h_1 - h_2$ , is as small as possible [52]. The given probability is usually high. The confidence level,  $1 - \alpha$ , which is often specified, is defined through the relation

$$\Pr[h_2 \leq p \leq h_1] = 1 - \alpha \quad (\text{A.7})$$

The interpretation of Equation (A.7) is that with probability  $1 - \alpha$ , which is referred as confidence, the left and right hand sides of the inequality bracket the true value.

Since  $\hat{p}$  is binomially distributed, it can be shown [52] that for the two sided interval,  $h_1$  and  $h_2$  are the respective solutions of

$$\sum_{k=0}^{\varphi} \binom{N}{k} h_1^k (1 - h_1)^{N-k} = F(h_1; \varphi, N - \varphi - 1) = \alpha/2 \quad (\text{A.8})$$

$$\sum_{k=\varphi}^N \binom{N}{k} h_2^k (1 - h_2)^{N-k} = F(h_2; \varphi - 1, N - \varphi) = \alpha/2 \quad (\text{A.9})$$

where  $F(x; \alpha, \beta)$  is the cumulative beta distribution and can be expressed by

$$F(x; \alpha, \beta) = \frac{(\alpha + \beta + 1)!}{\alpha! \beta!} \int_0^x t^\alpha (1 - t)^\beta dt \quad (\text{A.10})$$

The equations (A.8) and (A.9) must be solved iteratively. Fortunately for situations of usual interest, the value of  $p$ ,  $\varphi$ , and  $N$  encountered permits us to use well known approximations. It is known that the binomial distribution converges to the Poisson distribution as  $p$  or  $\hat{p} \rightarrow 0$ ,  $N \rightarrow \infty$ , and  $N_p$  remains constant. The binomial distribution converges to the normal distribution as  $N \rightarrow \infty$ . The normal approximation to the binomial yields the statement

$$\Pr \left\{ \frac{N}{N + d_\alpha^2} \left[ \hat{p} + \frac{d_\alpha^2}{2N} - d_\alpha \sqrt{\frac{\hat{p}(1 - \hat{p})}{N} + \left( \frac{d_\alpha}{2N} \right)^2} \right] \leq p \leq \frac{N}{N + d_\alpha^2} \left[ \hat{p} + \frac{d_\alpha^2}{2N} + d_\alpha \sqrt{\frac{\hat{p}(1 - \hat{p})}{N} + \left( \frac{d_\alpha}{2N} \right)^2} \right] \right\} = 1 - \alpha \quad (\text{A.11})$$

where  $p$  is the true value of the BER and  $d_\alpha$  is chosen so that the following relationship

is satisfied

$$\int_{-d_\alpha}^{d_\alpha} \frac{1}{\sqrt{2\pi}} e^{-t^2/2} dt = 1 - \alpha \quad (\text{A.12})$$

The generalization referred to the above is obtained if we assume that  $\hat{p} \neq 0$ . In that case we set  $\hat{p} = 10^{-\zeta}$  and  $N = \varphi 10^\zeta$ , with  $\zeta$  not necessarily an integer [52]. For virtually every case of interest, the approximations  $N/(N + d_\alpha^2) \approx 1$  and  $p(1 - p) \simeq p$  are more than amply satisfied. We can express Equation (A.11) as

$$\Pr[y_+ \leq p \leq y_-] = 1 - \alpha \quad (\text{A.13})$$

where the confidence interval  $(y_+, y_-)$  is given by [52]

$$y_\pm = 10^{-\zeta} \left\{ 1 + \frac{d_\alpha^2}{2\varphi} \left[ 1 \pm \sqrt{\frac{4\varphi}{d_\alpha^2} + 1} \right] \right\} \quad (\text{A.14})$$

A general rule that  $N$  should be on the order of  $10/P_e$  [52]. This coincides with a vertical slice at  $N = 10^{\zeta+1}$ , which produces a confidence interval of about  $(2\hat{p}, 0.5\hat{p})$ , i.e. a factor of about 2 on the BER, which is generally considered a reasonable uncertainty.

# Bibliography

- [1] J. G. Proakis, *Digital Communications*, 4th ed. New York, N.Y.: McGraw-Hill, Inc., 2001.
- [2] T. S. Rappaport, *Wireless communications: Principles and Practice*. Upper Saddle River, New Jersey, 07458, USA: Prentice Hall, 1996, ISBN 0-13-375536-3.
- [3] W. C. Jakes, Jr., *Microwave Mobile Communications*. New York, NY, USA: Wiley, 1974, ISBN 0-471-43720-4.
- [4] D. Gesbert, M. Shafi, D. shan Shiu, P. J. Smith, and A. Naguib, “From theory to practice: An overview of MIMO space-time coded wireless systems,” *IEEE Journal on Selected Areas in Communications*, vol. 21, no. 3, pp. 281–302, Apr. 2003.
- [5] V. Tarokh, H. Jafarkhani, and A. R. Calderbank, “Space-time block codes from orthogonal designs,” *IEEE Transactions on Information Theory*, vol. 45, no. 5, pp. 1456–1467, July 1999.
- [6] I. E. Telatar, “Capacity of multi-antenna Gaussian channels,” *European Transactions on Telecommunications*, vol. 10, no. 6, pp. 585–595, November/December 1995.
- [7] E. Biglieri, J. Proakis, and S. Shamai, “Fading channels: Information-theoretic and communications aspects,” *IEEE Transactions on Information Theory*, pp. 2619–2692, October 1998.

- [8] G. J. Foschini, Jr. and M. J. Gans, “On limits of wireless communication in a fading environment when using multiple antennas,” *Wireless Personal Communication*, March 1998.
- [9] A. Paulraj, D. Gore, R. Nabar, and H. Bolcskel, “An overview of MIMO communications - a key to gigabit wireless,” *Proceedings of the IEEE*, vol. 92, no. 2, pp. 198 – 218, February 2004.
- [10] L. Zheng and N. C. D. Tse, “Diversity and multiplexing: A fundamental trade-off in multiple-antenna channels,” *IEEE Transactions on Information Theory*, vol. 49, no. 5, pp. 1073–1096, 2003.
- [11] D. Tse and P. Viswanath, *Fundamentals of Wireless Communication*. Cambridge University Press, 2005.
- [12] R. Heath, Jr and A. Paulraj, “Switching between multiplexing and diversity based on constellation distance,” in *Proceedings of Allerton Conference on Communications, Control, and Computing*, October 2000.
- [13] V. Tarokh, N. Seshadri, and A. R. Calderbank, “Space-time codes for high data rate wireless communication: Performance criterion and code construction,” *IEEE Transactions on Information Theory*, pp. 744–765, March 1998.
- [14] H. Jafarkhani, *Space-Time Coding Theory and Practice*. Cambridge University Press, 2005.
- [15] S. M. Alamouti, “A simple transmit diversity technique for wireless communications,” *IEEE Journal on Selected Areas in Communications*, vol. 16, no. 8, pp. 1451–1458, October 1998.
- [16] 3GPP TSG Ran WG1, “Multiplexing and channel coding (FDD),” 3GPP TR 25.212 V 6.7.0 (2005), Tech. Rep., December 2005.

- [17] —, “Multiple input and multiple output in UTRA,” 3GPP TR 25.876 V 1.8.0 (2005), Tech. Rep., October 2005.
- [18] —, “Physical channels and modulation (release 8),” 3GPP TR 36.211 V 1.2.2 (2005), Tech. Rep., August 2007.
- [19] —, “Physical layer aspect for evolved UTRA,” 3GPP TR 25.814 V 1.0.3 (2006), Tech. Rep., February 2006.
- [20] 3GPP2, “Physical layer for ultra mobile broadband (UMB) air interface specification,” 3GPP2 C S0084 V 1.0 (2007), Tech. Rep., April 2007.
- [21] IEEE 802.11n/D1.10, “Local and metropolitan area network specific requirements - part 11: wireless lan media access control (MAC) and physical layer (PHY) specifications,” IEEE, Tech. Rep., December 2005.
- [22] O. Tirkkonen and A. Hottinen, “Square-matrix embeddable space-time block codes for complex signal constellations,” *IEEE Transactions on Information Theory*, vol. 48, no. 2, pp. 383–395, February 2002.
- [23] W. Su and X.-G. Xia, “On space-time block codes from complex orthogonal designs,” *Wireless Personal Communications*, pp. 1 – 26, 2003.
- [24] H. Jarfarkhani, “A quasi-orthogonal space-time block code,” *IEEE Transactions on Communications*, vol. 49, no. 1, pp. 1–4, January 2001.
- [25] N. Sharma and C. Papadias, “Improved quasi-orthogonal codes through constellation rotation,” *IEEE Transactions on Communications*, vol. 51, no. 3, pp. 332–335, 2003.
- [26] L. Dalton and C. Georghiades, “A full-rate, full-diversity four-antenna quasi-orthogonal space-time block code,” *IEEE Transactions on Wireless Communications*, vol. 4, no. 2, pp. 363–366, March 2005.

- [27] D. Wang and X. Xia, "Optimal diversity product rotations for quasi-orthogonal STBC with MPSK symbols," *IEEE Communications Letters*, vol. 9, no. 5, pp. 420–422, May 2005.
- [28] W. Su and X. Xia, "Signal constellation for quasi-orthogonal space-time block codes with full diversity," *IEEE Transactions on Information Theory*, vol. 50, no. 10, pp. 2331–2347, 2004.
- [29] V. Tarokh, H. Jafarkhani, and A. R. Calderbank, "Space-time block codes for high data rate wireless communications: Performance results," *IEEE Journal on Selected Areas in Communications*, vol. 17, no. 3, pp. 451–460, March 1999.
- [30] J. Hou, M. Lee, and J. Park, "Matrices analysis of quasi-orthogonal space-time block codes," *IEEE Communications Letters*, vol. 7, no. 8, pp. 385–387, August 2003.
- [31] V. Tarokh, A. Naguib, N. Seshadri, and A. Calderbank, "Space-time codes for high data rate wireless communication: performance criteria in the presence of channel estimation errors, mobility, and multiple paths," *IEEE Transactions on Communications*, vol. 47, no. 2, pp. 199 – 207, February 1999.
- [32] Y. Zhang and D. Li, "Performance of space-time transmit diversity over time-selective fading channels," in *Proceedings of 9th IEEE Asia Pacific Conference on Communications*, 2003, pp. 402–405.
- [33] P. Schulz-Rittich, J. Baltersee, and G. Fock, "Channel estimation for DS-CDMA with transmit diversity over frequency selective fading channels," in *Proceedings of the IEEE Vehicular Technology Spring Conference (VTC-Spring)*, May 2001, pp. 1973–1977.
- [34] A. Vielmon, D. Li, and J. Barry, "Performance of transmit diversity over time-varying Rayleigh-fading channels," in *Proceedings of IEEE Global Communications Conference (GLOBECOM)*, November 2001, pp. 3242–3246.

- [35] K. Vanganuru and A. Annamalai, “Analysis of transmit diversity schemes: Impact of fade distribution, spatial correlation and channel estimation errors,” in *Proceedings of the IEEE Wireless Communications and Networking Conference (WCNC)*, March 2003, pp. 247 – 251.
- [36] J. Wang, M. Simon, M. Fitz, and K. Yao, “On the performance of space-time codes over spatially correlated Rayleigh fading channels,” *IEEE Transactions on Communications*, vol. 52, pp. 877 – 881, June 2004.
- [37] E. Jorswieck and A. Sezgin, “Impact of spatial correlation on the performance of orthogonal space-time block codes,” *IEEE Communications Letters*, vol. 8, pp. 21 – 23, January 2004.
- [38] R. Buehrer and N. Kumar, “The impact of channel estimation error on space-time block codes,” in *Proceedings of the IEEE Vehicular Technology Fall Conference (VTC-Fall)*, September 2002, pp. 1921–1925.
- [39] J. Jootar, J. Zeidler, and J. Proakis, “Performance of Alamouti space-time code in time-varying channels with noisy channel estimates,” in *Proceedings of the IEEE Wireless Communications and Networking Conference (WCNC)*, vol. 1, March 2005, pp. 498–503.
- [40] —, “On the performance of concatenated convolutional code and Alamouti space-time code with noisy channel estimates and finite-depth interleaving,” January 2006, to be published.
- [41] J. Cavers, “An analysis of pilot symbol assisted modulation for Rayleigh fading channels,” *IEEE Transactions on Vehicular Technology*, vol. 40, no. 4, pp. 686–693, November 1991.
- [42] S. Haykin, *Adaptive Filter Theory*, 4th ed. Prentice Hall, 2002.
- [43] G. Turin, “The characteristic function of Hermitian quadratic forms in complex normal variables,” *Biometrika*, vol. 47, pp. 199–201, June 1960.

- [44] B. Hochwald and T. Marzetta, “Unitary space-time modulation for multiple-antenna communications in Rayleigh fading,” *IEEE Transactions on Information Theory*, vol. 46, no. 2, pp. 343–364, March 2000.
- [45] T. L. Marzetta and B. M. Hochwald, “Capacity of a mobile multiple-antenna communication link in Rayleigh flat fading,” *IEEE Transactions on Information Theory*, vol. 45, no. 1, pp. 139–157, January 1999.
- [46] B. Hughes, “Differential space-time modulation,” *IEEE Transactions on Information Theory*, vol. 46, no. 7, pp. 2567 – 2578, November 2000.
- [47] B. Hochwald and W. Sweldens, “Differential unitary space-time modulation,” *IEEE Transactions on Communications*, vol. 48, no. 12, pp. 2041 – 2052, December 2000.
- [48] V. Tarokh and H. Jafarkhani, “A differential detection scheme for transmit diversity,” *IEEE Journal on Selected Areas in Communications*, vol. 18, pp. 1169 – 1174, July 2000.
- [49] H. Jarfarkhani and V. Tarokh, “Multiple transmit antenna differential detection from generalized orthogonal design,” *IEEE Transactions on Information Theory*, vol. 47, no. 6, pp. 2626–2631, September 2001.
- [50] M. Tao and R. Cheng, “Differential space-time block codes,” in *Proceedings of IEEE Global Communications Conference (GLOBECOM)*, vol. 2, San Antonio, TX, November 2001, pp. 1098–1102.
- [51] Y. Zhu and H. Jafarkhani, “Differential modulation based on quasi-orthogonal codes,” *IEEE Transactions on Wireless Communications*, vol. 4, no. 6, pp. 3018–3030, November 2005.
- [52] M. C. Jeruchim, “Techniques for estimating the bit error rate in the simulation of digital communication systems,” *IEEE Journal on Selected Areas in Communications*, vol. SAC - 2, no. 1, pp. 153–170, January 1984.